



THE INVESTIGATION OF THE EFFECTS AND CELLULAR MECHANISMS OF  
KAEMPFEROL ON REGULATING ION TRANSPORT IN COLONIC EPITHELIUM



JANJIRA THAWEEWATTANODOM

Graduate School Srinakharinwirot University

2022

การศึกษาฤทธิ์และกลไกการออกฤทธิ์ในระดับเซลล์ของแคมเฟอร์อลในการควบคุมการขนส่ง  
ไอออนผ่านเยื่อผนังลำไส้ใหญ่



เจนจิรา ทวีวัฒนินดม

ปริญญาานิพนธ์นี้เป็นส่วนหนึ่งของการศึกษาตามหลักสูตร  
ปรัชญาดุษฎีบัณฑิต สาขาวิชาชีวภาพการแพทย์  
คณะแพทยศาสตร์ มหาวิทยาลัยศรีนครินทรวิโรฒ  
ปีการศึกษา 2565  
ลิขสิทธิ์ของมหาวิทยาลัยศรีนครินทรวิโรฒ

THE INVESTIGATION OF THE EFFECTS AND CELLULAR MECHANISMS OF  
KAEMPFEROL ON REGULATING ION TRANSPORT IN COLONIC EPITHELIUM



JANJIRA THAWEEWATTANODOM

A Dissertation Submitted in Partial Fulfillment of the Requirements  
for the Degree of DOCTOR OF PHILOSOPHY  
(Biomedical Sciences)

Faculty of Medicine, Srinakharinwirot University

2022

Copyright of Srinakharinwirot University

THE DISSERTATION TITLED  
THE INVESTIGATION OF THE EFFECTS AND CELLULAR MECHANISMS OF KAEMPFEROL ON  
REGULATING ION TRANSPORT IN COLONIC EPITHELIUM

BY  
JANJIRA THAWEEWATTANODOM

HAS BEEN APPROVED BY THE GRADUATE SCHOOL IN PARTIAL FULFILLMENT  
OF THE REQUIREMENTS FOR THE DOCTOR OF PHILOSOPHY  
IN BIOMEDICAL SCIENCES AT SRINAKHARINWIROT UNIVERSITY

-----  
(Assoc. Prof. Dr. Chatchai Ekpanyaskul, MD.)  
Dean of Graduate School  
-----

ORAL DEFENSE COMMITTEE

..... Major-advisor	..... Chair
(Prof.Chatsri Deachapunya, Ph.D.)	(Jarinthorn Teerapompuntakit, Ph.D.)
..... Co-advisor	..... Committee
(Assoc. Prof.Sutthasinee Poonyachoti, D.V.M., Ph.D.)	(Assoc. Prof.Wanlaya Tanechpongamb, Ph.D.)
	..... Committee
	(Asst. Prof.Yamaratee Jaisin, Ph.D.)

Title	THE INVESTIGATION OF THE EFFECTS AND CELLULAR MECHANISMS OF KAEMPFEROL ON REGULATING ION TRANSPORT IN COLONIC EPITHELIUM
Author	JANJIRA THAWEEWATTANODOM
Degree	DOCTOR OF PHILOSOPHY
Academic Year	2022
Thesis Advisor	Professor Chatsri Deachapunya , Ph.D.
Co Advisor	Associate Professor Sutthasinee Poonyachoti , D.V.M., Ph.D.

Kaempferol is a flavonol, mostly found in plants and identified as the most potent stimulator of Cl<sup>-</sup> secretion in airway epithelial cells. This study aims to investigate the effects and cellular mechanisms of kaempferol on ion transport in colonic epithelial T84 cells. The cytotoxicity of kaempferol on T84 cells was examined by MTT assay. The electrical parameters were measured using the Ussing chamber technique. CFTR protein expression was determined by western blot. The results showed that kaempferol treatments (1, 5, 10, 50, and 100 μM) for 24 and 48 h had no toxicity to T84 cells. In intact monolayers, the apical and basolateral addition of kaempferol exerted a biphasic short circuit current ( $I_{sc}$ ) response. Concentrations of less than 50 μM induced a concentration-dependent increase in  $I_{sc}$  with an  $EC_{50}$  of 8.18 μM whereas high concentration inhibited  $I_{sc}$ . Kaempferol (50 μM)-increased  $I_{sc}$  was inhibited by CFTR inhibitors (Glibenclamide and NPPB) or NKCC blocker (bumetanide), but not CaCC inhibitors (CaCCinh-A01 and DIDS) or the Na<sup>+</sup> channel blocker. The ion substitution tests indicated that kaempferol-increased  $I_{sc}$  was dependent on Cl<sup>-</sup> secretions. In amphotericin B-permeabilized monolayers, kaempferol-stimulated apical Cl<sup>-</sup> current ( $I_{Cl}$ ) was inhibited by Cl<sup>-</sup> inhibitors (CFTRinh-172 and CaCCinh-A01). Kaempferol had no additive effects in the presence of forskolin or 8cpt-cAMP. Moreover, kaempferol activated the basolateral K<sup>+</sup> current ( $I_{KB}$ ). The kaempferol-stimulated  $I_{Cl}$  was decreased by protein kinase A inhibitor (H89) whereas it was not abolished by tyrosine kinase inhibitors (AG490 and tyrphostin A23) or tyrosine phosphatase inhibitor (vanadate). Kaempferol treatment for 24 h increased CFTR protein expression. Conclusively, kaempferol activates Cl<sup>-</sup> secretion through activating apical Cl<sup>-</sup> current and basolateral K<sup>+</sup> current in T84 cells. Its mechanism may involve the cAMP/PKA pathway along with increasing CFTR protein expression. The findings indicated the therapeutic benefit of using kaempferol to promote fluid secretion into the intestinal lumen which can be used to treat constipation.

Keyword : T84 cells, Kaempferol, Short circuit current, Apical chloride current, cAMP/PKA pathway



## ACKNOWLEDGEMENTS

This study was achieved at the Department of Physiology, Faculty of Medicine, Srinakarinwirot University, Thailand, and the Department of Physiology, Faculty of Veterinary Science, Chulalongkorn University, Thailand. The study has been supported by research grants from the Faculty of Medicine at Srinakarinwirot University.

I would like to express my sincere gratitude to my advisor, Prof. Dr. Chatsri Deachapunya, for her supervision and guidance. I appreciate her unending support and insightful suggestions to assist me in thinking critically about my research, as well as her encouragement and ongoing advice during my Ph.D. study. I have learned a lot during this time and have become a better scientist.

I deeply appreciate my co-advisor, Assoc. Prof. Dr. Sutthasinee Poonyachoti for her kindness, encouragement, valuable suggestions, and problem-solving thinking in my research study. Thank you for making me positive and confident.

I would like to thank my committee in this dissertation, Asst. Prof. Dr. Orapin Gerdprasert, Assoc. Prof. Dr. Wanlaya Tanechpongthamb, Asst. Prof. Dr. Yamaratee Jaisin, and Dr. Jarinthorn Teerapornpuntakit, for their valuable comments on this dissertation.

My special thanks are also given to my lab colleagues, Dr. Muttarin Lothong, Wannaporn Chayalak, and Norathee Buathong, for their assistance and teaching about lab techniques such as MTT colorimetric assay, Ussing chamber, and Western blot analysis.

Lastly, my most important goes to my family and my best friends. Thanks for their advice that help me through problems and obstacles during my study. I am deeply grateful for their unconditional support, motivation, and constant encouragement.

JANJIRA THAWEEWATTANODOM

## TABLE OF CONTENTS

	Page
ABSTRACT .....	D
ACKNOWLEDGEMENTS.....	F
TABLE OF CONTENTS.....	G
LIST OF TABLES.....	L
LIST OF FIGURES .....	M
CHAPTER 1 INTRODUCTION.....	1
Hypotheses of the Study.....	6
Objectives of the Study.....	6
CHAPTER 2 LITERATURE REVIEW.....	7
2.1 Gastrointestinal tract.....	7
2.2 Colonic epithelium .....	9
2.2.1 Structure and function.....	9
2.2.2 Tight junction .....	10
2.3 Colonic ion transport.....	13
2.3.1 Sodium absorption .....	13
2.3.2 Chloride secretion .....	15
2.3.3 Potassium secretion .....	16
2.4 Colonic transport proteins and regulation .....	17
2.4.1 Channels.....	17
A. The amiloride-sensitive epithelial sodium channel (ENaC) .....	17
B. Apical chloride channels .....	18



C. Apical potassium channel .....	22
D. Basolateral potassium channels .....	22
2.4.2 Exchangers.....	24
A. Sodium-proton exchanger (NHE) .....	24
B. Chloride-bicarbonate exchanger (DRA) .....	24
2.4.3 Cotransporter .....	25
A. Sodium-potassium-chloride cotransporter (NKCC) .....	25
2.5 Signaling pathway regulation of colonic ion transport .....	25
2.5.1 Cyclic adenosine monophosphate signaling pathway .....	25
2.5.2 Calcium signaling pathway .....	27
2.5.3 Cyclic guanosine monophosphate signaling pathway .....	29
2.5.4 Tyrosine kinase and tyrosine phosphatase signaling pathways .....	30
2.6 Kaempferol.....	31
2.6.1 Structure & source.....	31
2.6.2 Bioavailability.....	32
2.6.3 Biological action .....	34
2.6.4 Kaempferol safety .....	35
Conceptual framework .....	37
CHAPTER 3 RESEARCH METHODOLOGY .....	38
3.1 Cell line.....	38
3.2 Materials and reagents .....	40
3.3 Experimental procedures.....	42
3.3.1 Cell culture.....	42

3.3.2 Cytotoxicity assay.....	42
3.3.3 Ussing chamber experiments .....	44
3.3.4 Western blot analysis .....	49
3.4 Statistical analyses.....	51
3.5 Experimental Protocols .....	52
Part 1. Evaluation of the cytotoxic effect of kaempferol.....	52
Part 2. Investigation of the effects of kaempferol on the ion transport across the intact monolayer.....	52
2.1 The direct effect of kaempferol on basal short circuit current .....	52
2.2 Effect of kaempferol on ionic basis of ion transport .....	54
Part 3. Investigation of the effect of kaempferol on the apical membrane permeability in the permeabilized monolayer .....	59
3.1 The effect of kaempferol on the apical membrane permeability .....	59
3.2 The effect of kaempferol on the basolateral membrane permeability ...	63
Part 4. Evaluation of the underlying mechanism of kaempferol through cAMP- dependent protein kinase, tyrosine kinase and tyrosine phosphatase signaling pathway .....	64
4.1 The effect of kaempferol on cAMP-dependent protein kinase signaling pathway.....	64
4.2 The effect of kaempferol on tyrosine kinase and tyrosine phosphatase signaling pathways .....	64
Part 5. Examination of the effect of kaempferol on CFTR protein expression .....	66
CHAPTER 4 RESULTS.....	67
Part 1. The cytotoxic effect of kaempferol .....	67

Part 2. The effects of kaempferol on the ion transport across the intact monolayer ...	69
2.1 The effect of kaempferol on basal short circuit current .....	69
2.2 Ionic basis of kaempferol-stimulated short circuit current.....	73
2.2.1 Effect of kaempferol on transepithelial sodium ion transport .....	73
2.2.2 Effect of kaempferol on transepithelial chloride ion transport.....	75
2.2.3 Effect of ion substitution on kaempferol-increased short circuit current .....	79
2.2.4 Effect of kaempferol on forskolin-activated chloride secretion .....	81
Part 3. The effect of kaempferol on the apical membrane permeability in the permeabilized monolayer .....	83
3.1 The effect of kaempferol on the apical chloride current.....	83
3.1.1 The direct effect of kaempferol on the apical chloride current .....	83
3.1.2 The effect of kaempferol on cAMP-activated chloride current .....	86
3.1.3 The effect of kaempferol on Ca <sup>2+</sup> -activated chloride current .....	89
3.2 The effect of kaempferol on the basolateral membrane permeability.....	91
Part 4. Evaluation of the underlying mechanism of kaempferol through cAMP- dependent protein kinase, tyrosine kinase and tyrosine phosphatase signaling pathway .....	92
4.1 The effect of kaempferol on cAMP-dependent protein kinase signaling pathway .....	92
4.2 The effect of kaempferol on tyrosine kinase and tyrosine phosphatase signaling pathway .....	94
Part 5. The effect of kaempferol on the ion transport protein expression .....	96
CHAPTER 5 SUMMARY DISCUSSION AND SUGGESTION .....	98

Conclusion ..... 108

REFERENCES..... 110

VITA ..... 132



## LIST OF TABLES

	Page
Table 1 Materials and reagents .....	40



## LIST OF FIGURES

	Page
Figure 1 The structure of the intestinal epithelial tight junction (TJ) and associated proteins.....	12
Figure 2 The model of electroneutral Na <sup>+</sup> absorption in the proximal colonic epithelium. ....	14
Figure 3 The model of electrogenic Na <sup>+</sup> absorption in the distal colonic epithelium. ....	14
Figure 4 The model of Cl <sup>-</sup> secretion through luminal CFTR, CaCC, or other Cl <sup>-</sup> channels in the colonic epithelium.....	16
Figure 5 The model of K <sup>+</sup> secretion in the distal colonic epithelium. ....	17
Figure 6 The structure of ENaC comprises $\alpha$ , $\beta$ , and $\gamma$ subunits containing cytoplasmic NH <sub>2</sub> and COOH termini. ....	18
Figure 7 Structure of CFTR.....	20
Figure 8 Cellular roles of CaCC. ....	21
Figure 9 cAMP signaling pathways in the colonic epithelium stimulated by VIP or PG. .	27
Figure 10 Ca <sup>2+</sup> -dependent signaling pathways in the colonic epithelium by acetylcholine, carbachol or substance P. ....	29
Figure 11 cGMP signaling pathways in the colonic epithelium.....	30
Figure 12 Structure of kaempferol.....	32
Figure 13 The bioavailability of dietary flavonol after the ingestion of aglycone and glycoside forms. ....	33
Figure 14 Therapeutic effects of kaempferol on a variety of disorders.....	34
Figure 15 Ussing chamber setup for studying the effect of kaempferol on short circuit current in T84 cell monolayer.....	45

Figure 16 The action of amphotericin B on permeabilization of human cell membranes. .....	47
Figure 17 Model for studying the effect of kaempferol on apical $\text{Cl}^-$ current in amphotericin B-permeabilized T84 cell monolayer .....	48
Figure 18 Model for studying the effect of kaempferol on basolateral $\text{K}^+$ current ( $I_{\text{KB}}$ ) in amphotericin B-permeabilized T84 cell monolayer .....	49
Figure 19 Protocol for studying a single dose of kaempferol on short circuit current in T84 cell monolayer .....	53
Figure 20 Protocol for studying the concentration-dependent short circuit current response of kaempferol in T84 cell monolayer .....	53
Figure 21 Protocol for studying the effect of kaempferol on short circuit current when added into each side of T84 cell monolayer.....	54
Figure 22 Protocol for studying the effect of kaempferol on sodium absorption in T84 cell monolayer .....	55
Figure 23 Protocol for evaluating the effect of kaempferol on chloride secretion via CFTR, CaCC, or NKCC in T84 cell monolayer.....	56
Figure 24 Protocol for studying the effect of kaempferol-activated short circuit current under $\text{Cl}^-$ free, $\text{HCO}_3^-$ free, or $\text{Cl}^-$ - $\text{HCO}_3^-$ free condition in T84 cell monolayer .....	57
Figure 25 Protocol for testing the effect of kaempferol on the forskolin-activated short circuit current.....	58
Figure 26 Protocol for testing the effect of forskolin on the kaempferol-activated short circuit current.....	58
Figure 27 Protocol for investigating the effect of kaempferol on apical chloride current in permeabilized T84 cell monolayer .....	59
Figure 28 Protocol for investigating the effect of kaempferol-activated apical chloride current via ENaC, CFTR, or CaCC in permeabilized T84 cell monolayer .....	60

Figure 29 Protocol for investigating the effect of kaempferol on CaCC before using CaCC inhibitor in permeabilized T84 cell monolayer .....	60
Figure 30 Protocol for evaluating the effect of kaempferol on the cAMP-activated apical chloride current in the permeabilized basolateral membrane of T84 monolayer .....	61
Figure 31 Protocol for evaluating the effect of kaempferol on the 8cpt-activated apical chloride current in the permeabilized basolateral membrane of T84 monolayer .....	61
Figure 32 Protocol for evaluating the effect of kaempferol on the Ca <sup>2+</sup> -activated apical chloride current in the permeabilized basolateral membrane of T84 monolayer .....	62
Figure 33 Protocol for evaluating the effect of kaempferol on the basolateral potassium current in the permeabilized apical membrane of T84 monolayer.....	63
Figure 34 Protocol for assessing the effect of kaempferol on cAMP-dependent protein kinase A signaling pathway.....	64
Figure 35 Protocol for assessing the effect of kaempferol on tyrosine kinase signaling pathway .....	65
Figure 36 Protocol for assessing the effect of kaempferol on tyrosine phosphatase signaling pathway .....	65
Figure 37 The cytotoxic effect of kaempferol in T84 cells. ....	68
Figure 38 The effective concentration of kaempferol on basal short circuit current in T84 cells.....	70
Figure 39 The effect of DMSO on basal short circuit current in T84 cells.....	70
Figure 40 Concentration dependent kaempferol-activated short circuit current. ....	71
Figure 41 The effect of kaempferol on basal short circuit current when added to each side of the membrane. ....	72
Figure 42 Effect of the Na <sup>+</sup> channel blocker amiloride on the kaempferol-activated short circuit current in T84 cells. ....	74



Figure 43 Effect of CFTR Cl <sup>-</sup> channel inhibitors on the kaempferol-activated short circuit current in T84 cells. ....	76
Figure 44 Effect of CaCC Cl <sup>-</sup> channel inhibitors on the kaempferol-activated short circuit current in T84 cells. ....	77
Figure 45 Effect of the NKCC cotransporter blocker bumetanide on the kaempferol-activated short circuit current in T84 cells. ....	78
Figure 46 Effect of Cl <sup>-</sup> and HCO <sub>3</sub> <sup>-</sup> substitution on the kaempferol-activated short circuit current in T84 cells. ....	80
Figure 47 Effect of kaempferol on forskolin-activated transepithelial chloride secretion. ....	82
Figure 48 The effect of kaempferol on apical chloride current in the basolaterally permeabilized T84 monolayer. ....	84
Figure 49 The effect of the Na <sup>+</sup> channel blocker and Cl <sup>-</sup> channel inhibitors on the kaempferol-activated apical chloride current in the basolaterally permeabilized T84 monolayer. ....	85
Figure 50 The effect of the CFTR Cl <sup>-</sup> channel inhibitor on the kaempferol-activated apical chloride current in the basolaterally permeabilized T84 monolayer. ....	85
Figure 51 The effect of kaempferol on forskolin-activated chloride current in the basolaterally permeabilized T84 monolayer. ....	87
Figure 52 The effect of kaempferol on 8-cpt-cAMP-activated chloride current in the basolaterally permeabilized T84 monolayer. ....	88
Figure 53 The effect of kaempferol on Ca <sup>2+</sup> -activated chloride current in the basolaterally permeabilized T84 monolayer. ....	90
Figure 54 The effect of kaempferol on the basolateral potassium current in the apically permeabilized T84 monolayer. ....	91
Figure 55 The effect of protein kinase A inhibitor H89 on the kaempferol-activated apical chloride current in the basolaterally permeabilized T84 monolayer. ....	93

Figure 56 The effect of tyrosine kinase and tyrosine phosphatase inhibitors on the kaempferol-activated apical chloride current in the basolaterally permeabilized T84 monolayer. ....	95
Figure 57 Effect of kaempferol on CFTR protein expression in T84 cells. ....	97
Figure 58 The model illustrates the effect and cellular mechanism of kaempferol on T84 cells.....	108



## CHAPTER 1

### INTRODUCTION

The colonic epithelium is essential for the homeostasis of the digestive tract by regulating transepithelial ions and water transport between the intestinal lumen and the blood circulation. Under physiological conditions, approximately 1.3–1.8 liters of electrolyte-rich fluid are absorbed daily by the colon.<sup>(1)</sup> Furthermore, secretion of mucus and electrolytes is another crucial role of the colon, which is balanced by absorption. Net transport of electrolytes and water across the colonic epithelium depends on the ion transport machinery, composed of several ion channels, membrane transporters, pumps, and water channels distributed along the luminal and the basolateral membrane. The function of these transport proteins leads to the results of well-balanced absorption and secretion.

The primary determinant of fluid absorption is the amount of sodium ( $\text{Na}^+$ ) absorption. In the proximal colon, electroneutral  $\text{Na}^+$  transport occurs via  $\text{Na}^+/\text{H}^+$  and  $\text{Cl}^-/\text{HCO}_3^-$  exchangers in the luminal membrane, resulting in  $\text{NaCl}$  absorption. In the distal colon, electrogenic absorption via amiloride-sensitive  $\text{Na}^+$  channels (ENaC) is the predominant mechanism of  $\text{Na}^+$  absorption which is under the influence of aldosterone.<sup>(2)</sup> Under this circumstance,  $\text{Cl}^-$  secretion is caused by cystic fibrosis transmembrane conductance regulator (CFTR) channels and other  $\text{Cl}^-$  channels, for instance,  $\text{Ca}^{2+}$ -activated chloride channels (CaCC). The transepithelial  $\text{Cl}^-$  secretion processes depend on the combined activity of several transport proteins by which the  $\text{Na}^+/\text{K}^+$ -ATPase located on the basolateral membrane generates the  $\text{Na}^+$  gradient, leading to the combined movement of  $\text{Na}^+$ ,  $\text{K}^+$ , and  $\text{Cl}^-$  into the cells via basolateral  $\text{Na}^+/\text{K}^+/\text{2Cl}^-$  cotransporter (NKCC). Then,  $\text{Cl}^-$  are mainly secreted via the CFTR  $\text{Cl}^-$  channel in the apical membrane,<sup>(3)</sup> producing an osmotic gradient and resulting in a subsequent fluid movement from the basolateral interstitium into the lumen. In addition, basolateral  $\text{K}^+$  channels play an essential role in recycling  $\text{K}^+$ , which hyperpolarized membrane and creates electrical driving force required for  $\text{Cl}^-$  secretion.<sup>(1)</sup> Besides, the epithelial cell can maintain  $\text{K}^+$  homeostasis through secreting  $\text{K}^+$  by the distal colon.<sup>(4)</sup>

In general, the process of  $\text{Na}^+$  absorption occurs to a greater extent than  $\text{Cl}^-$  and  $\text{K}^+$  secretion to prevent the loss of water and electrolytes from the body.<sup>(5)</sup> Although the net effect is  $\text{Na}^+$  absorption,  $\text{Cl}^-$  and  $\text{K}^+$  secretion plays a crucial role in preventing epithelial surface dehydration and controlling luminal pH. Previous research has demonstrated that the pH level of the gastrointestinal lumen promotes both innate immunity and epithelial barrier function.<sup>(6)</sup> Moreover, an appropriate level of luminal fluid for digestive process depends on fluid secretion, mainly driven by  $\text{Cl}^-$  secretion.<sup>(7)</sup> This  $\text{Cl}^-$  secretion leads to a suitable environment for enzymatic digestion, nutrient absorption, and stool movement.<sup>(8)</sup> Hence,  $\text{Cl}^-$  secretion followed by fluid secretion promotes the colonic epithelial barrier to protect against infection and increases fluidity to reduce constipation.

$\text{Cl}^-$  secretion in the colon is regulated by hormones, neurotransmitters and various substances that are mediated through intracellular signaling cascades, such as cyclic adenosine monophosphate (cAMP) signaling pathway and  $\text{Ca}^{2+}$  signaling pathway or controlled by a direct activation of the CFTR  $\text{Cl}^-$  channel. The cAMP signaling pathway is demonstrated by activators of cAMP (e.g., vasoactive intestinal peptide, prostaglandins). These activators bind to their specific membrane G-protein coupled receptors (GPCRs) which leads to stimulation of adenylate cyclase (AC) to convert adenosine triphosphate (ATP) to cAMP.<sup>(9)</sup> The increased cAMP, in turn, activates protein kinase A (PKA), which phosphorylates transport proteins to increase CFTR channel activity.<sup>(10, 11)</sup> Furthermore, proline-rich tyrosine kinases (Pyk2) and Src family kinases (SFK) may directly phosphorylate CFTR to promote CFTR activity.<sup>(12, 13)</sup> These tyrosine kinases can also cause robust activation of quiescent CFTR channels.<sup>(14)</sup> The tyrosine kinase induced direct activation of CFTR is independent of protein kinase A and protein kinase C. Phosphorylation of CFTR on tyrosine residues by c-Src and Pyk2 produces chloride currents that are 80% greater than those generated through PKA.<sup>(14)</sup> Furthermore, the  $\text{Cl}^-$  secretion by colonic epithelium can be regulated by  $\text{Ca}^{2+}$  signaling pathway.<sup>(15)</sup> The  $\text{Ca}^{2+}$  signaling pathway is stimulated by muscarinic agonists that bind to GPCRs via muscarinic M3 receptor<sup>(15, 16)</sup> to stimulate  $\text{G}\alpha_q$ . Phospholipase C (PLC) is

activated when  $G\alpha_q$  is active, and phosphatidylinositol 4,5-bisphosphate ( $PIP_2$ ) is converted to inositol triphosphate ( $IP_3$ ) and diacylglycerol (DAG).  $IP_3$  elevates intracellular  $Ca^{2+}$  levels whereas DAG stimulates specific kinds of protein kinase C. The increased intracellular  $Ca^{2+}$  stimulates  $Cl^-$  secretion via  $CaCC$ .<sup>(17, 18)</sup>

Maintaining proper  $Na^+$  absorption and  $Cl^-$  secretion keeps the body in physiological homeostasis. However, malfunction in the absorption and secretion through the colonic epithelium can lead to diarrhea or constipation. For example, dysfunction of  $Na^+$  absorption has been found in patients with chronic pain receiving opioids. An opioid agonist binding to peripheral  $\mu$ -opioid receptors in the GI tract reduces bowel tone, slows peristaltic activity, and decreases mucosal secretions. Hence, these effects cause slow intestinal transit, subsequently increase  $Na^+$  and fluid absorption and finally lead to opioid-induced constipation (OIC).<sup>(19)</sup>

Dysfunction of  $Cl^-$  secretion can also cause diarrhea or constipation. Alteration in  $Cl^-$  transport observed in secretory diarrhea has been associated with the enterotoxins of several species of bacteria that cause increases in cAMP to activate CFTR channels, resulting in overstimulation of  $Cl^-$  secretion.<sup>(1)</sup> Conversely, the decrease in  $Cl^-$  secretion is a common cause of chronic constipation in the elderly that severely affects the quality of life. Studying of active ion transport in the rabbit colon has been found to relate with the aging process.<sup>(20)</sup> In mature animals, cAMP-dependent  $Cl^-$  secretion declines significantly while  $Na^+$  absorption does not. This discovery is supported by a reduction in stool water content and the number of colonic crypts containing non-goblet cells. This is consistent with studies in human rectal and colonic biopsies which indicate that cAMP-dependent and cholinergic  $Cl^-$  secretion is highest in neonates and lowest in the elderly.<sup>(21)</sup> In addition, the decrease in  $Cl^-$  secretion observed in cystic fibrosis patients is due to not only impairing cAMP-dependent  $Cl^-$  conductance but also enhancing  $Na^+$  absorption as assessed by Ussing chamber technique in human rectal biopsies.<sup>(22)</sup> Thus, alterations in ion transport activity and function lead to ion transport-related disorders which require medication for treatment or, in severe cases, may require hospitalization.<sup>(23, 24)</sup> For this reason, a promising natural compound that are capable of

modulating ion transport has been received much attention as it will help attenuate these ion transport-related disorders and even reduce adverse events or chemical residues in patients using modern medicines.

Flavonoids belong to the group of plant polyphenols widely found in fruits, soybeans, and vegetables which are ingested by humans as a regular diet.<sup>(25)</sup> Several studies have reported a wide variety of pharmacological effects of flavonoids on mammalian cells and tissues, such as anti-oxidative, anti-inflammatory, anti-mutagenic, and anti-carcinogenic effects.<sup>(26)</sup> However, the transport-related properties of flavonoids are limited to some classes of flavonoids, especially flavonol, which consists of quercetin, kaempferol, myricetin, and isorhamnetin. Among flavonol compounds, quercetin gets the most extensive study on the control of ion transport in the intestine. Quercetin induces  $\text{Cl}^-$  secretion in rat small intestine and colon, which is observed by an increase in short-circuit current ( $I_{\text{SC}}$ ) in Ussing technique<sup>(27)</sup> and activation of the basolateral  $\text{K}^+$  channel in rat distal colon mucosa.<sup>(28)</sup> Quercetin also stimulates  $\text{Cl}^-$  secretion via the CaCC in human colon adenocarcinoma cells. In intestinal tissues, quercetin increases  $I_{\text{SC}}$  by increasing calcium concentration via L-type  $\text{Ca}^{2+}$  channel and activating basolateral NKCC,  $\text{Na}^+/\text{K}^+$ -ATPase, and  $\text{K}^+$  channels.<sup>(29)</sup> In addition, previous studies with baicalein, a flavone type of flavonoid, have demonstrated its effect on stimulating  $\text{Cl}^-$  secretion in human colonic epithelial cells through an increase in intracellular cAMP and PKA activity.<sup>(30, 31)</sup> However, the cellular mechanisms of flavonol in the colonic epithelial cells are still unclear, especially in kaempferol.

Kaempferol is a flavonol compound widely distributed in grapes, broccoli, tomatoes, spinach, and tea. A report has shown that kaempferol stimulate electrogenic  $\text{Cl}^-$  secretion on the T84 colonic adenocarcinoma cell line, but the effect is less potent than quercetin under basal condition while myricetin produces minimal responses.<sup>(32)</sup> Conversely, kaempferol can produce the maximum effect of  $\text{Cl}^-$  secretion in human airway epithelium, followed by apigenin, quercetin, and genistein, respectively, on cAMP-activated  $\text{Cl}^-$  secretion by forskolin.<sup>(33)</sup> This study suggested that kaempferol is the highest potency of all tested flavonoids, identified by the significant effect on short

circuit current. Interestingly, the mechanism of action for flavonoids appears to depend on the stimulation level of the cAMP-PKA system.<sup>(33)</sup> Nevertheless, based on electrophysiological studies, information is limited concerning the effects and mechanisms of kaempferol on the absorptive and secretory function of the intestinal epithelia. This draws our attention to investigate the effect and cellular mechanism of kaempferol on the modulation of ion transport in colonic epithelium using the human colonic adenocarcinoma cell line (T84). These cells were commonly used as a cell model of colonic epithelial cells to study transepithelial ion transport as they exhibit several ion channels and transporters such as CFTR, CaCC, ENaC, basolateral NKCC, and several other vital components involved in multi-level ion transport.<sup>(34, 35)</sup>

The findings obtained from the present study may provide more scientific information about the effect and significant mechanisms of using kaempferol regarding ion transport regulation in colonic epithelium. It also provides data as a candidate substance in the flavonol group to be developed as a drug for treating ion transport-related disorders.

### Hypotheses of the Study

1. Kaempferol can increase the basal short circuit current in the colonic epithelial T84 cell monolayer.
2. Kaempferol can increase the apical chloride current in the basolaterally membrane permeabilized T84 monolayer.
3. Kaempferol may activate chloride secretion through CFTR and CaCC via cAMP, intracellular calcium, and tyrosine kinase and tyrosine phosphatase signaling pathways.
4. Kaempferol can increase the expression of CFTR proteins.

### Objectives of the Study

1. To investigate the effect of kaempferol on basal transport property in colonic epithelial T84 cell monolayer
2. To identify the effect of kaempferol on chloride secretion through CFTR and CaCC in colonic epithelial T84 cell monolayer
3. To evaluate the cellular mechanisms of action of kaempferol involved in cAMP, intracellular calcium, and tyrosine kinase and tyrosine phosphatase signaling pathways
4. To elucidate the genomic effect of kaempferol on the expression of CFTR protein



## CHAPTER 2

### LITERATURE REVIEW

#### 2.1 Gastrointestinal tract

The gastrointestinal tract (GI tract) consisting of several organs forms a long tube starting from the mouth to the anus. The mouth, esophagus, stomach, duodenum, jejunum, and ileum comprise the upper GI tract, whereas the colon, rectum, and anus comprise the lower GI tract. The principal functions of the GI tract are digestion of food, absorption of nutrients and vitamins, secretion of water and salt, and excretion of waste products. Several organs accomplish these functions with diverse functions ranging from the mouth to the anus.<sup>(36)</sup> Peristalsis of the esophagus is an activity of muscle contractions that moves food from the pharynx into the stomach. After digestion by gastric acid and digestive enzymes, chyme, the breakdown products of the food bolus, passes the pyloric sphincter and enters the duodenum. In order to facilitate nutrient absorption in the small intestine, the mechanism of digestion then breaks down the carbohydrates, lipids, and proteins into shorter molecules. Several auxiliary organs, including the salivary glands, pancreas, liver, and gallbladder, assist the digestive process. After the luminal contents reaching the colon, they are referred to as feces and are able to be eliminated through the rectum and anal canal.<sup>(37)</sup>

The cross-sectional structure of the GI tract from the lumen outward is divided into four layers: mucosa, submucosa, muscularis, and serosa or adventitia.<sup>(38)</sup> The mucosal layer is lined with composed of epithelial cells capable of absorption and secretion. The submucosal layer contains the nervous, lymphatic, and connective tissue systems. The muscle layer is composed of both longitudinal and circular smooth muscles. The connective tissue that borders the digestive system is referred to as adventitia above the diaphragm and serosa below it. The serosal layer or adventitia comprises blood arteries, lymphatics, and nerves.

Furthermore, the GI tract contains various cell types, each with a unique role. Epithelial cells are the major cell type in the gastrointestinal epithelium. These cells line the inner surface of the GI tract and are responsible for absorbing nutrients and water

from ingested foods and secreting immunoglobulins.<sup>(39, 40)</sup> Goblet cells can produce mucus to keep the gastrointestinal tract moist and prevent digestive enzymes from causing intestinal mucosa damage.<sup>(41)</sup> Enteroendocrine cells (EECs) are specialized endoderm-derived epithelial cells that secrete hormones for regulating digestion, nutrient absorption, and intestinal motility.<sup>(42)</sup> They respond to changes in the luminal content by secreting signaling molecules that diffuse into the circulation and function as classical hormones on distant targets and paracrine on nearby cells. Additionally, proper digestion and digestive tract health require a complex system of neurological activities coordinated by the central nervous system (CNS) and the enteric nervous system (ENS).<sup>(43, 44)</sup>

Paneth cells are commonly found in the small intestine and can also be present in the colonic epithelium. They protect the gastrointestinal tract from pathogenic bacteria by directly detecting enteric pathogens via MyD88-dependent activation of toll-like receptor (TLR) 4 and by activating a wide variety of antimicrobial agents.<sup>(45)</sup> Microfold (M) cells are specialized intestinal cells that help transport bacteria or other intestinal antigens from the epithelial surface to dendritic cells to initiate immune responses.<sup>(46)</sup> Tuft cells play a role in immunity to parasites by secreting cytokines for parasite clearance.<sup>(47)</sup> Immune cells, which include lymphocytes, macrophages, and dendritic cells, help to protect the GI tract from pathogens and foreign invaders.<sup>(48)</sup> Stem cells continuously regenerate the GI epithelium that maintains the health and function of the epithelium.<sup>(49)</sup>

The largest part of the GI system consists of the small intestine and colon, which are in the abdominal cavity.<sup>(50)</sup> The colon is the final part of the GI tract by which its structure originates at the ileocecal valve extending to the anus. The three primary functions of the colon are absorption of electrolyte-rich fluid (90% of sodium and water accessing the proximal colon<sup>(1)</sup>), production and absorption of vitamins, and transport of wastes to the rectum which approximately 0.2–0.4 liter is excreted in the stool.<sup>(51)</sup> The structural wall of the colon consists of multiple layers from the lumen outward, including the mucosa, submucosa, muscular layer, and serosa.<sup>(52)</sup> The innermost surface of the

colon is composed of the epithelial layer playing a pivotal role in transport massive amounts of sodium and water across the mucosa to the blood side of the colon.

## 2.2 Colonic epithelium

### 2.2.1 Structure and function

The colonic epithelium is the single-cell layer consisting of three primary structures: epithelial cells, tight junction, and basement membrane. The adjacent epithelial layer cells are sealed with tight junction forming the epithelial barrier and separating the plasma membrane into two compartments: apical membrane facing the intestinal lumen and basolateral membrane close to the blood circulation.<sup>(53)</sup> The distinct structural and functional differences between the apical and basolateral membranes organize an apical-to-basal polarity of epithelial cells, which regulates the vectorial transport of ions and nutrients across the colonic epithelium cell monolayers during their secretory and absorptive functions.<sup>(54)</sup>

In addition, the colonic epithelium is composed of specialized cells with several functions that differentiate from stem cells at the invagination structure known as crypt base. Colonocytes with absorptive functions are the most epithelial cells distributed over specialized epithelial lineages, including EECs and secretory goblets.<sup>(55)</sup> The main functions of colonocytes (surface epithelium) are absorption of water and electrolytes; however, the secretion of electrolytes can occur at the surface epithelium. Likewise, goblet cells are primarily responsible for the secretion of electrolytes and mucus. Therefore, both surface epithelium and crypts are the locations of electrolytes secretion, which is primarily mediated by  $\text{Cl}^-$  channel as identified by the patch-clamp technique.<sup>(1)</sup>

The ion transport function of the colonic epithelium relies on various transport proteins, i.e., ion channels, transporters, and pumps, located either on the apical or basolateral membrane. These transport proteins play important roles in transporting large amounts of essential electrolytes such as sodium, potassium, and chloride, leading to net absorption of electrolytes under physiological conditions.

Furthermore, net absorption occurs in the surface epithelium more than in crypt cells because the surface epithelium has a greater density of  $\text{Na}^+$  channels. However, net secretion of electrolytes can occur when the colonic epithelium is stimulated by secretagogues such as vasoactive intestinal peptide, prostaglandins, and heat-labile toxin from *Escherichia coli*. Although the net results of ion transport are absorption of sodium chloride ( NaCl) , potassium chloride ( KCl) , and water for maintaining homeostasis, secretion of NaCl and KCl occurs at a much greater extent than absorption as evidenced in secretory diarrhea.<sup>(1)</sup> The fluid secretion by the colonic epithelium lubricates the surface of the epithelium, thus safeguarding the mucosa at the site of mechanical stress and facilitating stool movement. The fluid secretion process is mainly generated by chloride secretion across the epithelial cells, and this creates an osmotic gradient for pulling water, along with sodium passively following via the paracellular space into the lumen of the intestinal tract.<sup>(8,56)</sup>

### 2.2.2 Tight junction

Tight junctions are intercellular adhesion complexes generated by the number and composition of several proteins joining at the apical part of the adjacent epithelial cells. The tight junction can be classified as two types of barriers. The paracellular barrier controls selective paracellular permeability, or the passive transport of ions, solutes, and water between epithelial cells. The intramembrane barrier prevents membrane components from being exchanged between the apical and basolateral cell surface domains. Both barriers are physically located on intramembrane strands and are most likely structurally connected.<sup>(57)</sup> Therefore, the tight junction is critical for preserving the function of the intestinal barrier by regulating the permeability of the paracellular transport pathway.<sup>(53)</sup> Ions can readily pass through the tight junction, but large molecules and proteins cannot. The ion permeability of the tight junction is evaluated using transepithelial electrical resistance measurements.<sup>(58)</sup>

The functional proteins of a tight junction are transmembrane proteins that connect adjacent cell membranes and proteins in the peripheral membrane. Tight

junction integrity is continuously modulated by integral transmembrane proteins and their interactions with peripheral membrane proteins. Occludin, claudins, junctional adhesion molecule (JAM), and tricellulin are examples of transmembrane proteins that link together to control the permeation of ions and small solutes through the tight junction. All three members of the zonula occludens (ZO) family, i.e., ZO-1, ZO-2, and ZO-3, are peripheral membrane adaptor proteins that facilitate interaction with integral membrane proteins, the actin cytoskeleton, and other signaling proteins (figure 1).<sup>(53)</sup> However, the claudin composition of tight junctions regulates ion permeability, creating gated ion-selective paracellular pores across the paracellular transport barrier. The function of tight junction barrier is also regulated by the phosphorylation, distribution, and expression levels of tight junction proteins. Intracellular signaling pathways contain protein kinase A (PKA), protein kinase C (PKC), protein kinase G (PKG), phosphatase, myosin light chain (MLCK), mitogen-activated protein kinases (MAPK), phosphoinositide 3-kinase (PI3K), and Rho signaling pathways are indicated to regulate tight junction permeability. responsible for their stringent regulation.<sup>(59, 60)</sup>

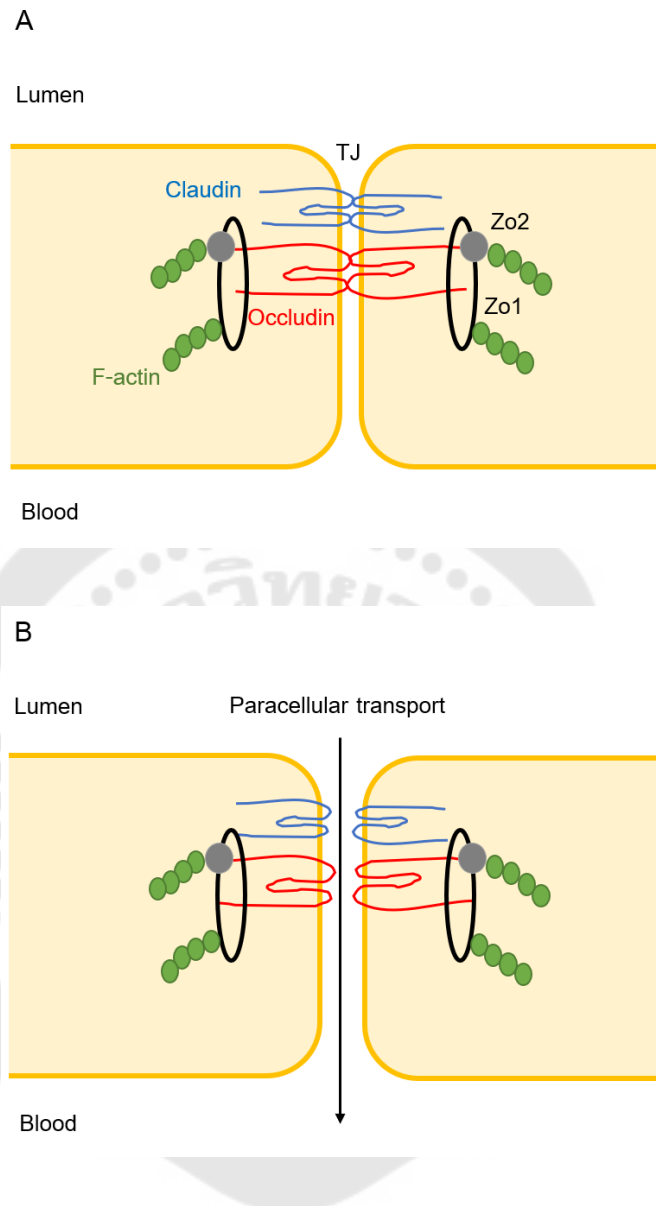


Figure 1 The structure of the intestinal epithelial tight junction (TJ) and associated proteins. **(A)** The association of claudin, occludin, ZO-1 and -2, and F-actin results in the formation of a TJ structure. **(B)** Once the TJ opens in response to stimulation from the luminal side, transport of extracellular components from the intestinal lumen to blood occurs via paracellular transport. Adapted from Lee.<sup>(53)</sup>

## 2.3 Colonic ion transport

### 2.3.1 Sodium absorption

The principal function of the human colonic epithelium is the absorption of electrolytes which the primary electrolyte of absorption is sodium ( $\text{Na}^+$ ).  $\text{Na}^+$  absorption by electroneutral process depends on  $\text{Na}^+/\text{H}^+$  and  $\text{Cl}^-/\text{HCO}_3^-$  exchange located on the luminal membrane leading to  $\text{NaCl}$  absorption. In addition,  $\text{Na}^+$  absorption can happen by electrogenic absorption through luminal  $\text{ENaC}$ .<sup>(61)</sup> However, absorptive processes in the human colonic epithelium are complex and exhibit significant regional differences. In the proximal colon, electroneutral absorption is the primary process of  $\text{NaCl}$  absorption which  $\text{Cl}^-/\text{HCO}_3^-$  exchange functions together with  $\text{Na}^+/\text{H}^+$  exchange (NHE). This process is dependent on intracellular carbonic anhydrases, which generate  $\text{H}^+$  and  $\text{HCO}_3^-$  from  $\text{CO}_2$  and  $\text{H}_2\text{O}$ . With the activity of basolateral  $\text{Na}^+/\text{K}^+$ -ATPase,  $\text{Na}^+$  enters across the apical membrane by  $\text{Na}^+/\text{H}^+$  exchangers (e.g., NHE2 and NHE3) down electrochemical gradient while  $\text{Cl}^-$  entry occurs via apical  $\text{Cl}^-/\text{HCO}_3^-$  exchangers (DRA).<sup>(62)</sup> Subsequently,  $\text{Na}^+$  leaves the cell through the  $\text{Na}^+/\text{K}^+$ -ATPase and  $\text{Cl}^-$  via chloride channel-2 (CLC-2) at the basolateral membrane.  $\text{K}^+$  that enters the cell by  $\text{Na}^+/\text{K}^+$ -ATPase at the basolateral membrane leaves the cell via basolateral  $\text{K}^+$  channels (KCNN4 and KCNQ/1 KCNE3) and is used for continuous action of  $\text{Na}^+/\text{K}^+$ -ATPase, thus resulting in electroneutral  $\text{NaCl}$  absorption (figure 2).<sup>(1, 62)</sup> In the distal colon,  $\text{Na}^+$  absorption is primarily electrogenic process which occurs via amiloride-sensitive epithelial  $\text{Na}^+$  channels ( $\text{ENaC}$ ).<sup>(2)</sup> The accumulated  $\text{Na}^+$  in the interstitial fluid of the blood side creates hyperosmotic driving force for passive  $\text{Cl}^-$  movement through the paracellular pathway (figure 3).<sup>(1, 62)</sup>

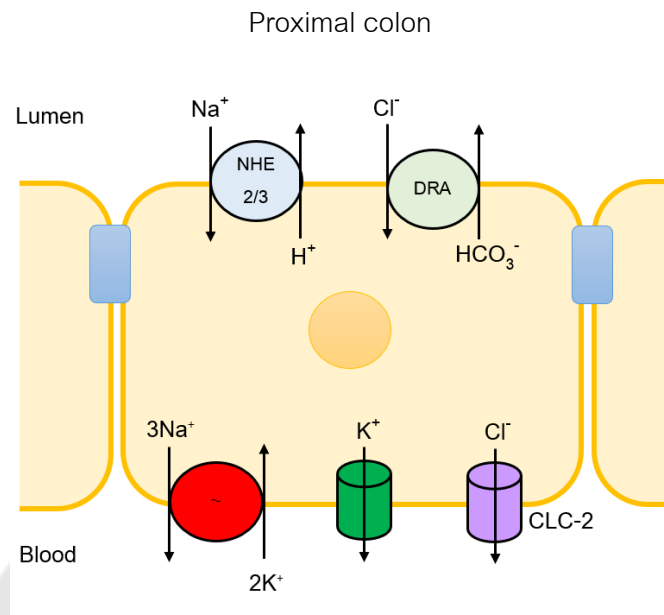


Figure 2 The model of electroneutral  $\text{Na}^+$  absorption in the proximal colonic epithelium. Adapted from Kunzelmann and Mall; Rao.<sup>(1, 62)</sup>

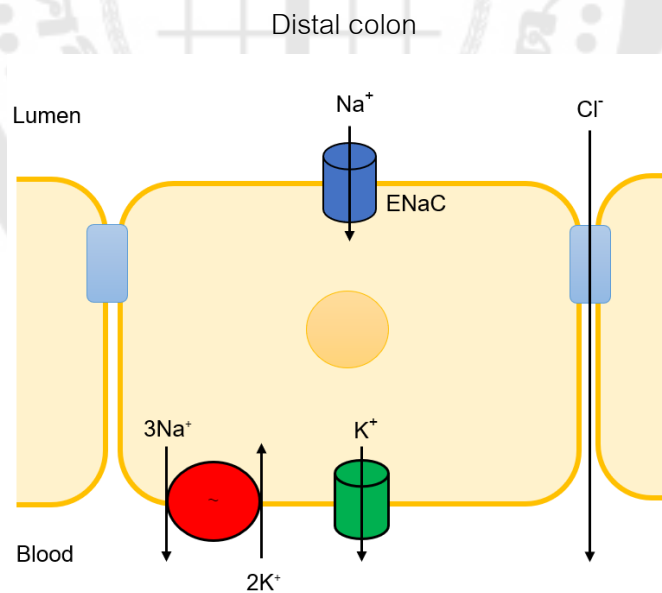


Figure 3 The model of electrogenic  $\text{Na}^+$  absorption in the distal colonic epithelium. Adapted from Kunzelmann and Mall; Rao.<sup>(1, 62)</sup>



### 2.3.2 Chloride secretion

The colonic epithelium also plays an essential function in electrolyte secretion, which is counterbalanced by absorption. Electrolyte secretion by the colonic epithelium will hydrate and lubricate the mucosa which help protect cells from physical injury from mechanical stress, prevent bacterial overgrowth and virulence, and promote stool passage.<sup>(63)</sup> The colonic secretion mainly involves  $\text{Cl}^-$  and  $\text{K}^+$  secretion. Although  $\text{Cl}^-$  secretion can occur throughout the colon, it is predominantly found in crypt cells and slightly found in the surface epithelia of the proximal and distal colon. Meanwhile,  $\text{K}^+$  is only secreted by the distal colon.<sup>(1, 62)</sup> The processes of  $\text{Cl}^-$  secretion require basolateral  $\text{Na}^+/\text{K}^+$ -ATPase activity to provide the driving force for  $\text{Cl}^-$  entry via basolateral  $\text{Na}^+-2\text{Cl}^-$ - $\text{K}^+$  cotransporters (NKCC). The accumulative  $\text{Cl}^-$  then exits the cells through CFTR channel,  $\text{Ca}^{2+}$ -activated  $\text{Cl}^-$  channel (CaCC) or others on the apical membranes. Electrogenic  $\text{Cl}^-$  or  $\text{K}^+$  secretion changes can be assessed by measuring short circuit current ( $I_{\text{SC}}$ ) and potential difference (PD).<sup>(64)</sup>

Furthermore, intracellular  $\text{Na}^+$  from basolateral  $\text{Na}^+-2\text{Cl}^-$ - $\text{K}^+$  cotransporter exits via basolateral  $\text{Na}^+/\text{K}^+$ -ATPase, while the  $\text{K}^+$  primarily exits via basolateral  $\text{K}^+$  channels. Besides,  $\text{K}^+$  may occasionally exit the cell via apical membrane channels. For this reason,  $\text{Cl}^-$  secretion is driven by an interplay between the basolateral  $\text{Na}^+/\text{K}^+$ -ATPase and the basolateral  $\text{K}^+$  channels (Figure 4),<sup>(62)</sup> which maintains the electronegative properties of the cell membrane. Thus, colonic electrolyte secretion is largely dependent on the active transepithelial  $\text{Cl}^-$  secretion. The  $\text{Cl}^-$  movement from the blood side into the lumen will generate the electrical and osmotic gradient driving the passive transport of  $\text{Na}^+$  and water via paracellular route into the lumen.<sup>(62)</sup>

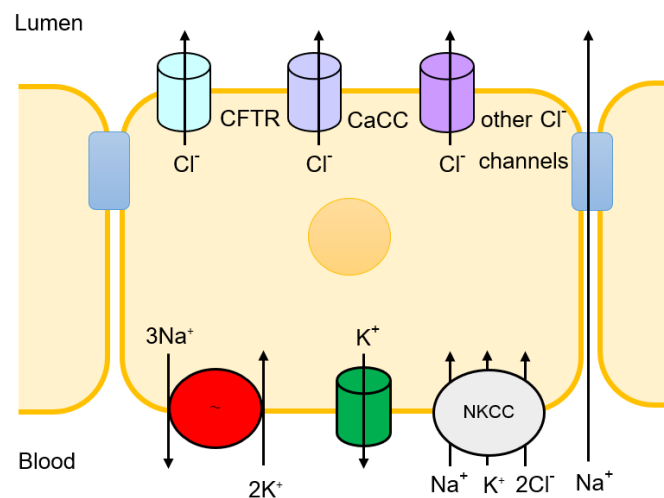


Figure 4 The model of  $\text{Cl}^-$  secretion through luminal CFTR, CaCC, or other  $\text{Cl}^-$  channels in the colonic epithelium. Adapted from Rao.<sup>(62)</sup>

### 2.3.3 Potassium secretion

Potassium secretion also adds to net fluid secretion in the distal colon. In diarrheal diseases, an increase in this secretion leads to loss of  $\text{K}^+$  in feces, as demonstrated in cholera. The amount of fecal  $\text{K}^+$  in healthy subjects is 10 mEq/day as compared with 119 mEq/day in cholera-infected subjects.  $\text{K}^+$  concentration of approximately 90% is excreted by the kidneys and 10% in the stool in a healthy adult. Nonetheless, colonic  $\text{K}^+$  secretion may be crucial for  $\text{K}^+$  homeostasis, particularly in patients with end-stage kidney disease. Distal colonic  $\text{K}^+$  secretion is uncoupled with  $\text{Cl}^-$  secretion<sup>(63)</sup> and has a significant role when luminal values exceed 25 mEq/L. The processes of active secretion of  $\text{K}^+$  occur by  $\text{Na}^+/\text{K}^+$  ATPase and, under stimulated secretory conditions, via  $\text{Na}^+-2\text{Cl}^--\text{K}^+$  cotransporters to allow  $\text{K}^+$  entry across the basolateral membrane.<sup>(65, 66)</sup> Then,  $\text{K}^+$  exits across the apical membrane via KCNMA1 channels, the primary apical channel for  $\text{K}^+$  secretion. In other part of the intestine, basolateral  $\text{K}^+$  channels such as KCNQ1/KCNE3, and KCNN4 are also required for the exit of  $\text{K}^+$  across the basolateral membrane (figure 5) as well as stabilizing the membrane potential (figure 5).<sup>(62)</sup>

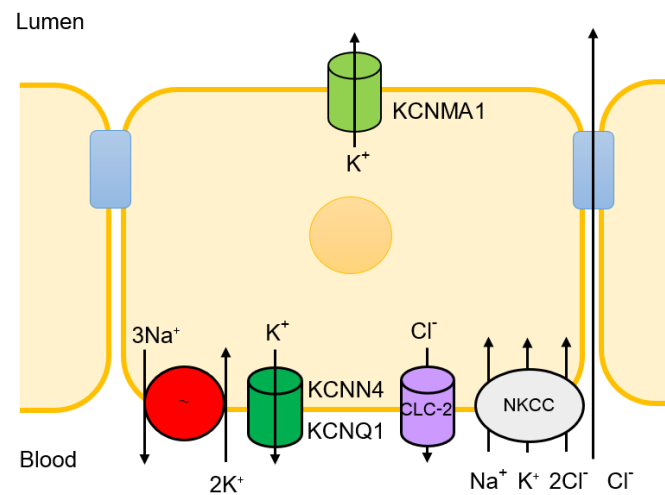


Figure 5 The model of  $K^+$  secretion in the distal colonic epithelium. Adapted from Rao.<sup>(62)</sup>

## 2.4 Colonic transport proteins and regulation

### 2.4.1 Channels

#### A. The amiloride-sensitive epithelial sodium channel (ENaC)

ENaC facilitates the cell entry of  $Na^+$  from the luminal fluid in a variety of reabsorbing epithelia.<sup>(67)</sup> High expression of ENaC on the apical membranes of colonic epithelial cells<sup>(68)</sup> confirms a role in regulating fecal  $Na^+$  excretion contributing to  $Na^+$  homeostasis. ENaC has been extensively characterized in renal and airway epithelial models. ENaC is a multimeric protein composed of  $\alpha$ ,  $\beta$ , and  $\gamma$  subunits with  $NH_2$  and  $COOH$  termini (Figure 6).<sup>(69)</sup> It is relatively permeable to  $Na^+$ ,  $H^+$ , and  $Li^+$ .<sup>(70)</sup> Several glycosylated proteins in the extracellular loops of the receptors are hypothesized to facilitate ENaC function.

ENaC is crucial for the maintenance of  $Na^+$  and extracellular volume homeostasis. The rate-limiting step in electrogenic  $Na^+$  absorption is ENaC uptake into colonocytes.<sup>(71)</sup> ENaC is controlled by various hormones including aldosterone and is inhibited by amiloride and its analogs. Amiloride, a diuretic, has a high sensitivity to these channels. Aldosterone normally stimulates the channel by increasing the number

of apical membrane channels synthesized via exocytosis of intracellular vesicles.<sup>(2, 72)</sup> Corticosteroids also stimulate ENaC in the colon by increasing transcription of the  $\alpha$  and  $\beta$  subunits. Mutations that result in an increased function cause an increase in extracellular volume, whereas mutations that result in a decreased function may result in salt-wasting conditions characterized by alterations in  $K^+$  balance.

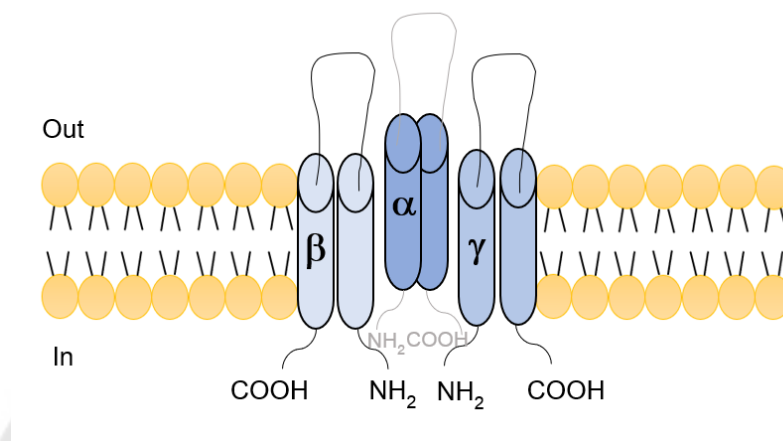


Figure 6 The structure of ENaC comprises  $\alpha$ ,  $\beta$ , and  $\gamma$  subunits containing cytoplasmic  $NH_2$  and  $COOH$  termini. Adapted from Warnock.<sup>(69)</sup>

### B. Apical chloride channels

- **The cystic fibrosis transmembrane conductance regulator (CFTR)**

CFTR, a  $Cl^-$  channel activated by cAMP, was first cloned by Riordan and a coworker in 1989.<sup>(73)</sup> In cystic fibrosis, over 900 different mutations in the CFTR gene result in decreased  $Cl^-$  and  $Na^+$  transport and impaired secretion or absorption of electrolytes.<sup>(74)</sup> CFTR is predominantly localized at the apical membrane of epithelial cells, and it is recycled constitutively between subapical vesicles and the plasma membrane.<sup>(75)</sup> CFTR is expressed in the stomach, pancreas, hepatobiliary ducts, and intestine.

The channel is implanted as dimers in the apical membrane, where their 12 transmembrane domains form the pore for  $Cl^-$  secretion.<sup>(76)</sup> CFTR is unique among ATP-binding cassette protein that is known to function as an ion channel. CFTR

comprises highly glycosylated membrane proteins with two remarkable homologous motifs (figure 7).<sup>(77)</sup> Each motif consists of a hexa-helical membrane-spanning domain (MSD1: TM1-6 and MSD2: TM7-12) and a nucleotide-binding domain (NBD1 and NBD2, separately). The regulatory (R) domain which divides the two motifs contains protein consensus sequences mostly by PKA phosphorylation as well as PKGII phosphorylation. Both N- and C-termini are in the cytoplasm and can interact with cooperated signaling and anchoring proteins.<sup>(78)</sup>

Cl<sup>-</sup> and other anions, especially HCO<sub>3</sub><sup>-</sup>, are mainly transported by CFTR. Cl<sup>-</sup> secretion through CFTR can be regulated by PKA phosphorylation of the regulatory R domain and ATP binding to and dimerization of the NBDs. Even though two NBDs contain many ATPase sites, only one in the NBD2 can catalyze ATP hydrolysis. This hydrolysis of ATP does not contribute to the energy supply of the transport process, but it is required for CFTR gating. The presence of ATP activates the phosphorylated form of CFTR, comparable to a ligand-gated channel.<sup>(62)</sup> PKA stimulates CFTR in most tissues and intestines, while PKGII, PKC, and Ca<sup>2+</sup>/Ca<sup>2+</sup>-calmodulin activate CFTR in the intestine. Ca<sup>2+</sup> appears to activate CFTR indirectly through activating K<sup>+</sup> channels. Both PKA and cGMP increase CFTR activity in intestinal cell lines and native tissues by modifying the open probability of the channel and increasing the existence of channels at the apical membrane.<sup>(35, 75, 79, 80)</sup> Additionally, cAMP- and Ca<sup>2+</sup>-activated Cl<sup>-</sup> secretion are most likely due to the influence of endogenous secretagogues such as prostaglandins, vasoactive intestinal polypeptide (VIP), acetylcholine (ACh), histamine, secretin, leukotrienes, serotonin, adenosine, and nitric oxide (NO).<sup>(68, 81)</sup> Conversely, the opening of the CFTR channel is inhibited by various CFTR inhibitors. For example, the sulphonylurea drugs, glibenclamide and diphenylamine-2-carboxylate, and 5-nitro-2-(3-phenylpropyl-amino)benzoate (NPPB) are widely used as CFTR inhibitors. These substances inhibit CFTR and other Cl<sup>-</sup> channels and transporters with IC<sub>50</sub> values commonly greater than 100 μM.<sup>(82)</sup> Other than that, selective inhibitor CFTRinh-172 has been applied for detecting CFTR currents in various cell types.<sup>(83)</sup> Therefore, these CFTR inhibitors were used to identify the effect of kaempferol through the CFTR channel.

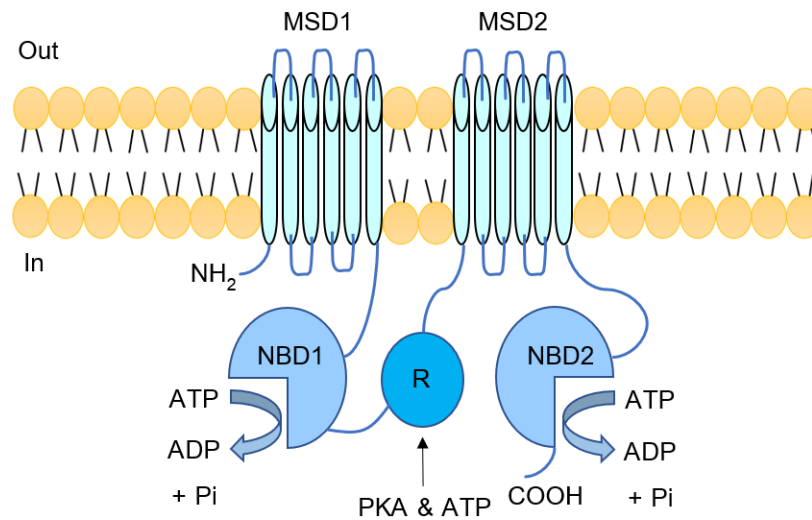


Figure 7 Structure of CFTR. Adapted from Sheppard and Welsh.<sup>(77)</sup>

- **Calcium-activated chloride channel (CaCC)**

CaCC is an anion-selective channel that is activated by increased cytosolic  $\text{Ca}^{2+}$ . CaCC was most likely initially detected in *Xenopus* oocytes about two decades ago<sup>(84)</sup> and has been found in epithelial cells, vascular endothelial cells, neurons, smooth and cardiac muscle cells.<sup>(85)</sup> CaCC activity is required to  $\text{Cl}^-$  secretion and other anions, such as  $\text{HCO}_3^-$ , in epithelial cells.<sup>(86)</sup> The newly identified CaCC, anoctamin 1 (TMEM16A; Ano1), has been discovered in the basolateral membrane rather than the apical membrane of adult intestinal epithelial cells.<sup>(87-92)</sup>

The TMEM16A protein is one of ten anoctamin family members, including proteins with eight transmembrane segments and projecting N- and C-termini into the intracellular medium.<sup>(93)</sup> Recent cryo-electron microscopy structures of TMEM16A in the unbound and  $\text{Ca}^{2+}$ -bound states demonstrate that  $\text{Ca}^{2+}$  interacts directly with the pore.<sup>(94, 95)</sup> These are functionally outward rectifying channels that are inhibited by niflumic acid (NFA), 4,4-diisothiocyano-2,2-stilbenedisulfonic acid (DIDS),

Ca<sup>2+</sup>-activated Cl<sup>-</sup> channel inhibitor (CaCCinh-A01),<sup>(96)</sup> and activated by Ca<sup>2+</sup>/Ca<sup>2+</sup>-calmodulin kinase II (CaMKII) (Figure 8).<sup>(97)</sup>

CaCC is induced in the apical membrane of airway epithelia by application of calcium ionophores, ATP and UTP.<sup>(98-101)</sup> NFA does not prevent carbachol-stimulated Cl<sup>-</sup> secretion, and apical ATP and UTP only evoke transient K<sup>+</sup> secretion in the colon.<sup>(102)</sup> There has been evidence of coordinated regulation of CaCC and CFTR. For example, TMEM16A knockout animals lack Ca<sup>2+</sup>-activated Cl<sup>-</sup> secretion. In CFTR knockout mice, carbachol fails to stimulate Cl<sup>-</sup> secretion but does affect changes in cell volume. It has been suggested that the TMEM16A located in the basolateral membrane regulates cell volume while they are engaged in secretion when present in the apical membrane.<sup>(103, 104)</sup>

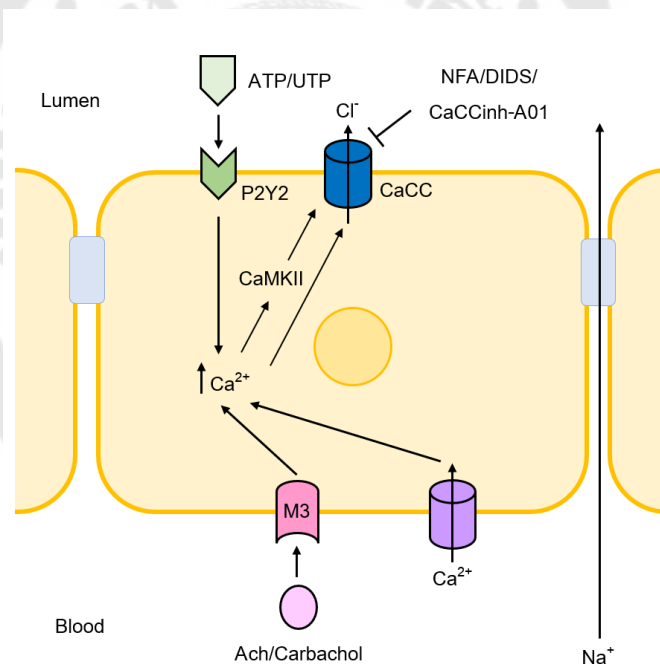


Figure 8 Cellular roles of CaCC. Adapted from De La Fuente and co-worker.<sup>(97)</sup>

### C. Apical potassium channel

- Calcium-activated potassium channel subunit alpha-1 (KCNMA1 channel)

The KCNMA1 channel (also known as BK or MaxiK) is the primary  $K^+$  channel responsible for  $K^+$  secretion in rat and mouse colons. It is the only  $K^+$  channel found in the apical membrane of human colonic epithelial cells.<sup>(105)</sup> However, this does not contribute to the driving force for  $Cl^-$  secretion.<sup>(106)</sup> The KCNMA1 channel has a tetrameric structure with two subunits:  $\alpha$  subunit, which forms the pore and contains voltage and  $Ca^{2+}$ -sensing domains, and  $\beta$  subunit (1-4), which modulates the voltage and  $Ca^{2+}$ -sensing domains of the  $\alpha$  subunit.

The KCNMA1 channel is under the control of secondary hyperaldosteronism, dietary  $K^+$  influx, cAMP, and  $Ca^{2+}$ . Colonic  $K^+$  channels are peculiar in that they are only sensitive to mineralocorticoids and not to glucocorticoids. The action of aldosterone in raising both  $K^+$  secretion and  $K^+$  absorption can counterbalance each other. The regulation of numerous  $K^+$  channels may involve temporal separation of signaling,<sup>(107)</sup> structural compartmentalization via scaffolding proteins, or functional compartmentalization, as demonstrated by the role of PDEs in inhibiting the release of paracrine modulators such as ATP or preventing cAMP distribution.<sup>(108-110)</sup> Furthermore, carbachol has been shown to promote  $K^+$  secretion.<sup>(111)</sup> Ussing chamber experiments with the human rectal mucosa found a cholinergic regulation of apical  $K^+$  conductance. On the other hand, tetraethylammonium, iberiotoxin, paxilline, and quinidine were shown to inhibit the KCNMA1 channels.<sup>(1)</sup>

### D. Basolateral potassium channels

$K^+$  channels located at the basolateral membrane functions to hyperpolarize membrane potential and provide the electrical driving force for  $Cl^-$  secretion and  $Na^+$  absorption. Two main types of  $K^+$  channels that determine basolateral  $K^+$  conductance in the mammalian colon are controlled by intracellular  $Ca^{2+}$  and cAMP.<sup>(81, 112-114)</sup>



- **Basolateral cAMP-activated K<sup>+</sup> channels**

The KCNQ1/KCNE channel (also known as KVLQT1) is a basolateral K<sup>+</sup> channel that is triggered by elevated intracellular cAMP.<sup>(81, 115, 116)</sup> As previously proven for the rat and rabbit colon, the chromanol compound 293B explicitly inhibits this type of K<sup>+</sup> channel.<sup>(115, 116)</sup> The KCNQ1 channel is composed of 12  $\alpha$  subunits. The conducting  $\alpha$ KCNQ1 subunit must interact with the regulatory  $\beta$ KCNE (1-5) subunits at physiological pH to form the K<sup>+</sup> channel pore. On the basolateral and apical membranes of the intestine, high levels of expression of KCNQ1/KCNE1 and KCNQ1/KCNE3 have been observed, respectively.<sup>(62)</sup> Although the function of cAMP-sensitive K<sup>+</sup> channels is known in the rat and mouse colons and possibly in T84 cells, the role of cAMP in human colonic crypts is less clear.

- **Basolateral Ca<sup>2+</sup>-activated K<sup>+</sup> channels**

The KCNN4 channel, also called KCa3.1, is the essential basolateral K<sup>+</sup> channel to keep the hyperpolarized driving force required for Cl<sup>-</sup> secretion. KCNN4 channels are found in the basolateral and apical membranes of T84 cells, rats, mice, and the human colon.<sup>(117)</sup> The channels show differential splice variant expression. For example, KCNN4a and b have six transmembrane domains expressed in smooth muscle and the basolateral membrane of the small intestine, respectively. In contrast, KCNN4c only has five transmembrane domains and functions as an apical channel. The channel is regulated by Ca<sup>2+</sup>, calmodulin and cAMP.<sup>(106)</sup> 1-ethyl-2-benzimidazolone (1-EBIO) activates this K<sup>+</sup> channel.<sup>(118, 119)</sup> In patch-clamp experiments, the channel can be inhibited by imidazole compounds such as NS004 and the anti-fungal drug clotrimazole.<sup>(120)</sup> Similarly, clotrimazole significantly decreased Cl<sup>-</sup> secretion activated by high levels of intracellular Ca<sup>2+</sup>, cAMP, or cGMP in T84 cells and the colonic mucosa of mice and rabbits.<sup>(121)</sup>

## 2.4.2 Exchangers

### A. Sodium-proton exchanger (NHE)

The  $\text{Na}^+/\text{H}^+$  exchanger is secondary active transporter that employs the  $\text{Na}^+$  gradient to exchange extracellular  $\text{Na}^+$  for intracellular  $\text{H}^+$ . Three distinct NHE subtypes have been identified in the colonic epithelium thus far. NHE1 is expressed in the basolateral membrane and does not affect the depletion of  $\text{Na}^+$ . Both NHE2 and NHE3 are expressed on the apical membrane of colonic epithelial cells, with NHE3 contributing significantly more to  $\text{Na}^+$  absorption under control conditions.<sup>(122)</sup>

Nine members of the NHE family have 12 transmembrane helices and intracellular N-terminal and C-terminal domains. The C termini include many protein kinase consensus sequences and serve as the loci for complicated regulation.<sup>(123)</sup> NHE2 and NHE3 are differentially expressed by having higher expression in the proximal colon and lower expression in the distal colon<sup>(122, 124)</sup>; moreover, a new third kind of  $\text{Cl}^-$ -dependent NHE has been discovered in the apical membranes of rat crypt cells.<sup>(125)</sup> This exchanger can be stimulated when plasma aldosterone levels rise in response to a sodium deficiency.<sup>(126)</sup>

### B. Chloride-bicarbonate exchanger (DRA)

The  $\text{Cl}^-/\text{HCO}_3^-$  exchanger, also known as downregulated in adenoma (DRA), is derived from the SLC26A3 gene which was initially identified as the DRA gene.<sup>(127)</sup> This protein is predicted to contain ten to twelve transmembrane spanning membrane lipids with cytoplasmic N and C termini, all of which are essential for its activity and regulation. DRA is mainly found in the apical membrane of surface colonocytes, the duodenal lower villus region, and the ileum.<sup>(128-130)</sup> The  $\text{Cl}^-/\text{HCO}_3^-$  exchanger works to move  $\text{HCO}_3^-$  into the cell in exchange with  $\text{Cl}^-$ . Meanwhile, the  $\text{Na}^+/\text{H}^+$  exchanger NHE3 functions simultaneously with the apical  $\text{Cl}^-/\text{HCO}_3^-$  exchanger and is thus required for  $\text{Na}^+$  and  $\text{Cl}^-$  electroneutral absorption.<sup>(131)</sup>

Most of the research on  $\text{Cl}^-/\text{HCO}_3^-$  exchange regulation has been on activity measurements, which have been validated in some cases by measurements of transporter protein modulation. In conclusion,  $\text{Cl}^-/\text{HCO}_3^-$  exchange function is induced by glucocorticoids, neuropeptide Y, lysophosphatidic acid, and sphingosine-1

phosphate, and reduced by pro-inflammatory cytokines and these substances that stimulate the production of intracellular  $\text{Ca}^{2+}$ , cAMP, and cGMP.<sup>(132-135)</sup>

### 2.4.3 Cotransporter

#### A. Sodium-potassium-chloride cotransporter (NKCC)

The  $\text{Na}^+2\text{Cl}^-K^+$  cotransporter is a secondary active transporter that transports  $1\text{Na}^+ : 1\text{K}^+ : 2\text{Cl}^-$  into and out of cells in a coupled manner. The NKCC family comprises two isoforms, namely NKCC1 and NKCC2.<sup>(136)</sup> NKCC1 is found throughout the body and essential for cell volume control, ion homeostasis, and  $\text{Cl}^-$  secretion. In the secretory epithelia of the colon, NKCC1 is located on the basolateral membrane and inhibited by furosemide and bumetanide. However, azosemide inhibits its activity more effectively.<sup>(137)</sup> NKCC2 is predominantly expressed in the apical membrane of the thick ascending limb of the loop of Henle and the macula densa.<sup>(136)</sup>

NKCCs have N-linked glycosylation sites between transmembrane segments with N- and C-terminus. The N-terminus comprises the phosphothreonine sites necessary for NKCC1 activity.<sup>(136)</sup> NKCC1 is regulated in several ways, including cAMP-induced increases in cell surface expression, PKA-mediated direct phosphorylation, or regulation by additional protein kinases and phosphatases.<sup>(138, 139)</sup> Simultaneous stimulation of NKCC1 and ion channels is required for the control of  $\text{Cl}^-$  secretion through apical CFTR channels. cAMP and  $\text{Ca}^{2+}$  may stimulate NKCC indirectly by activating  $\text{Cl}^-$  and  $\text{K}^+$  channels, respectively. Moreover, reduced intracellular  $\text{Cl}^-$  and cellular volume enhance the phosphorylation and activity of NKCC.

## 2.5 Signaling pathway regulation of colonic ion transport

### 2.5.1 Cyclic adenosine monophosphate signaling pathway

The primary regulation of colonic ion transport is neurohumoral stimulation of cyclic adenosine monophosphate (cAMP). cAMP is known to influence the activity of protein kinase, which is one of the mechanisms involved in controlling cell function.<sup>(140)</sup> The increased intracellular cAMP  $[\text{cAMP}]_i$  can activate transepithelial  $\text{Cl}^-$  secretion.

Multiple external stimuli that bind to membrane receptors activate this second messenger cascades. The binding of cAMP stimulators (e.g., vasoactive intestinal peptide, prostaglandin) to specific membrane G-protein coupled receptors (GPCRs) triggers  $G\alpha_s$  to stimulate transmembrane adenylate cyclase (tmAC). The tmAC localized to the basolateral membrane of epithelial cells converts adenosine triphosphate (ATP) to cAMP.<sup>(9)</sup> Besides, cAMP being generated by soluble AC (sAC) is found in the cytosol and mitochondria activated by  $Ca^{2+}$  and  $HCO_3^-$ .<sup>(141)</sup> Both the tmAC and sAC are present in the colonic epithelia.<sup>(142)</sup>

Several previous reports show that CFTR mediated  $Cl^-$  secretion are activated by protein kinases A (PKA)-dependent phosphorylation and binding of ATP.<sup>(10, 11)</sup> This phosphorylation of transport proteins increases CFTR channels or decreases the function of DRA/PAT-1 or NHE3 antiporters when cAMP levels rise. The PKA-dependent phosphorylation of CFTR channels occurs mainly in the R domain.<sup>(143, 144)</sup> The access of PKA to the numerous consensus sites, including serine and threonine phosphorylation sites in the R domain, determines the open probability of the CFTR channels.<sup>(143)</sup> For this reason, the cAMP signaling pathway stimulation leads to increase  $Cl^-$  secretion. However, cAMP can be made to have different effects in different parts of the cell by attaching to special proteins called scaffolding proteins such as A-Kinase Anchoring Protein (AKAP).<sup>(62)</sup> Additionally, cAMP works via the guanine nucleotide exchange factor, Epac, which stimulates phospholipase C (PLC) via RAP2. The cAMP-Epac pathway is hypothesized to be signalling crosstalk between cAMP and  $Ca^{2+}$  in the intestine that has not been discovered (figure 9).<sup>(62)</sup> Furthermore, the regulation of colonic ion transport involved by stimulation of cAMP can be studied using cAMP activators. For example, forskolin is an activator of adenylate cyclase that increases the synthesis of intracellular cAMP used for investigating the role of cAMP in the opening of CFTR or other cellular processes of the gastrointestinal tract.<sup>(145)</sup> 8cpt-cAMP is a selective activator of cAMP-dependent PKA.<sup>(146)</sup>

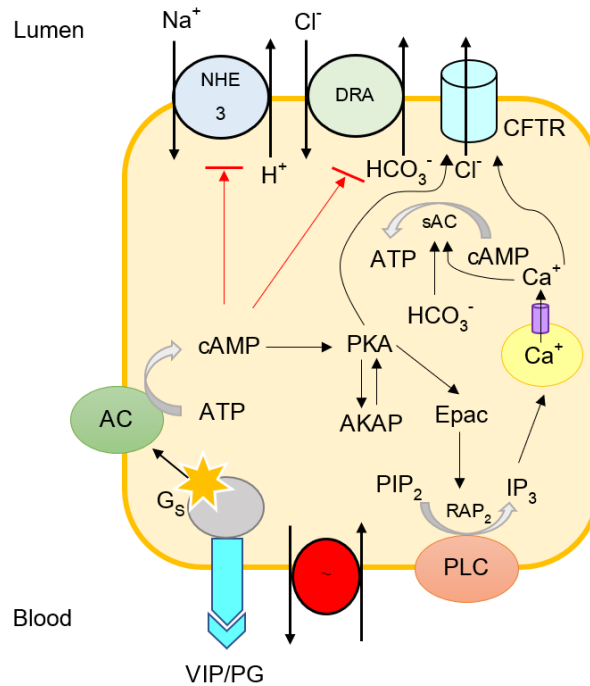


Figure 9 cAMP signaling pathways in the colonic epithelium stimulated by VIP or PG. Adapted from Rao.<sup>(62)</sup>

### 2.5.2 Calcium signaling pathway

Intracellular  $\text{Ca}^{2+}$  [ $\text{Ca}^{2+}$ ]<sub>i</sub> has a multiplicity effect on the colonic epithelium. The effects of activation of muscarinic M3 receptors on [ $\text{Ca}^{2+}$ ]<sub>i</sub> levels and  $\text{Ca}^{2+}$  conductance have been investigated in considerable detail. The receptors responsible for acetylcholine receptor-mediated  $\text{Cl}^-$  secretion in rat colonic epithelium belong to the M3 class.<sup>(15, 16)</sup> Acetylcholine or carbachol, classified as a cholinergic agonist, can bind to GPCRs via muscarinic M3 to stimulate  $\text{G}\alpha_q$ , whereas substance P stimulates  $\text{Ca}^{2+}$  channels (figure 10). The activated  $\text{G}\alpha_q$  induces phospholipase C- $\beta$  (PLC) to hydrolyze phosphatidylinositol 4,5-bisphosphate ( $\text{PIP}_2$ ) and release diacylglycerol (DAG) and inositol 1,4,5-trisphosphate ( $\text{IP}_3$ ).  $\text{IP}_3$  binds to specific  $\text{IP}_3$  receptors ( $\text{IP}_3\text{R}$ ) and causes  $\text{Ca}^{2+}$  release from the endoplasmic reticulum (ER). The  $\text{IP}_3\text{R}$  binding proteins, the  $\text{Ca}^{2+}$ -release channel binding protein (IRBIT), compete with the  $\text{IP}_3$  receptor in their

phosphorylated state (IRBIT-P). IRBIT-Ps are established class of signaling molecules in regulating various ion transporters including CFTR, NHE3, and PAT-1.<sup>(17, 18)</sup>

The intracellular  $\text{Ca}^{2+}$  can either directly activate  $\text{Ca}^{2+}$  channels or indirectly via  $\text{Ca}^{2+}$ -calmodulin activate specific protein kinases (PKs) and phosphatases (PPs), and cytoskeletal proteins. DAG acts as  $\text{Ca}^{2+}$  to stimulate some isoforms of protein kinase C (PKC) (figure 10).<sup>(62)</sup> Numerous reports indicate the PKC activation of CFTR for apical  $\text{Cl}^-$  secretion in the colonic epithelium. Furthermore, the increased  $[\text{Ca}^{2+}]_i$  can stimulate basolateral  $\text{Ca}^{2+}$ -activated  $\text{K}^+$  channels leading to  $\text{Cl}^-$  secretion.<sup>(12, 147)</sup> In addition,  $[\text{Ca}^{2+}]_i$  induced activation of  $\text{Cl}^-$  secretion can be studied using  $\text{Ca}^{2+}$  ionophore A23187 to increase  $[\text{Ca}^{2+}]_i$  level.<sup>(148)</sup>

$\text{Ca}^{2+}$ -activated  $\text{Cl}^-$  channels (CaCC), recently identified as anoctamin 1 (TMEM16A; Ano1), are discovered in the basolateral membranes greater than apical membranes of adult colonic epithelial cells.<sup>(90, 104, 149)</sup> Additionally, it may be found in ER near the basolateral membrane. Ano1 modulates intracellular  $\text{Ca}^{2+}$  signaling in response to the activation of Gq-coupled receptors via the muscarinic M3 receptor. Moreover, Ano1 helps maintain the driving force produced by activating basolateral  $\text{Ca}^{2+}$ -activated  $\text{K}^+$  channels to promote  $\text{Ca}^{2+}$ -activated  $\text{Cl}^-$  secretion. There are two possible mechanisms of the function of the Ano1 protein. First, Ano1 may be found in the ER, which may increase the amount of  $\text{Ca}^{2+}$  released into the cell through  $\text{IP}_3$  receptors.<sup>(150, 151)</sup> Second, Ano1 may connect the ER to the cell membrane, which could help activate another basolateral  $\text{K}^+$  channel called KCNN4  $\text{K}^+$  channels.<sup>(152)</sup> Nevertheless, free  $[\text{Ca}^{2+}]_i$  is quickly removed from the cell by  $\text{Ca}^{2+}$ -dependent ATPases or  $\text{Na}^+/\text{Ca}^{2+}$  exchangers in the basolateral membrane or ER, and  $[\text{Ca}^{2+}]_i$  reserves are restored via transient receptor potential (TRP) channels.

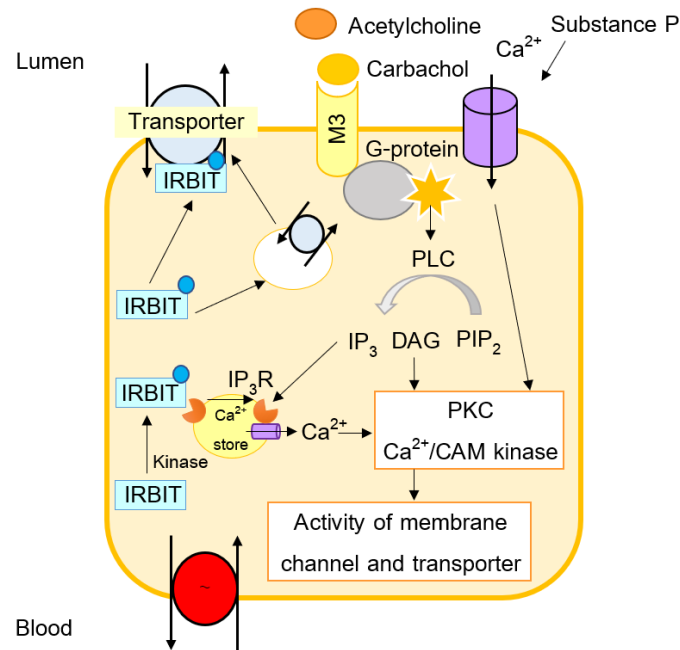


Figure 10  $\text{Ca}^{2+}$ -dependent signaling pathways in the colonic epithelium by acetylcholine, carbachol or substance P. Adapted from Rao.<sup>(62)</sup>

### 2.5.3 Cyclic guanosine monophosphate signaling pathway

Cyclic guanosine monophosphate (cGMP) can stimulate CFTR mediated  $\text{Cl}^-$  secretion through cGMP-regulated protein kinase G type II. Certain agents (e.g., GTP, guanosine triphosphate; STa, heat-stable enterotoxin) bind to membrane guanylate cyclase (mGC, also known as GUCY2C), which acts as both receptor and enzymatic activity, located only on the apical membrane of colonic epithelial cells.<sup>(153)</sup> When GUCY2C is activated, it produces cGMP from GTP. Meanwhile, activators like nitric oxide (NO) can be used to synthesize cGMP from soluble GC (sGC). cGMP activates an enzyme known as PKG2. This enzyme is attached to the cell membrane through the myristoylation process and can also be controlled by anchoring proteins, especially NHERF4. PKG2 phosphorylates target transport proteins similar to the way PKA works and then activates CFTR channels for  $\text{Cl}^-$  secretion. Additionally, nucleotide transporters can transport cGMP across the basolateral membrane, where it works on nociceptive nerve terminals to alleviate pain.<sup>(62)</sup> Furthermore, cGMP can inhibit specific

phosphodiesterase (PDE), leading to an increase in intracellular cAMP (figure 11).<sup>(62)</sup> cGMP-specific phosphodiesterase 5 (PDE5) is expressed in human colonic epithelial cells and appears to regulate intracellular cGMP concentrations.<sup>(154)</sup>

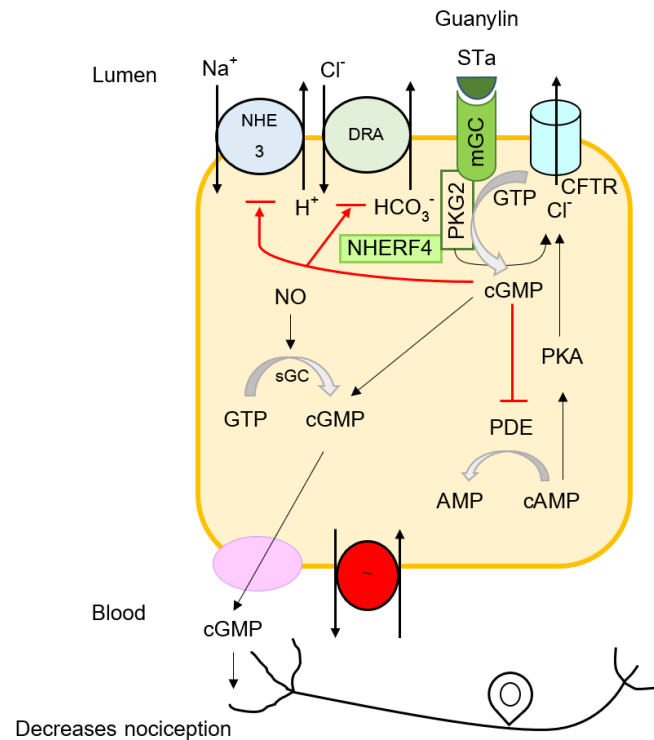


Figure 11 cGMP signaling pathways in the colonic epithelium. Adapted from Rao.<sup>(62)</sup>

#### 2.5.4 Tyrosine kinase and tyrosine phosphatase signaling pathways

Apart from the above, signaling pathways involving phosphorylation and dephosphorylation of tyrosine have been shown to regulate ion transport. The phosphorylated state of CFTR is controlled by both protein kinases and phosphatases. Many research investigations have shown that tyrosine kinases can influence the gating of CFTR either directly or indirectly. Direct tyrosine kinase regulation has been demonstrated through the exposure of membrane regions to a non-receptor tyrosine kinase<sup>(155)</sup> and the sensitivity of muscarinic activation of CFTR to tyrosine kinase inhibitors.<sup>(13)</sup> Indirect regulation has also been reported via a pathway that involves tyrosine phosphorylation, revealing a serine/threonine protein kinase phospho-acceptor



site in NBD1.<sup>(156, 157)</sup> In addition, tyrosine phosphorylation is a direct stimulus for CFTR activation that induce chloride currents in baby hamster kidney (BHK) cells, which are 80% as large as those activated by PKA. Thus, PKA-independent activation by tyrosine phosphorylation has implications for the functions of CFTR.<sup>(14)</sup> Meanwhile, tyrosine phosphatases are a broad enzyme family that catalyzes the removal of phosphate groups from tyrosine residues. Inhibition of tyrosine phosphatase by vanadate enhances the activity of the CFTR and stabilizes an open state of the CFTR chloride channel.<sup>(158, 159)</sup> However, the opening of the CFTR channel involved by tyrosine kinase and tyrosine phosphatase can be studied using inhibitors of tyrosine kinase and phosphatase. For example, tyrphostin A23 is a broad-spectrum protein tyrosine kinase inhibitor and functions by binding to the active sites of the enzymes.<sup>(160)</sup> AG490 is a selective inhibitor of tyrosine kinase that has been extensively used for inhibiting the JAK/STAT3 pathway in vitro and in vivo.<sup>(161)</sup> A report has shown that pretreatment with tyrphostin A23 or AG490 can reduce flavonoid genistein-stimulated  $I_{SC}$ .<sup>(162)</sup> Vanadate is an inhibitor of the protein tyrosine phosphatase used to maintain the tyrosyl phosphorylation state of proteins during experiments in the laboratory.<sup>(163)</sup>

## 2.6 Kaempferol

### 2.6.1 Structure & source

Kaempferol is a tetrahydroxyflavone composed of two phenyl rings (rings A and B) linked to a heterocyclic ring (ring C) and has the additional hydroxyl groups at positions 3, 5, 7, and 4' (figure 12). Kaempferol is a yellow crystalline solid with a molecular mass of 286.23 g/mol and a melting point of 276-278 °C; the structural formula is 15 carbon, 10 hydrogen, and 6 oxygen ( $C_{15}H_{10}O_6$ ). It is slightly dissolved in water but very soluble in hot ethanol, ethers, and dimethyl sulfoxide (DMSO).<sup>(164)</sup>

Kaempferol is a natural flavonol, a subclass of flavonoid, mostly found in edible plants, such as onion, grapefruit, strawberry, and lettuce, as well as medicinal plants such as *Acacia nilotica* (L), *Aloe vera* (L), *Crocus sativus* (L.) and *Ginkgo biloba* (L.).<sup>(165)</sup>

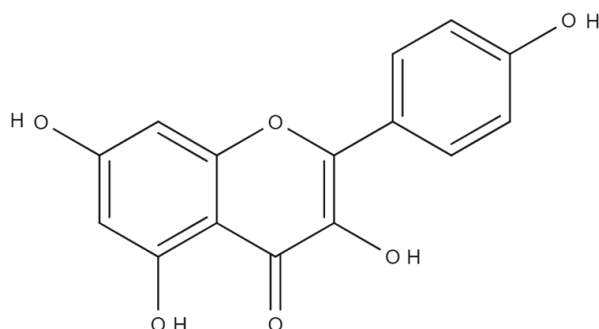


Figure 12 Structure of kaempferol

### 2.6.2 Bioavailability

The pharmacokinetic and pharmacodynamic properties of flavonol are studied both in vivo and in vitro experiments. Since kaempferol is a dietary flavonol that has therapeutic effects on various disorders, it must be effectively absorbed, distributed, metabolized, and eliminated in the human body. Kaempferol is often taken orally in the form of high and low-polarity glycosides. Glycosides with a high polarity show difficulty in absorption, whereas glycosides with a low polarity are readily absorbed. Kaempferol is a lipophilic compound that, like other flavonols, is absorbed through the small intestine via passive diffusion, facilitated diffusion, and active transport.<sup>(166)</sup> Additionally, intestinal enzymes metabolize flavonol kaempferol in the small intestine to flavonol-glucuronide. The normal floras of the colon metabolize the kaempferol glycoside to aglycones and subsequently to 4-methyl phenol, 4-hydroxyphenyl acetic acid, and phloroglucinol. Once being reabsorbed, kaempferol is metabolized in the liver by glucuronide conjugation and sulfate conjugation,<sup>(167-169)</sup> followed by absorption into the systemic circulation, distributed to different tissues, and finally eliminated via feces or urine (figure 13).<sup>(170-172)</sup> In a period of 24 hours, the body excretes an average of 1.9 percent of the kaempferol dosage.<sup>(173)</sup> Cao and colleagues have examined the bioavailability and pharmacokinetics of kaempferol in humans and revealed that a 14.97 mg/day dose of kaempferol resulted in a plasma concentration of 57.86 nM.

Additionally, 15 ug/L of kaempferol was detected in the blood after a daily intake of 27 mg of kaempferol from black tea containing 16 g of leaves brewed in one liter of boiling water.<sup>(174)</sup> Even though the amount of kaempferol that can be absorbed through the GI tract is remarkably small, it can still be effective for treating various diseases. For this reason, kaempferol might have therapeutic benefits even at low concentrations.

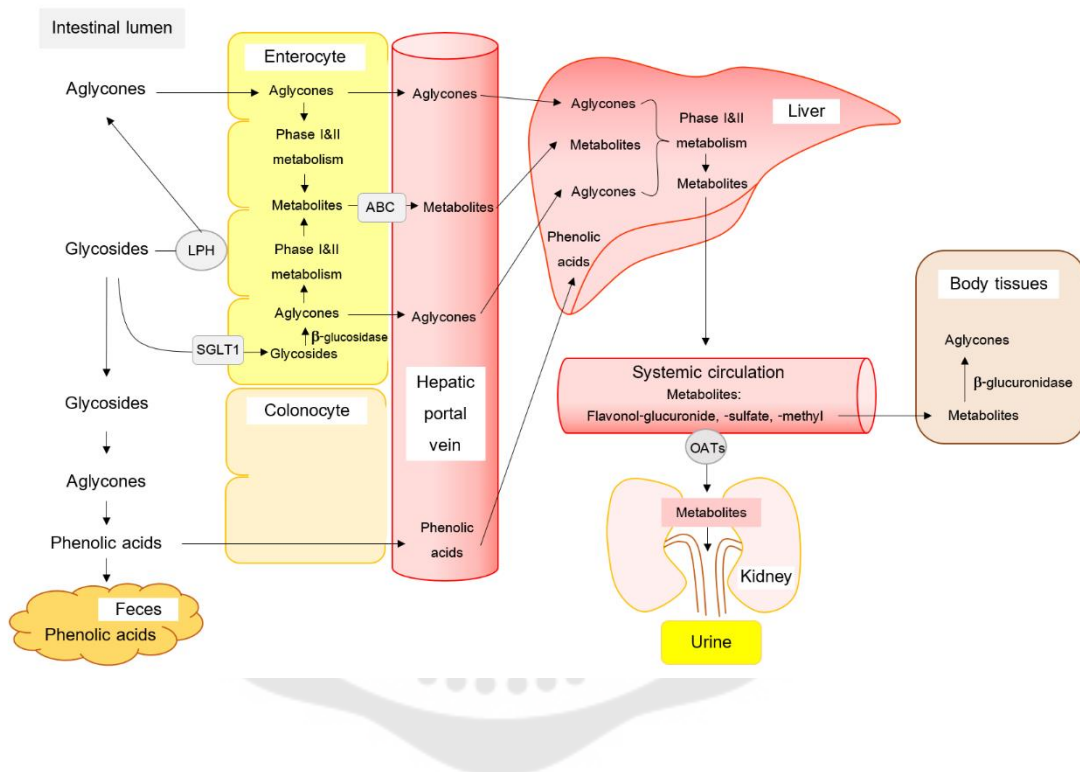


Figure 13 The bioavailability of dietary flavonol after the ingestion of aglycone and glycoside forms. Adapted from Dabeek and Marra.<sup>(172)</sup>

### 2.6.3 Biological action

#### Anti-cancer effects

Kaempferol has anti-cancer effects via several different mechanisms. Kaempferol is a potent promoter of apoptosis<sup>(175)</sup> and has been reported to stimulate host immunity, restrict tumor blood vessel formation, and enhance the sensitivity of other anti-cancer medications. Another anti-cancer mechanism of kaempferol involves increasing cellular DNA breakage.

#### Anti-inflammatory effects

Kaempferol decreases the levels of tumor necrosis factor (TNF- $\alpha$ ) and interleukin-1 (IL-1) induced by lipopolysaccharide (LPS) by increasing the number of activated macrophages and facilitating the nuclear translocation of NF- $\kappa$ B p65.<sup>(176)</sup> As inflammation can be defined as acute or chronic, the many categories of inflammatory disorders are studied separately to understand better the role of kaempferol in inflammatory disorders (figure 14).<sup>(177)</sup>

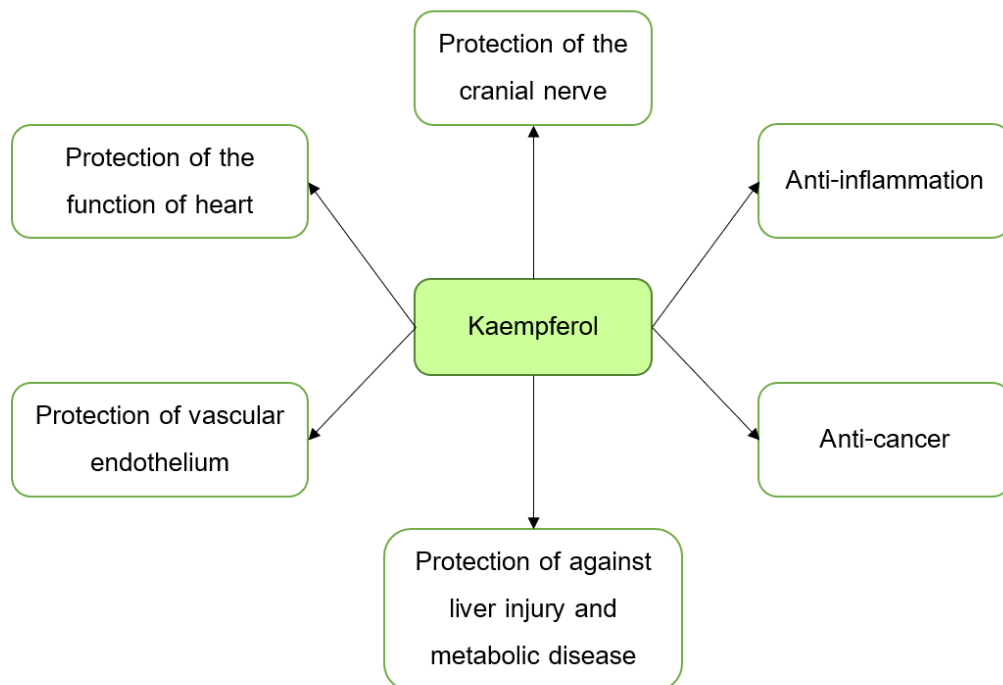


Figure 14 Therapeutic effects of kaempferol on a variety of disorders. Adapted from Ren and co-worker.<sup>(177)</sup>

### Transport-related effects

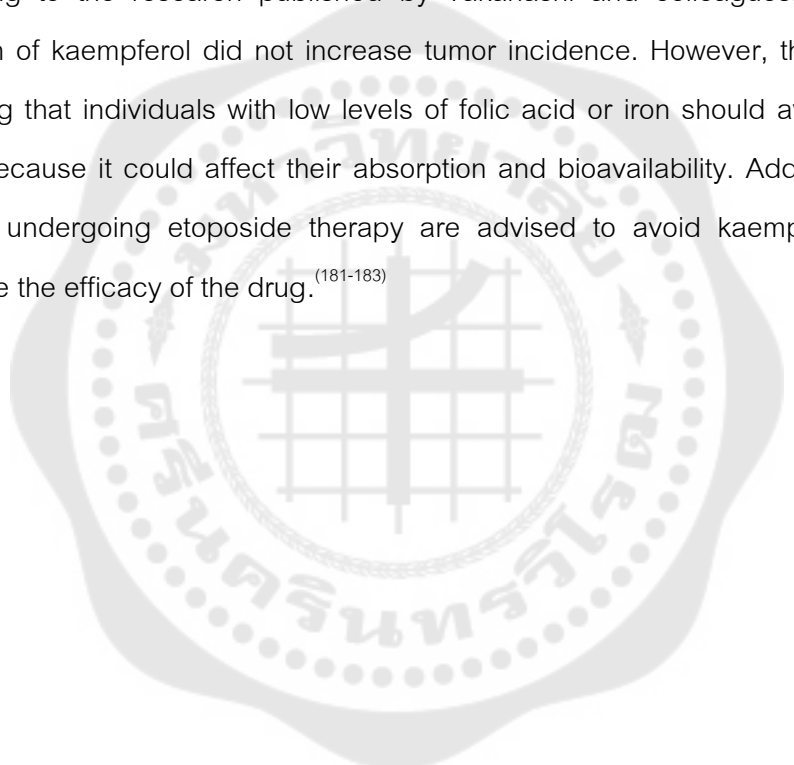
Previous study has established that the most prevalent flavonol, quercetin, promotes  $\text{Cl}^-$  secretion in rat small and large intestines as shown by an increase in short-circuit current ( $I_{\text{SC}}$ ) in Ussing experiment<sup>(27)</sup> and activates the basolateral  $\text{K}^+$  channel in rat distal colonic mucosa.<sup>(28)</sup> Additionally, quercetin induces the release of  $\text{Cl}^-$  via the CaCC in human colon cancer cells and increases  $I_{\text{SC}}$  in mouse intestinal tissue by increasing calcium concentration via the L-type calcium channel and activating basolateral NKCC,  $\text{Na}^+/\text{K}^+$ -ATPase, and  $\text{K}^+$  channels.<sup>(29)</sup>

According to one investigation, kaempferol can induce electrogenic  $\text{Cl}^-$  secretion on the colonic epithelium (T84); however, the effect of kaempferol is less potent than quercetin under basal conditions.<sup>(32)</sup> On the other hand, kaempferol had the greatest influence on  $\text{Cl}^-$  secretion in human airway epithelium, followed by apigenin, quercetin, and genistein. From this study, kaempferol has the highest potency of all flavonoids studied, as seen by its considerable effect on current. Interestingly, the mechanism of action of flavonoids relies on the degree to which forskolin stimulates the cAMP-PKA pathway.<sup>(33)</sup> However, the effects of kaempferol on the permeabilized monolayer condition and cellular mechanisms of action on regulating ion transport in human colonic epithelial cells are unknown.

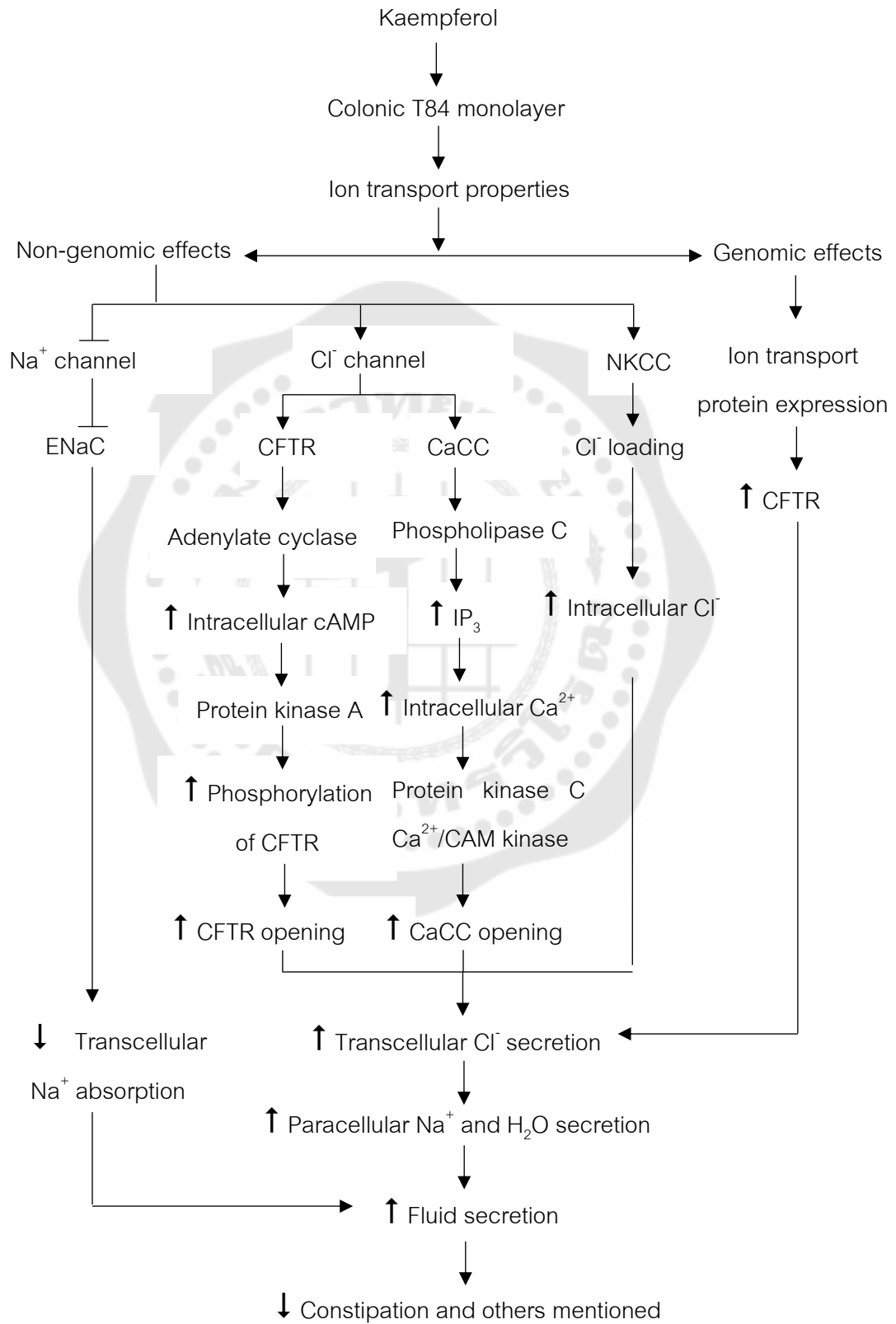
#### 2.6.4 Kaempferol safety

Different studies have shown contradictory findings regarding the safety and toxicity of kaempferol. Some studies claim that kaempferol is antimutagenic, whereas others believe it is genotoxic.<sup>(178)</sup> Although kaempferol exhibits antioxidant properties, it is also capable of acting to be a pro-oxidant. This pro-oxidant action may have an effect on genotoxicity.<sup>(179)</sup> By contributing a hydrogen atom, flavonoids neutralize free radicals and generate a phenoxyl radical. An interaction between the phenoxyl radical and the second radical leads to the formation of an antioxidant substance. However, a pro-oxidant is formed when the phenoxyl radical combines with oxygen species.<sup>(180)</sup>

Additionally, the pro-oxidant decreases copper and iron which are required for lipid peroxidation and hydroxyl radical production. The ability of kaempferol to act as a pro-oxidant has been shown to contribute to alterations in the levels and activities of enzymes with both antioxidant and pro-oxidant properties.<sup>(180)</sup> The DNA mutations caused by kaempferol can be the result of the genotoxic metabolite of kaempferol metabolism. The enzyme CYP 1A1 has been shown to be essential for this transformation. Kaempferol is carcinogenic and poisonous in vitro but not in vivo. According to the research published by Takanashi and colleagues, long-term oral ingestion of kaempferol did not increase tumor incidence. However, there are reports indicating that individuals with low levels of folic acid or iron should avoid kaempferol intake because it could affect their absorption and bioavailability. Additionally, cancer patients undergoing etoposide therapy are advised to avoid kaempferol as it can decrease the efficacy of the drug.<sup>(181-183)</sup>



### Conceptual framework



## CHAPTER 3

### RESEARCH METHODOLOGY

#### 3.1 Cell line

Human colonic adenocarcinoma cell line (T84) passage 56 purchased from American Type Culture Collection (Manassas, VA, USA) was used in this study. T84 cells are derived from a lung metastasis of colon carcinoma in a 72-year-old male. The T84 cell line has been extensively used as a model for studying transepithelial chloride transport, CFTR channel characteristics, and functional epithelial barriers.<sup>(34, 184)</sup> After being cultured, T84 cells developed the characteristics of colonic crypt epithelial cells, including the ability for vectorial electrolyte transport.<sup>(185)</sup> At confluence, these cells can form a monolayer which shows characteristics of mature absorptive epithelial cells in both structure and function. The transepithelial electrical resistance (TEER) is frequently used to evaluate the monolayer integrity after two to three weeks of maturation.<sup>(186-189)</sup>

The differentiated phenotype of T84 cells was characterized by the development of a polarized columnar structure, the formation of tight junctions, and the formation of microvilli protruded apical brush border.<sup>(188)</sup> Several previous studies have demonstrated that the cells are controlled by various hormones and neurotransmitters. In T84 cells, cAMP, cGMP, and calcium-related stimuli are three main categories that operate via distinct second messenger pathways. cAMP is a crucial second messenger that stimulates chloride secretion. Different stimuli, including vasoactive intestinal peptide (VIP), cholera toxin, and experimental compounds such as forskolin, activate adenylate cyclase resulting in an increase in intracellular cAMP and chloride secretion in T84 cells<sup>(190, 191)</sup>. Likewise, the heat-stable enterotoxin of *E. coli* and STa activate chloride secretion through an accumulation of cGMP by guanylyl cyclase<sup>(192)</sup>. Moreover, substances including carbachol and calcium ionophores can stimulate chloride secretion by increasing the level of free cytosolic calcium ( $[Ca^{2+}]_i$ )<sup>(191, 193)</sup>.

T84 cells can express colonocyte-specific enzymes, including colonocyte markers membrane spanning 4-domains A12 (*MS4A12*) and monocarboxylate transporter 1 (*MCT1* or *SLC16A1*)<sup>(34)</sup>. T84 cells also express  $Na^+/K^+$  ATPase,  $H^+/K^+$



ATPase,  $\text{Na}^+/\text{H}^+$  exchange,  $\text{Na}^+/\text{K}^+/\text{Cl}^-$  cotransport, and apical  $\text{Cl}^-$  channels necessary for ion transport process.<sup>(184)</sup> For this reason, the T84 monolayer is a well-established *in vitro* model system of the human colonic epithelium which is suitable for studying electrolyte transport pathways, particularly the chloride secretory mechanism.



### 3.2 Materials and reagents

Table 1 Materials and reagents

No.	Materials and reagents	Manufacturers
1.	30% Acrylamide/Bis-acrylamide	Bio-Rad, USA
2.	AG490	Sigma-Aldrich, USA
3.	Amiloride	Sigma-Aldrich, USA
4.	Amphotericin B	Sigma-Aldrich, USA
5.	Bicinchoninic acid assay (BCA assay)	Visual Protein, Taiwan
6.	Bumetanide	Sigma-Aldrich, USA
7.	Calcium-activated chloride channel inhibitor (CaCCinh)	Sigma-Aldrich, USA
8.	Ca <sup>2+</sup> ionophore A23187	Sigma-Aldrich, USA
9.	CFTRinh-172 (inh-172)	Sigma-Aldrich, USA
10.	8-(4-Chlorophenylthio)-adenosine-3',5' -cyclic monophosphate (8-CPT-cAMP)	Sigma-Aldrich, USA
11.	Corning® 100 mm culture dish	Corning, USA
12.	Corning® 60 mm culture dish	Corning, USA
13.	Corning® 96-well plate	Corning, USA
14.	Corning® 48-well plate	Corning, USA
15.	4,4'-Diisothiocyanatostilbene-2,2'-disulfonate (DIDS)	Sigma-Aldrich, USA
16.	Dimethyl sulfoxide (DMSO)	Sigma-Aldrich, USA
17.	Dulbecco's Modified Eagle's Medium (DMEM)	Gibco, USA
18.	Enhanced chemiluminescence (ECL)	Santa Cruz Biotechnology, USA
19.	ECL film	GE Healthcare, USA
20.	Forskolin	Sigma-Aldrich, USA
21.	Fetal bovine serum	Gibco, USA

Table 1 (continued)

No.	Materials and reagents	Manufacturers
22.	Glibenclamide	Sigma-Aldrich, USA
23.	H-89	Sigma-Aldrich, USA
24.	Horseradish peroxidase-conjugated goat anti-mouse IgG secondary antibody	Santa Cruz Biotechnology, USA
25.	Kaempferol	Sigma-Aldrich, USA
26.	Methanesulfonic acid	Sigma-Aldrich, USA
27.	Mouse monoclonal anti- $\beta$ -actin primary antibody	Santa Cruz Biotechnology, USA
28.	Mouse monoclonal anti-CFTR primary antibody	Santa Cruz Biotechnology, USA
29.	5-Nitro-2-(3-phenylpropylamino)benzoic acid (NPPB)	Sigma-Aldrich, USA
30.	Non-essential amino acid	Gibco, USA
31.	Penicillin-Streptomycin	Merck, Germany
32.	Phosphate Buffered Saline (PBS)	Gibco, USA
33.	Polyvinylidene difluoride (PVDF) membrane	Millipore, USA
34.	Snapwell™ insert with 0.4 $\mu$ m pore polycarbonate membrane	Corning, USA
35.	0.25% Trypsin/EDTA	Corning, USA
36.	Tyrphostin A23	Corning, USA
37.	Vanadate	Corning, USA

### 3.3 Experimental procedures

#### 3.3.1 Cell culture

T84 cells were cultured in a 1: 1 mixture of Dulbecco's modified Eagle's medium with 4.5 g/L of D-glucose and Ham's F12 Nutrient mixture (Gibco, USA) containing 5% fetal bovine serum (Gibco, USA), 100 U/mL penicillin, and 100 mg/L streptomycin (Merck, Germany). The cells were grown in a 100 mm culture dish and maintained in an incubator at 37° C with 5% CO<sub>2</sub> in air. Culture media was changed every other day. The cells at 80% confluence were dissociated with 0.05% trypsin-EDTA every 6-7 days and seeded into suitable cell culture vessels for experiments. For electrophysiological studies, the cells were seeded into the Snapwell insert with 0.4 µm pore polycarbonate membrane at 3x10<sup>5</sup> cells/well. Culture media were changed every other day until the cells formed complete monolayer within 10-14 days. Transepithelial electrical resistance (TEER) was measured by Millicell ERS-2 volt-ohm meter coupled to Ag/AgCl electrodes (EMD Millipore Corporation, USA) to determine the membrane integrity. The monolayer with a TEER of 1,500-3,000 Ω.cm<sup>2</sup> was selected for experiments. Besides, the cells were seeded into a 48-well plate for cytotoxicity assay, or a 60 mm culture dish for western blot analysis. Culture medium was changed every other day until the day of the experiment.

#### 3.3.2 Cytotoxicity assay

The MTT colorimetric assay was used to determine the cytotoxicity of kaempferol. It is based on the ability of NAD(P)H-dependent oxidoreductase enzymes to reduce a yellow tetrazolium salt (MTT) to purple formazan crystals. Thus, this assay was applied to quantify cell viability in terms of reductive activity, which is defined as the enzymatic reduction of the tetrazolium molecule to insoluble formazan crystals by dehydrogenases found in the mitochondria of living cells<sup>(194)</sup>. T84 cells were seeded into a 48-well plate at a density of 1x10<sup>5</sup> cells/well and cultured for 7 days in a humidified CO<sub>2</sub> incubator at 37°C. Afterward, the culture media were removed, followed by washing the cells with PBS. Then, the cells were divided into seven groups, i.e., complete media without any treatment (control group), complete media containing 0.01% (v/v) DMSO

(DMSO group), complete media containing kaempferol 1, 5, 10, 50 or 100  $\mu\text{M}$  (treatment groups) dissolved in 0.01% DMSO. The same amount of DMSO volume was added in all treatment and DMSO groups. The cells were then incubated for 24 h or 48 h in a  $\text{CO}_2$  incubator. Following incubation, the media were removed, and each well was added with 125  $\mu\text{l}$  of serum-free media containing 10% MTT solution (5 mg/mL in distilled water) and incubated for 3 h in a  $\text{CO}_2$  incubator. Then, all solutions in each well were removed. The cells were washed with PBS, added 100  $\mu\text{l}$  of DMSO, and incubated in the dark for 45 min.

All solutions were transferred to a 96-well plate for measuring the absorbance in terms of its optical density (OD) by a microplate reader (Biotek, USA) at 570 nm (wavelength of MTT-derived formazan) and 620 nm (wavelength of background). The OD unit of the DMSO and all treatment groups at 570 nm were subtracted by the culture media background OD unit at 620 nm before calculating cell viability. The maximum non-cytotoxic concentration was assessed as the concentration required to retain cell viability by 90% <sup>(170)</sup>. The percentage of cell viability was calculated as a percentage of the DMSO group using the following formula.

$$\text{Percentage of cell viability} = \frac{\text{Absorbance of treatment groups} \times 100}{\text{Absorbance of DMSO group}}$$

### 3.3.3 Ussing chamber experiments

- **Measurement of short-circuit current under basal condition**

The effect of kaempferol on ionic transport across T84 cell monolayers was studied by the Ussing technique. The T84 cells were seeded into the Snapwell insert at a density of  $3 \times 10^5$  cells/well and cultured for 10-14 days to form the complete monolayer. During the cell culture, TEER was measured to assess the cell monolayer integrity every other day by Millicell ERS-2 volt-ohm meter coupled to Ag/AgCl electrodes (EMD Millipore Corporation, USA). The complete monolayers, which had a TEER of 1,500-3,000  $\Omega \cdot \text{cm}^2$ , were selected for experiments. The monolayers were mounted in Ussing chambers containing standard Ringer solution pH 7.4 (in mM: 118 NaCl, 4.5 KCl, 2.5  $\text{CaCl}_2$ , 0.54  $\text{MgCl}_2$ , 25  $\text{NaHCO}_3$ , 1.5  $\text{NaH}_2\text{PO}_4$ ), maintained at 37°C and bubbled with 95%  $\text{O}_2$  and 5%  $\text{CO}_2$  (carbogen) as shown in figure 15. EVC-4000 voltage/current clamp (World Precision Instrument, USA) with Ag/AgCl electrodes were connected to bathing solution through 3 M KCl agar bridges for measuring short-circuit currents ( $I_{\text{SC}}$ ) and transepithelial potential difference (PD). Transepithelial conductance (G) was calculated by applying Ohm's law ( $G = I_{\text{SC}}/\text{PD}$ ). The monolayers were maintained under short-circuit conditions throughout the experiment, except when the PD value was measured before and after adding test compounds. The voltage clamp data was sent through a PowerLab 4/35 A/D converter and then saved on an Intel® Core™ i5-3570, 3.40 GHz, 3401 MHz Processors. After mounting the monolayer on the Ussing chamber, it was equilibrated for at least 30 min to establish a stable  $I_{\text{SC}}$  before adding test compounds. The  $I_{\text{SC}}$  was defined as the charge flow per time when the cell monolayer was short-circuited (PD was set to 0 mV). Using an apical site as a reference, a positive  $I_{\text{SC}}$  indicated the movement of positive charges from the apical side to the basolateral side (cation absorption), the movement of negative charges from the basolateral side to the apical side (anion secretion), or a combination of both processes.

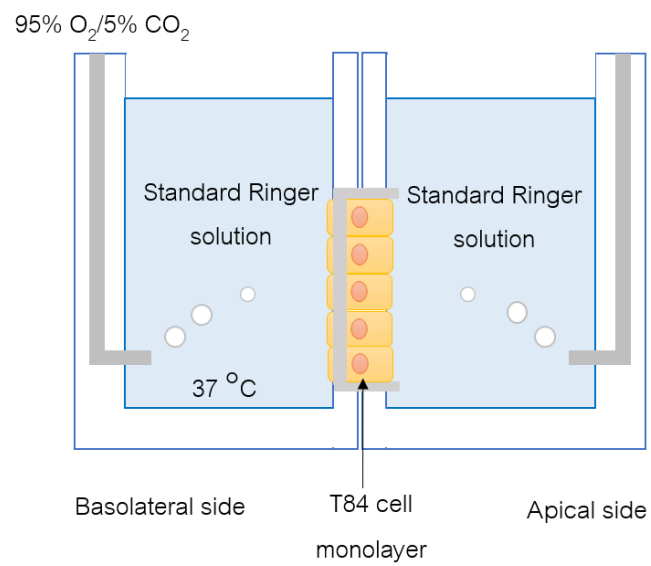
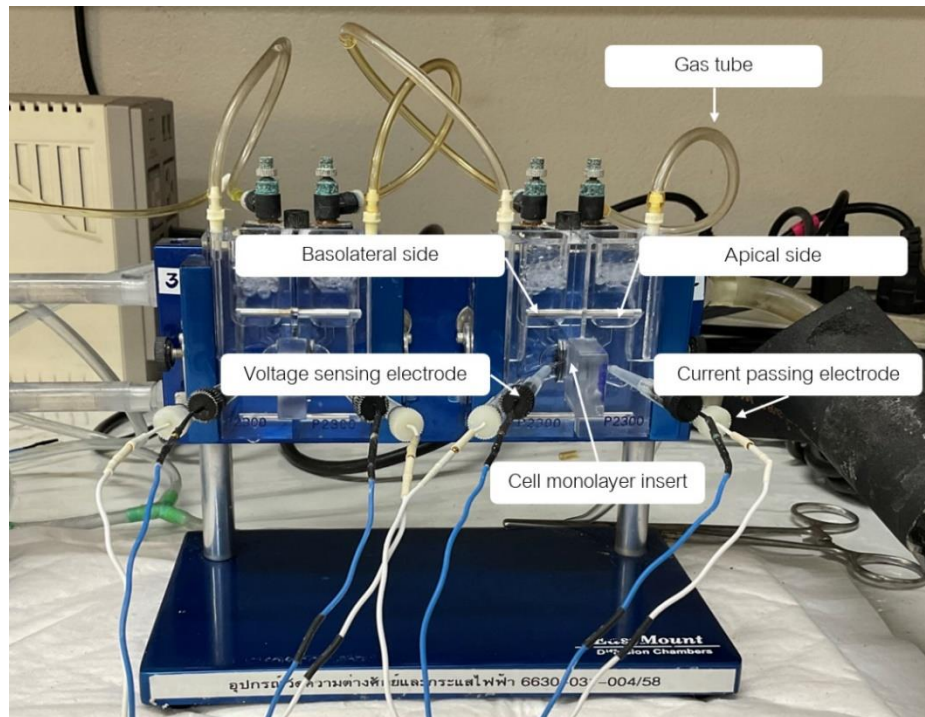


Figure 15 Ussing chamber setup for studying the effect of kaempferol on short circuit current in T84 cell monolayer

- **Measurement of short-circuit current under anion replacement condition**

In anion replacement experiments, T84 cell monolayers were mounted in Ussing chambers containing different Ringer solutions (pH 7.4) to investigate the type of anion in response to  $I_{SC}$  induced by kaempferol. Since stimulating the  $I_{SC}$  response could result from the transport of chloride, bicarbonate, or both, the effect of kaempferol were tested under  $Cl^-$  free,  $HCO_3^-$ -free or  $Cl^-$  and  $HCO_3^-$ -free Ringer solution. In  $Cl^-$  free solution, gluconate salts were used as a substitute for  $Cl^-$  (in mM: 118 Na-gluconic acid, 25  $NaHCO_3$ , 4.5 K-gluconic acid, 2.5 Ca-gluconic acid, 1.2  $NaH_2PO_4$ , 0.54 Mg-gluconic acid), and bubbled with carbogen, while in  $HCO_3^-$  free solution, HEPES buffer was used as a substitute for  $HCO_3^-$  (in mM: 118 NaCl, 25 HEPES buffer, 4.5 KCl, 2.5  $CaCl_2$ , 1.2  $NaH_2PO_4$ , 0.54  $MgCl_2$ ). Both  $HCO_3^-$  free and  $Cl^-$ - $HCO_3^-$  free Ringer solutions (in mM: 118 Na-gluconic acid, 25 HEPES buffer, 4.5 K-gluconic acid, 2.5 Ca-gluconic acid, 1.2  $NaH_2PO_4$ , 0.54 Mg-gluconic acid) were controlled at 37°C and aerated with 100%  $O_2$ . After a stable baseline, kaempferol was tested to obtain its maximum  $I_{SC}$  response.

- **Measurement of apical  $Cl^-$  current**

Since epithelial cell monolayers are composed of apical or basolateral membranes, the technique of selective membrane permeabilization was applied to study the transport activity of either the apical or basolateral membrane. This technique functionally eliminates the particular membrane from the electrical circuit by permeabilization with polyene antifungal amphotericin B which can form pores via binding to cholesterol in human cell membranes (figure 16).<sup>(195)</sup> The formation of pores contributes to increased membrane permeability and rapid leakage of monovalent and divalent ions, including  $K^+$ ,  $Na^+$ ,  $H^+$ ,  $Cl^-$  and  $Ca^{2+}$ .<sup>(195)</sup> Thus, by applying the amphotericin B to form pores and eliminate ionic resistance of one side of the membrane (such as basolateral side), the ionic change of another side of membrane (apical side) in response to test compounds can be determined.



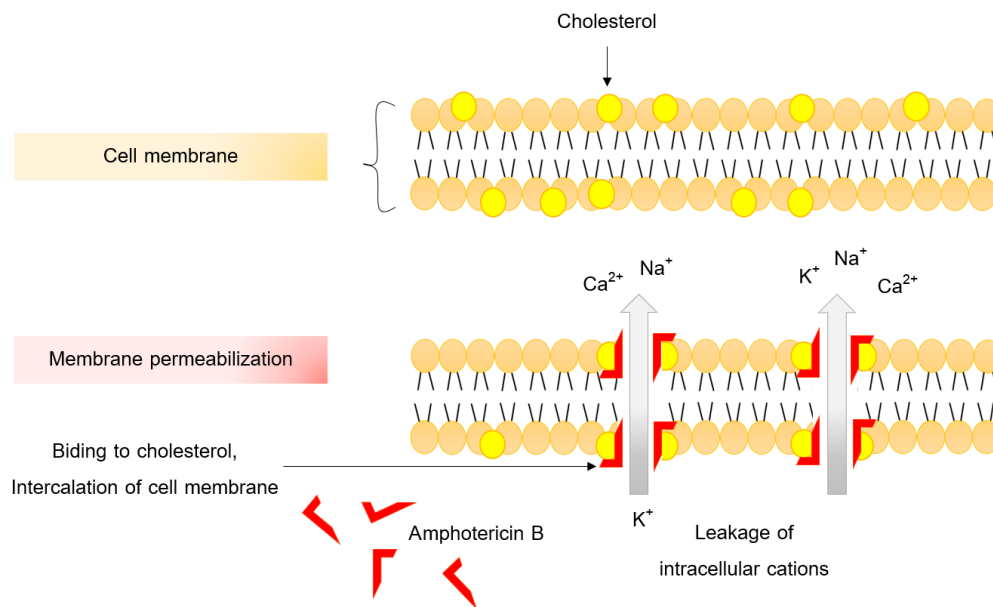


Figure 16 The action of amphotericin B on permeabilization of human cell membranes. The binding of amphotericin B to cholesterol causes the formation of pores, leading to increased membrane permeability and rapid leakage of monovalent and divalent ions, for example,  $\text{K}^+$ ,  $\text{Na}^+$ , and  $\text{Ca}^{2+}$ . Adapted from Bhattacharya and co-worker.<sup>(195)</sup>

In the experiment, apical  $\text{Cl}^-$  current ( $I_{\text{Cl}}$ ) was measured by the permeabilization of the basolateral side of the monolayers. The apical hemichamber was filled with a high concentrate KCl Ringer solution pH 7.4 (in mM: 111.5 KCl, 25  $\text{NaHCO}_3$ , 12 D-glucose, 1.8  $\text{Na}_2\text{HPO}_4$ , 1.25  $\text{CaCl}_2$ , 1  $\text{MgSO}_4$ , 0.2  $\text{NaH}_2\text{PO}_4$ ) while the basolateral hemichamber was filled with a  $\text{KMeSO}_4$  Ringer solution pH 7.4 (in mM: 120  $\text{KMeSO}_4$ , 20  $\text{KHCO}_3$ , 15 mannitol, 5  $\text{NaCl}$ , 2 calcium gluconate, 1.3  $\text{K}_2\text{HPO}_4$ , 1  $\text{MgSO}_4$ , 0.3  $\text{KH}_2\text{PO}_4$ ), maintained at  $37^\circ\text{C}$  and bubbled with carbogen. Then, amphotericin B ( $50 \mu\text{M}$ ) was added into the basolateral hemi-chamber to permeabilize the basolateral membrane, or in other words, to eliminate the basolateral membrane from the electrical circuit. Test compounds were added into the apical or basolateral hemi-chamber or both after the equilibration of the monolayer, and the data of  $I_{\text{Cl}}$  and PD will be recorded.

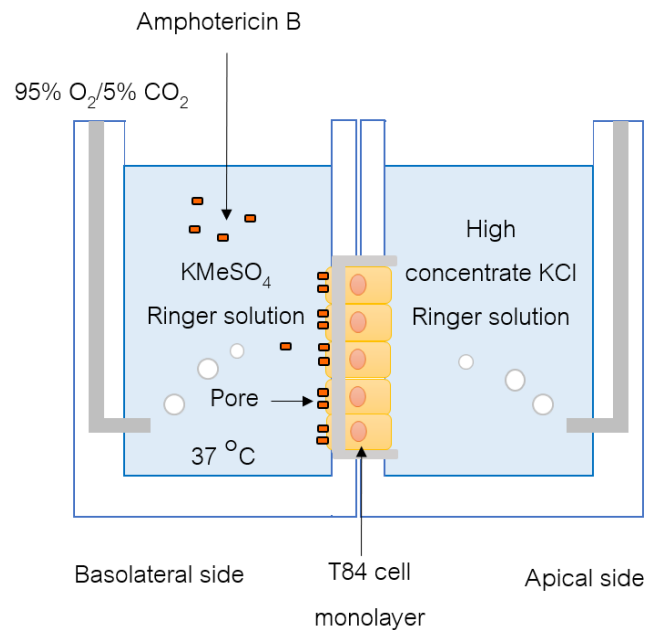


Figure 17 Model for studying the effect of kaempferol on apical  $\text{Cl}^-$  current in amphotericin B-permeabilized T84 cell monolayer

- **Measurement of basolateral  $\text{K}^+$  current**

Basolateral  $\text{K}^+$  current ( $I_{\text{KB}}$ ) was measured using amphotericin B-permeabilized apical membrane of the monolayers. In this experiment, the apical hemichamber was filled with a  $\text{KMeSO}_4$  Ringer solution, while the basolateral hemichamber was filled with a  $\text{NaMeSO}_4$  Ringer solution pH 7.4 (in mM: 120  $\text{NaMeSO}_4$ , 30 mannitol, 5  $\text{NaCl}$ , 3 calcium gluconate, 1  $\text{MgSO}_4$ , 20  $\text{KHCO}_3$ , 0.3  $\text{KH}_2\text{PO}_4$ , 1.3  $\text{K}_2\text{HPO}_4$ ). Afterward, amphotericin B (50  $\mu\text{M}$ ) was added to the apical hemi-chamber to permeabilize the apical membrane. All solutions were controlled at 37°C and bubbled with carbogen. After the equilibration of the monolayer, test compounds were added into the basolateral or apical hemi-chamber or both, and the data of  $I_{\text{KB}}$  and PD were recorded.

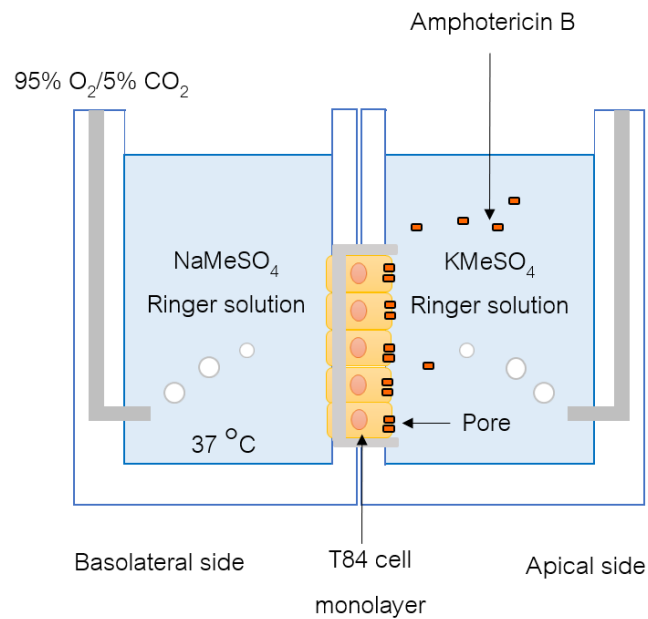


Figure 18 Model for studying the effect of kaempferol on basolateral K<sup>+</sup> current ( $I_{KB}$ ) in amphotericin B-permeabilized T84 cell monolayer

### 3.3.4 Western blot analysis

The effect of kaempferol on the expression of CFTR ion transport protein was determined using western blot analysis. T84 cells were plated in a 60 mm culture dish at a density of  $3 \times 10^5$  cells/well and cultured for 7 days at 37 °C in a CO<sub>2</sub> incubator. Then, the cells were treated with kaempferol 50 μM in complete media (dissolved in 0.01% v/v DMSO) or DMSO and incubated for 24 h. After completion of treatment, the cells were removed from the media containing kaempferol and washed twice with PBS. Total protein was isolated from the cells using a lysis buffer containing (in mM) 46.5 Tris (adjust pH 7.4), 150 mM NaCl, 1 EDTA, 1 NaF, 1 PMSF, 1% NP-40, and 1% protease inhibitor mixture (Sigma, USA). The cell lysate was transferred to an Eppendorf tube and incubated on ice for 30 min. Afterward, all solutions were centrifuged at a speed of 12,000 rpm at 4°C for 15 min, and the supernatant was collected to quantitate protein

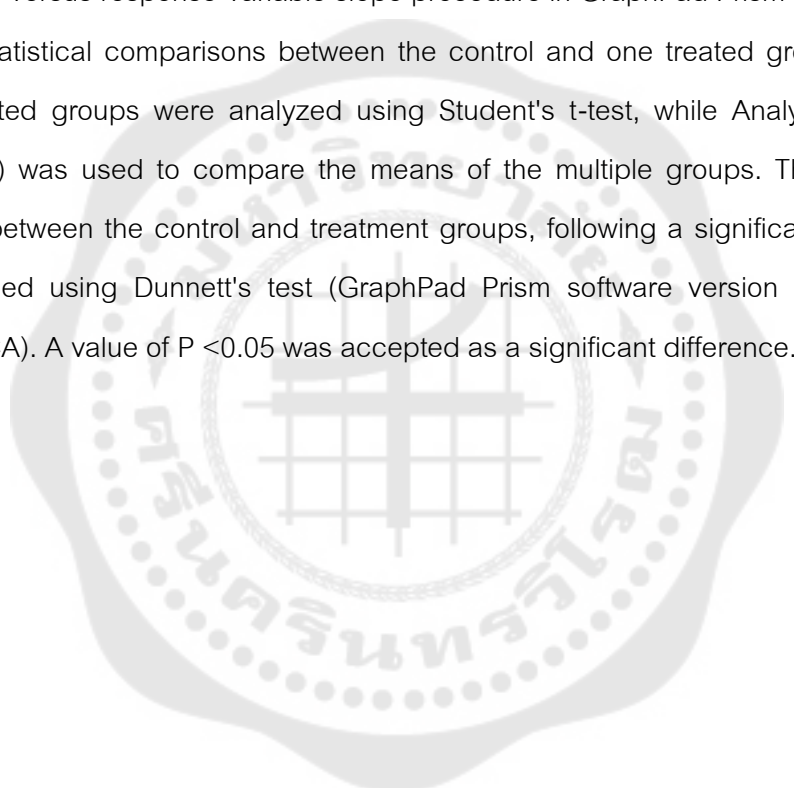
concentration by Bicinchoninic acid assay (BCA assay). The reagents B and A were mixed in a ratio of 1 to 50 for preparing Bicinchoninic acid and incubated in the dark at room temperature for 30 min. The standard bovine serum albumin (BSA) was prepared at the concentrations of 2000, 1500, 1000, 750, 500, 250, and 125  $\mu\text{g/ml}$ . The protein samples were diluted eightfold in nanopure water. A 100  $\mu\text{l}$  of BCA mixture was added to a 96-well plate and followed by mixing with 5  $\mu\text{l}$  of the BSA and protein samples. Then, the plate was enclosed with aluminum foil in an incubator for 30 min. After complete incubation, the plate was placed into a spectrophotometer for measuring the optical density (OD) of proteins at 570/620 nm. The protein concentration was calculated by comparing it with BSA standard curve.

An equal concentration of protein samples (60  $\mu\text{g/ml}$ ) was loaded into 7.5% Sodium Dodecyl Sulfate polyacrylamide gel electrophoresis (SDS-PAGE) for separating proteins based on their molecular weights. The mirror and comb of the western blot set were cleaned with methanol and set together for the setting gel. 7.5% resolving gel was loaded between the mirrors, followed by 4% stacking gel. The protein samples and loading dye were mixed in a ratio of 1:1 and heated at 65  $^{\circ}\text{C}$  for 5 min. The precision plus marker and the mixed samples were loaded into wells of the hardening gel. Then, the gel was run at 100 volts for 120 min. The separated proteins were transferred to the polyvinylidene difluoride (PVDF) membrane (Millipore, USA). The membrane was washed with 1X Tris-Tween 1 time (5 min/time), blocked with 5% non-fat milk in 1X Tris-tween for 1 h at room temperature, washed with 1X Tris-Tween 6 times, and incubated overnight at 4  $^{\circ}\text{C}$  with primary antibodies including mouse monoclonal anti-CFTR (1:100 dilution), and anti- $\beta$ -actin (1:1,000 dilution). Subsequently, the membrane was washed with 1X Tris-Tween 6 times before incubation with horseradish peroxidase-conjugated goat anti-mouse IgG secondary antibody (1:2,000 dilution) for 1 h at room temperature and washed again with 1X Tris-Tween 6 times. Immunoreactive signals were visualized by incubating the membrane with ECL substrate for 1 min. The membrane was imaged on the ChemiDoc Imaging System (Bio-Rad, USA) for 1 min. The target protein band was compared with  $\beta$ -actin. The band density of protein expression was calculated

using the Adobe Photoshop program (Adobe Photoshop CC 2020 software, USA) and ImageJ (NIH, USA).

### 3.4 Statistical analyses

Data were reported as mean  $\pm$  the standard error of the mean (SEM); values of n referred to the number of experiments in each group. EC<sub>50</sub> was calculated using log (agonist) versus response-variable slope procedure in GraphPad Prism software version 9.0.0. Statistical comparisons between the control and one treated group or between two treated groups were analyzed using Student's t-test, while Analysis of Variance (ANOVA) was used to compare the means of the multiple groups. The difference of means between the control and treatment groups, following a significant ANOVA, was determined using Dunnett's test (GraphPad Prism software version 8.0.2, Inc., San Diego, CA). A value of P <0.05 was accepted as a significant difference.



### 3.5 Experimental Protocols

#### Part 1. Evaluation of the cytotoxic effect of kaempferol

To assess the cytotoxicity of kaempferol, the MTT colorimetric assay was used to test the viability of T84 cells after incubation with kaempferol. T84 cells were seeded into a 48-well plate at a density of  $1 \times 10^5$  cells/well and cultured for 7 days in a CO<sub>2</sub> incubator at 37 °C. After that, the cells were treated with different concentrations of kaempferol (1, 5, 10, 50, and 100 μM) in complete media for 24 h and 48 h. The equivalent volume of DMSO used for dissolving kaempferol was added for vehicle control. After complete incubation, the media was removed, and each well was exposed to 125 μl of 10% MTT solution in complete media for 3 h in a CO<sub>2</sub> incubator at 37 °C. After removal of medium, the MTT-derived formazan was solubilized by 100 μl of DMSO, and the absorbance at wavelength 570/620 nm was measured by a microplate reader. The cytotoxic effect of kaempferol was reported as a percentage of cell viability when compared with the DMSO group. Concentrations of kaempferol that retain cell viability by 90% were non-cytotoxic.

#### Part 2. Investigation of the effects of kaempferol on the ion transport across the intact monolayer

##### 2.1 The direct effect of kaempferol on basal short circuit current

The effect of kaempferol on the ion transport across the T84 cell monolayer was studied by the Ussing technique. The monolayers grown in Snapwell inserts were mounted in the modified Ussing chamber bathed on both apical and basolateral sides with identical Ringer's solution, which was maintained at 37°C and bubbled with carbogen. At the start of experiment, the cell monolayers were equilibrated for 30 min to obtain a stable baseline with continuous recording of  $I_{sc}$ . The PD was intermittently recorded before and after adding the test compounds. Once the baseline was stable, a single dose of kaempferol (50 μM) was added to the apical and basolateral solutions to test the effect on basal short circuit current ( $I_{sc}$ ) (figure 19). The effect of DMSO on basal  $I_{sc}$  was verified by adding an equal volume of DMSO used to dissolve substances into the apical and basolateral solutions. Then, different

concentrations of kaempferol (1, 5, 10, 50, and 100  $\mu\text{M}$ ) were added into apical and basolateral solutions ( figure 20), and a concentration that produced the maximum response of  $I_{\text{SC}}$  was selected for studying the rest of the experiments. Moreover, the effective dose of kaempferol (50  $\mu\text{M}$ ) was tested for its effect on each side of the T84 cell monolayer by adding kaempferol into the apical or basolateral solution at a time (figure 21).

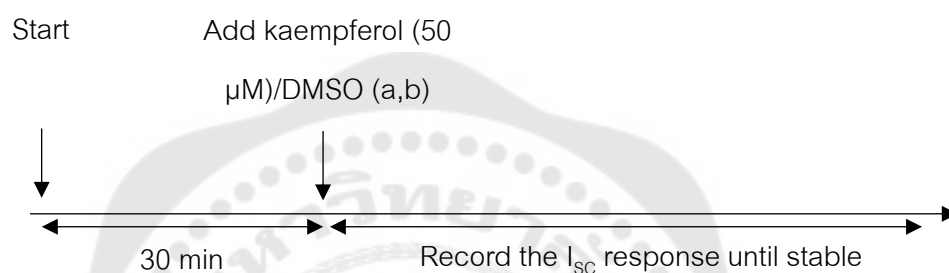


Figure 19 Protocol for studying a single dose of kaempferol on short circuit current in T84 cell monolayer (a = apical, b = basolateral)

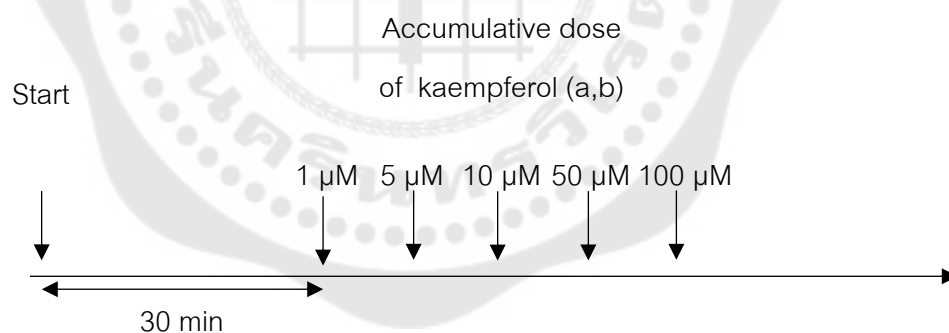


Figure 20 Protocol for studying the concentration-dependent short circuit current response of kaempferol in T84 cell monolayer (a = apical, b = basolateral)

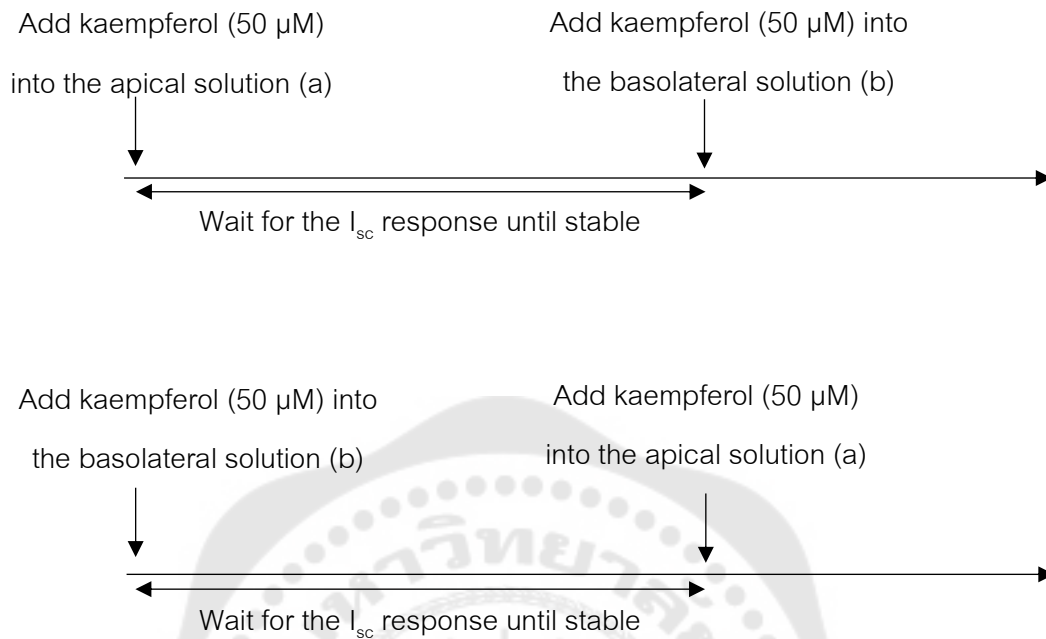


Figure 21 Protocol for studying the effect of kaempferol on short circuit current when added into each side of T84 cell monolayer

## 2.2 Effect of kaempferol on ionic basis of ion transport

### Effect of kaempferol on transepithelial sodium absorption

The effect of kaempferol on specific ion transport was determined using selective ion channel blockers in the T84 cell monolayer mounted in the Ussing chamber apparatus. Based on the  $I_{sc}$  recording, the positive  $I_{sc}$  could be a result of the process of transepithelial cation absorption or transepithelial anion secretion. To investigate the effect of kaempferol on sodium absorption, 10  $\mu\text{M}$  of amiloride was added into apical solution to block the epithelial sodium channels (ENaC) followed by kaempferol 50  $\mu\text{M}$  (figure 22).



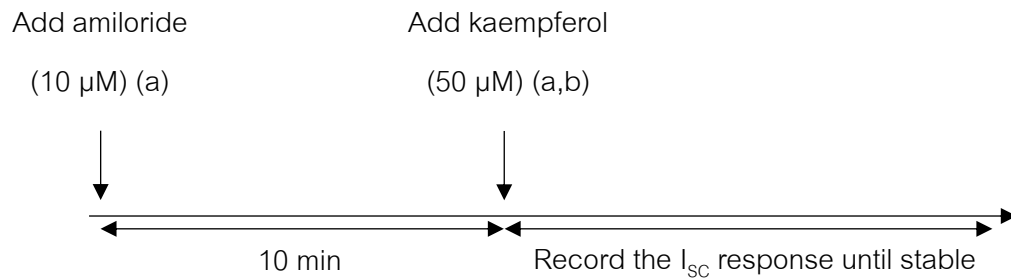


Figure 22 Protocol for studying the effect of kaempferol on sodium absorption in T84 cell monolayer

#### Effect of kaempferol on transepithelial chloride secretion

To further investigate the effect of kaempferol on transepithelial chloride secretion, we used a variety of pharmacological channels, transporter blockers, and anion substitution experiments to block chloride secretion. In colonic epithelium, chloride secretion that commonly occurs through two major types of chloride channels, CFTR and CaCC was tested for the kaempferol effect. After a stable baseline  $I_{SC}$ , CFTR channel inhibitors (50 μM of CFTR-172inh or 200 μM of glibenclamide) or a chloride channel blocker (100 μM of NPPB) were added into the apical solution for 10 min followed by kaempferol (50 μM). In a similar manner, CaCCinh-A01 (30 μM) or DIDS (100 μM) was added into the apical solution for 20 min to block the CaCC channels prior to the addition of kaempferol (50 μM). Furthermore, bumetanide (200 μM), a  $Na^+K^+Cl^-$  cotransporter (NKCC) blocker, was added into the basolateral solution for 10 min before kaempferol addition to examining the effect of kaempferol on the cellular uptake of  $Cl^-$  through NKCC cotransporter which influenced chloride secretion (figure 23).

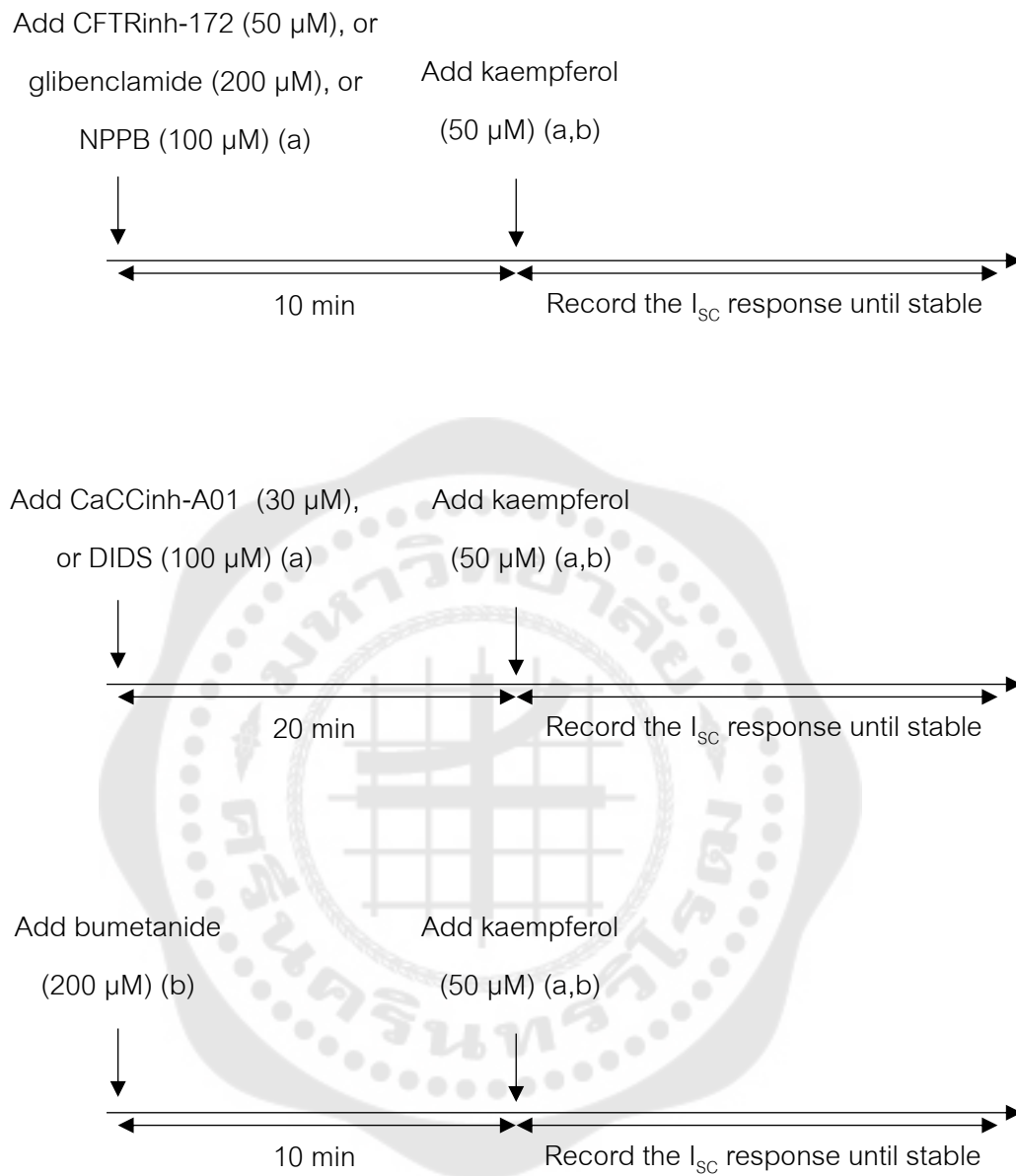


Figure 23 Protocol for evaluating the effect of kaempferol on chloride secretion via CFTR, CaCC, or NKCC in T84 cell monolayer

### Effect of ion substitution on kaempferol-activated short circuit current

Since the increased  $I_{SC}$  in response to kaempferol could be due to secretion of anion which mainly comprises chloride, bicarbonate, or both, we also determined the ionic basis of kaempferol-activated  $I_{SC}$  response by ion substitution testing. In the experiments, gluconate salts were substituted for  $Cl^-$ , and HEPES was substituted for  $HCO_3^-$ . Experiments under  $Cl^-$  free condition were bubbled with 95%  $O_2$  and 5%  $CO_2$ , while  $HCO_3^-$  free and  $Cl^-$ - $HCO_3^-$  free conditions were bubbled with 100%  $O_2$ . Following mounting the T84 monolayer in the Ussing chamber filled in both sides with  $Cl^-$  free,  $HCO_3^-$  free or  $Cl^-$ - $HCO_3^-$  free Ringer solution for at least 30 min, kaempferol (50  $\mu M$ ) was added to apical and basolateral solutions (figure 24).

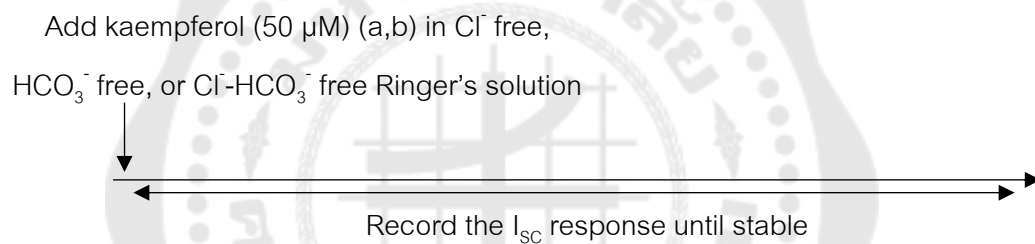


Figure 24 Protocol for studying the effect of kaempferol-activated short circuit current under  $Cl^-$  free,  $HCO_3^-$  free, or  $Cl^-$ - $HCO_3^-$  free condition in T84 cell monolayer

### Effect of kaempferol on cAMP-activated short circuit current

The modulatory effect of kaempferol on cAMP-activated transepithelial  $I_{sc}$  was tested in the presence of forskolin. Forskolin is an activator of adenylate cyclase that increases the synthesis of intracellular cAMP, leading to the opening of CFTR. After mounting the filter-grown cell monolayer in the Ussing chamber filled with the standard Ringer solution, forskolin (10  $\mu$ M) was firstly added and followed by kaempferol (50  $\mu$ M) (figure 25). Conversely, kaempferol (50  $\mu$ M) was added before adding forskolin (figure 26) to determine the kaempferol effect on the forskolin activated  $I_{sc}$ . The change in  $I_{sc}$  was measured when the current is stabilized.

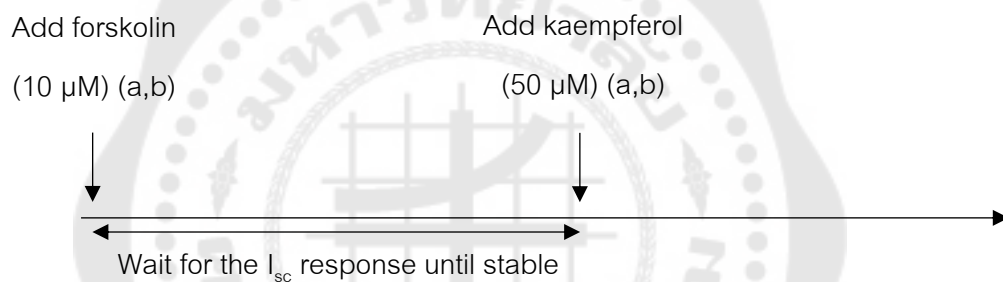


Figure 25 Protocol for testing the effect of kaempferol on the forskolin-activated short circuit current

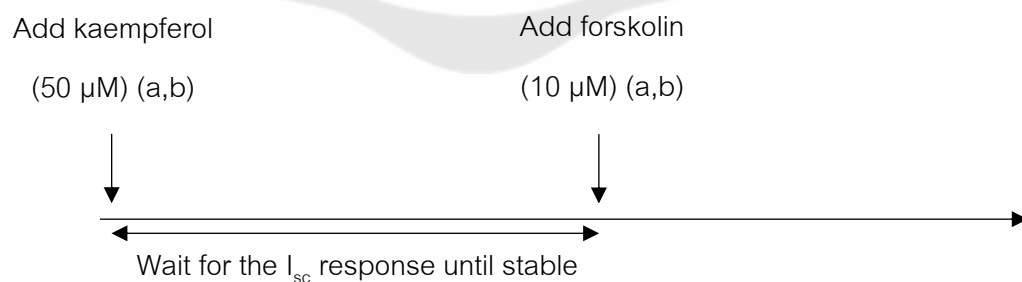


Figure 26 Protocol for testing the effect of forskolin on the kaempferol-activated short circuit current

### Part 3. Investigation of the effect of kaempferol on the apical membrane permeability in the permeabilized monolayer

#### 3.1 The effect of kaempferol on the apical membrane permeability

##### The direct effect of kaempferol on the apical chloride current

To study the effect of kaempferol on the apical membrane permeability, the basolateral membrane of the monolayer was permeabilized with amphotericin B for measuring only the apical membrane current. In this experiment, the T84 monolayers were mounted in the Ussing chamber by bathing the apical membrane with a high-concentrate KCl Ringer solution and the basolateral membrane with a  $\text{KMeSO}_4$  Ringer solution with amphotericin B ( $50 \mu\text{M}$ ) to measure the apical chloride current. After 30 min of equilibration, kaempferol ( $50 \mu\text{M}$ ) was added into apical and basolateral solutions to test the direct effect (figure 27). The kaempferol effect on the apical chloride current was also evaluated in the presence of amiloride ( $10 \mu\text{M}$ ), CFTRinh-172 ( $50 \mu\text{M}$ ) or CaCCinh-A01 ( $30 \mu\text{M}$ ) (figure 28). In another experiment, CFTRinh-172 ( $50 \mu\text{M}$ ) was firstly added before kaempferol and followed by CaCCinh-A01 (Figure 29).

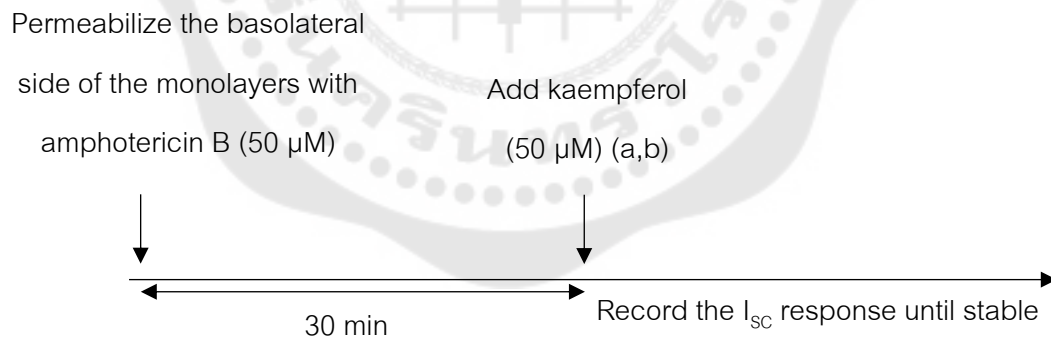


Figure 27 Protocol for investigating the effect of kaempferol on apical chloride current in permeabilized T84 cell monolayer

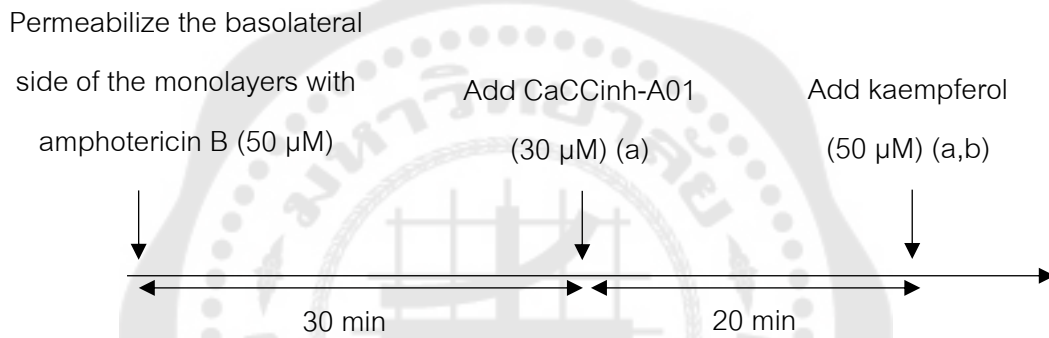
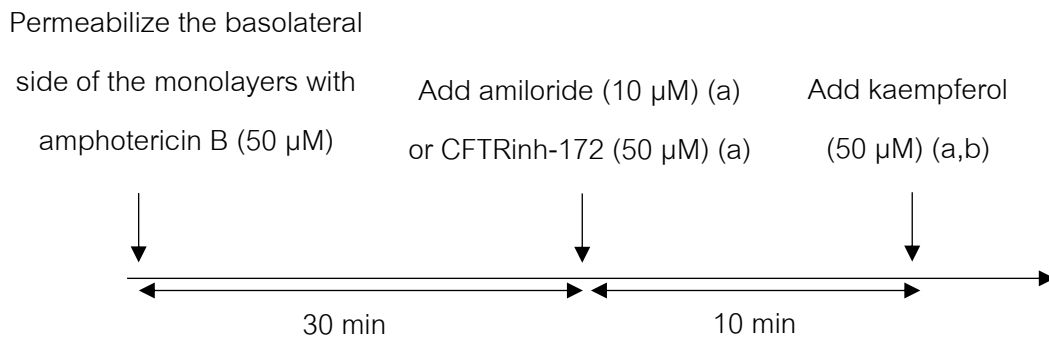


Figure 28 Protocol for investigating the effect of kaempferol-activated apical chloride current via ENaC, CFTR, or CaCC in permeabilized T84 cell monolayer

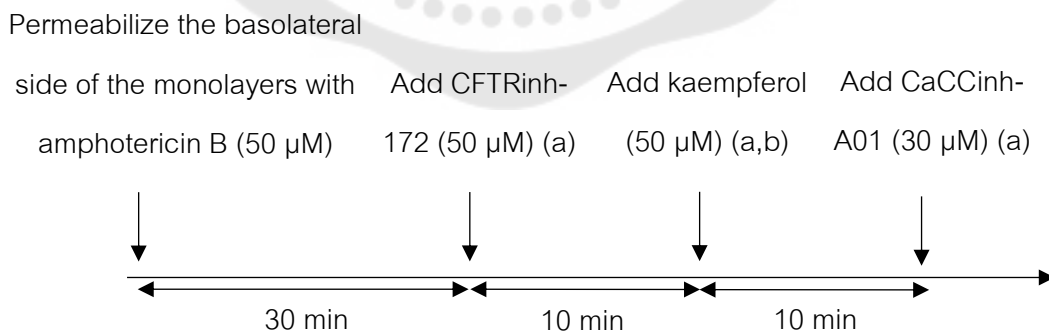


Figure 29 Protocol for investigating the effect of kaempferol on CaCC before using CaCC inhibitor in permeabilized T84 cell monolayer

### The effect of kaempferol on cAMP-activated apical chloride current

The effect of kaempferol on cAMP-activated apical chloride current was confirmed using forskolin and 8cpt-cAMP (a cAMP-analog). These experiments were performed in amphotericin B-permeabilized monolayers, as in protocol 3.1. After equilibration, forskolin (10  $\mu\text{M}$ ) or 8cpt-cAMP (100  $\mu\text{M}$ ) were administered to both apical and basolateral bathing buffer or the basolateral bathing buffer (figure 30), respectively, before adding kaempferol (50  $\mu\text{M}$ ). On the other hand, kaempferol was tested prior to the addition of forskolin or 8cpt-cAMP (figure 31).

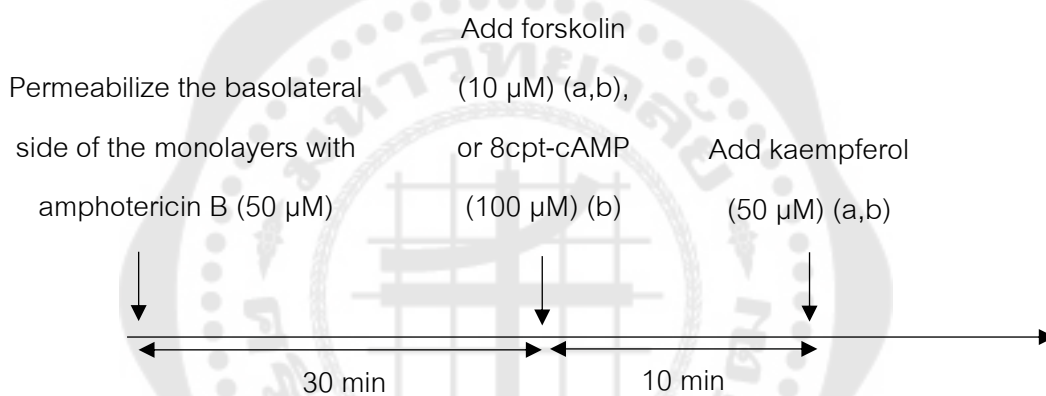


Figure 30 Protocol for evaluating the effect of kaempferol on the cAMP-activated apical chloride current in the permeabilized basolateral membrane of T84 monolayer

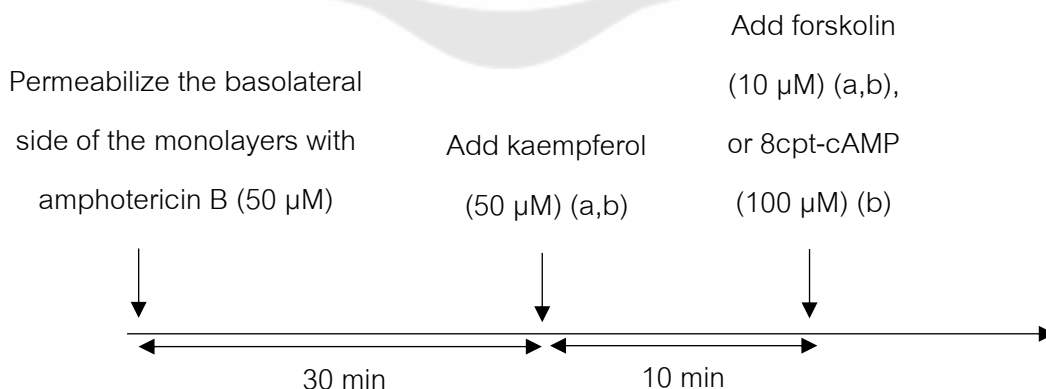


Figure 31 Protocol for evaluating the effect of kaempferol on the 8cpt-activated apical chloride current in the permeabilized basolateral membrane of T84 monolayer

### The effect of kaempferol on $\text{Ca}^{2+}$ -activated apical chloride current

The effect of kaempferol on  $\text{Ca}^{2+}$ -activated apical chloride current was determined using  $\text{Ca}^{2+}$  ionophore A23187 (a highly selective calcium ionophore), which increases intracellular  $\text{Ca}^{2+}$  levels<sup>(148)</sup>. Protocol 3.1 was used for this experiment, which was performed using amphotericin B-permeabilized monolayers. Following 30 min of permeabilization,  $\text{Ca}^{2+}$  ionophore A23187 (1  $\mu\text{M}$ ) was added to the apical solution, followed by kaempferol (50  $\mu\text{M}$ ) (figure 32).

Permeabilize the basolateral

side of the monolayers with  
amphotericin B (50  $\mu\text{M}$ )

Add  $\text{Ca}^{2+}$  ionophore  
(1  $\mu\text{M}$ ) (a)

Add kaempferol  
(50  $\mu\text{M}$ ) (a,b)

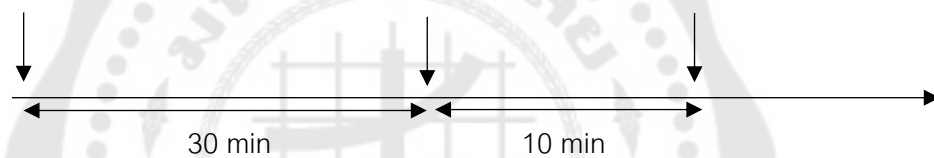


Figure 32 Protocol for evaluating the effect of kaempferol on the  $\text{Ca}^{2+}$ -activated apical chloride current in the permeabilized basolateral membrane of T84 monolayer



### 3.2 The effect of kaempferol on the basolateral membrane permeability

In studying the effect of kaempferol on the basolateral membrane permeability, the apical membrane of the monolayer was permeabilized with amphotericin B for measuring the basolateral membrane current ( $I_{KB}$ ). The apical membrane of the T84 monolayer was bathed with a  $KMeSO_4$  Ringer solution and permeabilized with amphotericin B ( $50 \mu M$ ), while the basolateral membrane was bathed with a  $NaMeSO_4$  Ringer solution. After equilibration,  $50 \mu M$  of kaempferol was added to both apical and basolateral solutions (figure 33). The data of  $I_{KB}$  and PD were recorded.

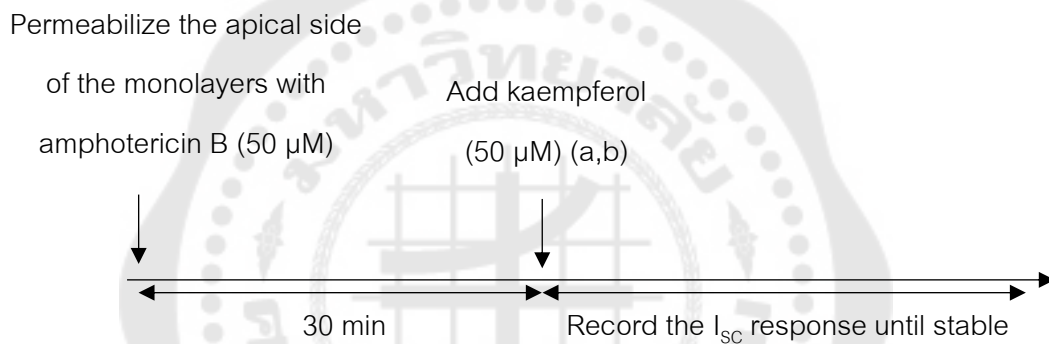


Figure 33 Protocol for evaluating the effect of kaempferol on the basolateral potassium current in the permeabilized apical membrane of T84 monolayer

## Part 4. Evaluation of the underlying mechanism of kaempferol through cAMP-dependent protein kinase, tyrosine kinase and tyrosine phosphatase signaling pathway

### 4.1 The effect of kaempferol on cAMP-dependent protein kinase signaling pathway

To evaluate the effect of kaempferol-activated  $\text{Cl}^-$  secretion was mediated by a cAMP-dependent protein kinase, the kaempferol response was tested using H89, a protein kinase A (PKA) inhibitor, to inhibit the cAMP-dependent PKA-activated apical chloride current. This experiment was performed in basolateral-to-apical  $\text{Cl}^-$  gradient condition in amphotericin B-permeabilized basolateral membrane. After equilibration, H89 (10  $\mu\text{M}$ ) was administered to the apical bathing solution for 30 min before kaempferol (50  $\mu\text{M}$ ) (figure 34).

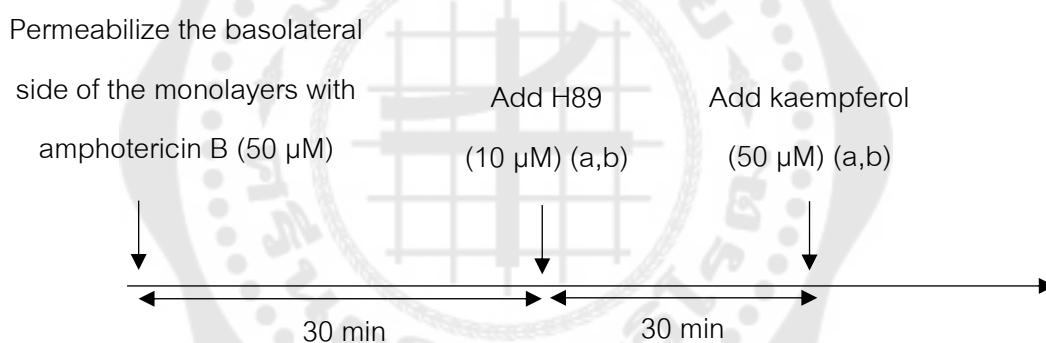


Figure 34 Protocol for assessing the effect of kaempferol on cAMP-dependent protein kinase A signaling pathway

### 4.2 The effect of kaempferol on tyrosine kinase and tyrosine phosphatase signaling pathways

Since both tyrosine kinase and tyrosine phosphatase controls the phosphorylation state of CFTR channels, we further investigated the effect of AG490 or tyrphostin A23 (tyrosine kinase inhibitors) or vanadate (tyrosine phosphatase inhibitor) on the kaempferol-activated apical  $\text{Cl}^-$  current response. The permeabilized basolateral side of the monolayers were added with AG490 (10  $\mu\text{M}$ ) or tyrphostin A23 (100  $\mu\text{M}$ ), tyrosine kinase inhibitors (figure 35), or vanadate (100  $\mu\text{M}$ ), tyrosine phosphatase

inhibitor (figure 36) to the apical and basolateral solutions for 30 min before the kaempferol treatment.

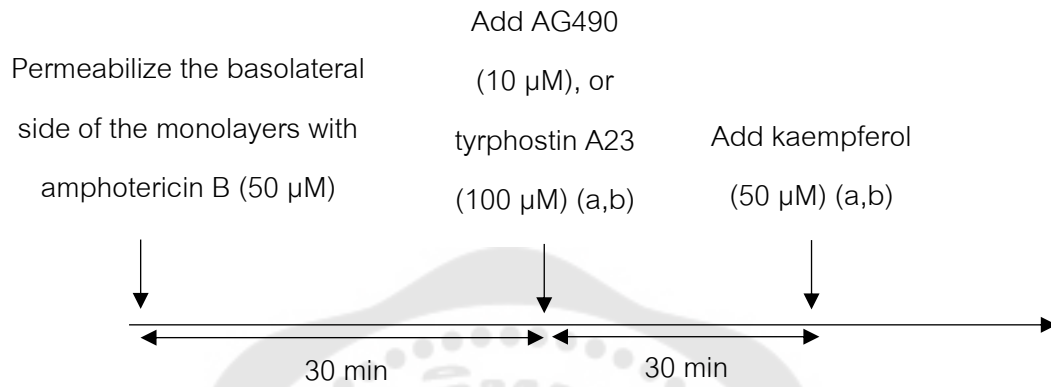


Figure 35 Protocol for assessing the effect of kaempferol on tyrosine kinase signaling pathway

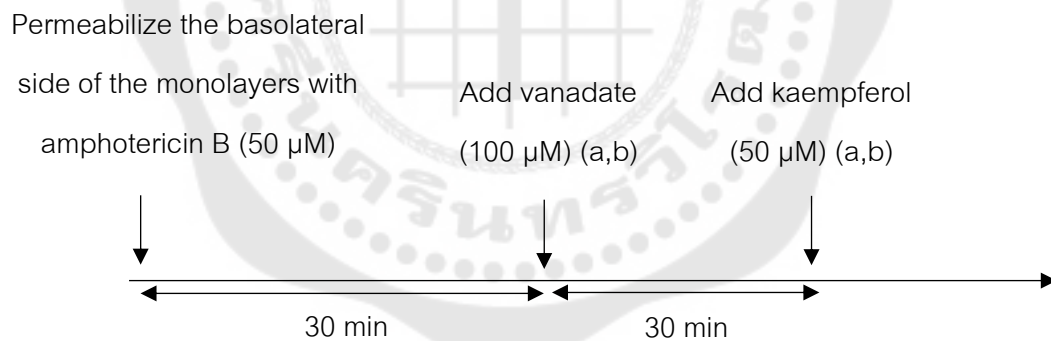


Figure 36 Protocol for assessing the effect of kaempferol on tyrosine phosphatase signaling pathway

### Part 5. Examination of the effect of kaempferol on CFTR protein expression

The effect of kaempferol on the expression of CFTR protein was evaluated using western blot analysis. T84 cells were treated with kaempferol (50  $\mu$ M or 100  $\mu$ M) or DMSO for 24 h and 48 h. The total proteins were isolated and determined for protein quantification by BCA protein assay. Then, the protein samples were separated in 7.5% SDS-PAGE, transferred into the PVDF membrane, and blocked with 5% non-fat milk for 1 h. Afterward, primary antibodies, including mouse monoclonal anti-CFTR and anti- $\beta$ -actin, were added to the membrane and incubated overnight at 4 °C, followed by horseradish peroxidase-conjugated goat anti-mouse IgG secondary antibody for 1 h. Subsequently, the membrane was added by the enhanced chemiluminescence (ECL) substrate to increase immunoreactive signals. Lastly, the immunoreactive bands were imaged on the ChemiDoc Imaging System. The band density of CFTR protein expression was calculated and compared with  $\beta$ -actin using the Adobe Photoshop program and ImageJ.

## CHAPTER 4

### RESULTS

#### Part 1. The cytotoxic effect of kaempferol

The cytotoxic effect on T84 cells of various concentrations of kaempferol used in this study was first determined using the MTT assay. Cells cultured for 7 days in complete media were incubated with kaempferol at concentrations of 1, 5, 10, 50, and 100  $\mu\text{M}$  for 24 or 48 h. The results showed that treatment with kaempferol 10 and 50  $\mu\text{M}$  for 24 and 48 h significantly increased T84 cell viability compared to corresponding DMSO ( $p < 0.05$ ). The increase in cell viability was proportional to the increased concentrations of kaempferol from 1 to 50  $\mu\text{M}$ . The increased T84 cell viability was mostly observed at both 24 and 48 h when treated with kaempferol 50  $\mu\text{M}$ . Regarding to treatment period, kaempferol 1 and 5  $\mu\text{M}$  seemed to increase cell viability at 24 h greater than 48 h, whereas kaempferol 10 and 50  $\mu\text{M}$  at 48 h seemed to be greater than 24 h. However, the kaempferol treatments at the same concentration did not significantly increase cell viability between 24 and 48 h. In addition, there was no change in cell viability following treatment with kaempferol 100  $\mu\text{M}$  for 24 and 48 h. (figure 37).

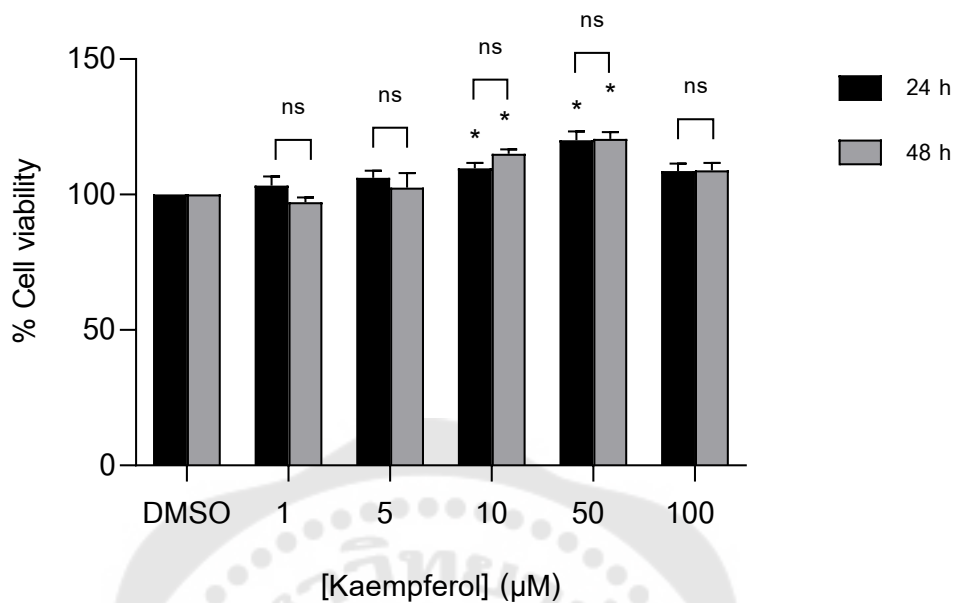


Figure 37 The cytotoxic effect of kaempferol in T84 cells. Cells incubated with 1-100 µM of kaempferol for 24 h and 48 h were assessed for cell viability using MTT colorimetric assay. Data showed the mean  $\pm$  SEM (n = 3-5) of % cell viability compared to the DMSO group. \*P < 0.05 compared to DMSO at specific incubation time by two-way ANOVA and Dunnett's post-hoc test. Non-statistical difference (ns) in % cell viability compared between 24 and 48 h at each treatment using two-way ANOVA and Sidak's multiple comparison post-test.

## Part 2. The effects of kaempferol on the ion transport across the intact monolayer

### 2.1 The effect of kaempferol on basal short circuit current

We first investigated the effect of kaempferol on basal ion transport properties in T84 cells using Ussing technique. Under basal condition where cell monolayers on Snapwell were set in Ussing chambers containing both sides with standard Ringer solution, the average  $I_{SC}$ , PD, and G values were  $1.07 \pm 0.10 \mu\text{A}/\text{cm}^2$ ,  $-1.12 \pm 0.13 \text{ mV}$ , and  $0.95 \pm 0.11 \text{ mS}/\text{cm}^2$  ( $n=54$ ), respectively. Addition of kaempferol ( $50 \mu\text{M}$ ) to both apical and basolateral solutions produced an increase in  $I_{SC}$  with a maximum response of  $19.54 \pm 1.57 \mu\text{A}/\text{cm}^2$  within 7-8 min, followed by a slight drop in  $I_{SC}$  and maintained continually for 90 min ( $n=8$ , figure 38). There were no changes in  $I_{SC}$  at any time point after the equivalent volume of vehicle control DMSO was implemented (figure 39). The addition of kaempferol at concentrations ranging from 1 to  $50 \mu\text{M}$  increased  $I_{SC}$  in a concentration-dependent manner, but  $100 \mu\text{M}$  decreased  $I_{SC}$  (figure 40A). An analysis of the kaempferol-induced accumulative  $I_{SC}$  response showed an  $EC_{50}$  value of  $8.18 \mu\text{M}$  and a maximal response at  $50 \mu\text{M}$  ( $n=3$ , figure 40B). Because kaempferol at a higher concentration ( $100 \mu\text{M}$ ) did not increase the  $I_{SC}$  further, the maximal response concentration ( $50 \mu\text{M}$ ) was used in the remaining tests.

To assess whether the apical or the basolateral membrane is responsible for kaempferol effect, we found that kaempferol stimulated  $I_{SC}$  response when firstly applied to the apical side and slightly increased  $I_{SC}$  after a subsequent addition to the basolateral side (figure 41A). Meanwhile, a basolateral addition of kaempferol produced a little increased  $I_{SC}$ , and a significant increase in  $I_{SC}$  was observed after an apical addition (figure 41B).

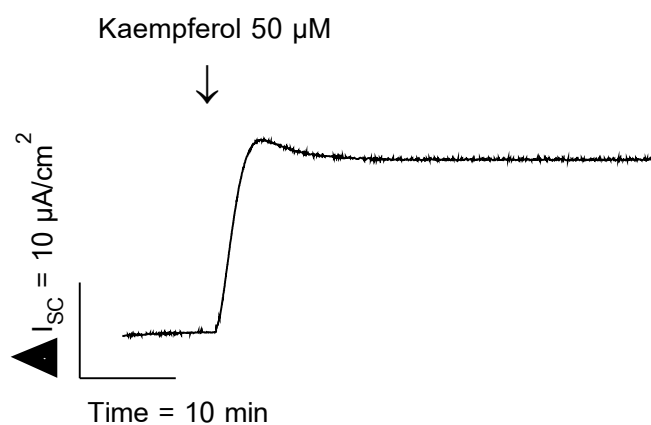


Figure 38 The effective concentration of kaempferol on basal short circuit current in T84 cells. A representative  $I_{\text{SC}}$  tracing showed the effect of kaempferol (50  $\mu\text{M}$ , apical and basolateral) (n=8) on the increase in the  $I_{\text{SC}}$  to a maximum response, followed by a slight decrease in the  $I_{\text{SC}}$  response and maintained continuously.

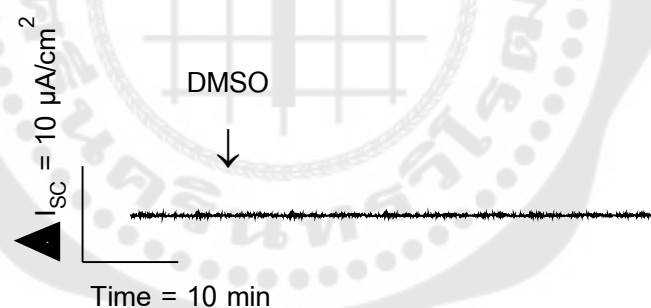


Figure 39 The effect of DMSO on basal short circuit current in T84 cells. A representative  $I_{\text{SC}}$  tracing showed the effect of vehicle DMSO (0.01% DMSO, apical and basolateral) (n=3) on no change in the  $I_{\text{SC}}$  response.



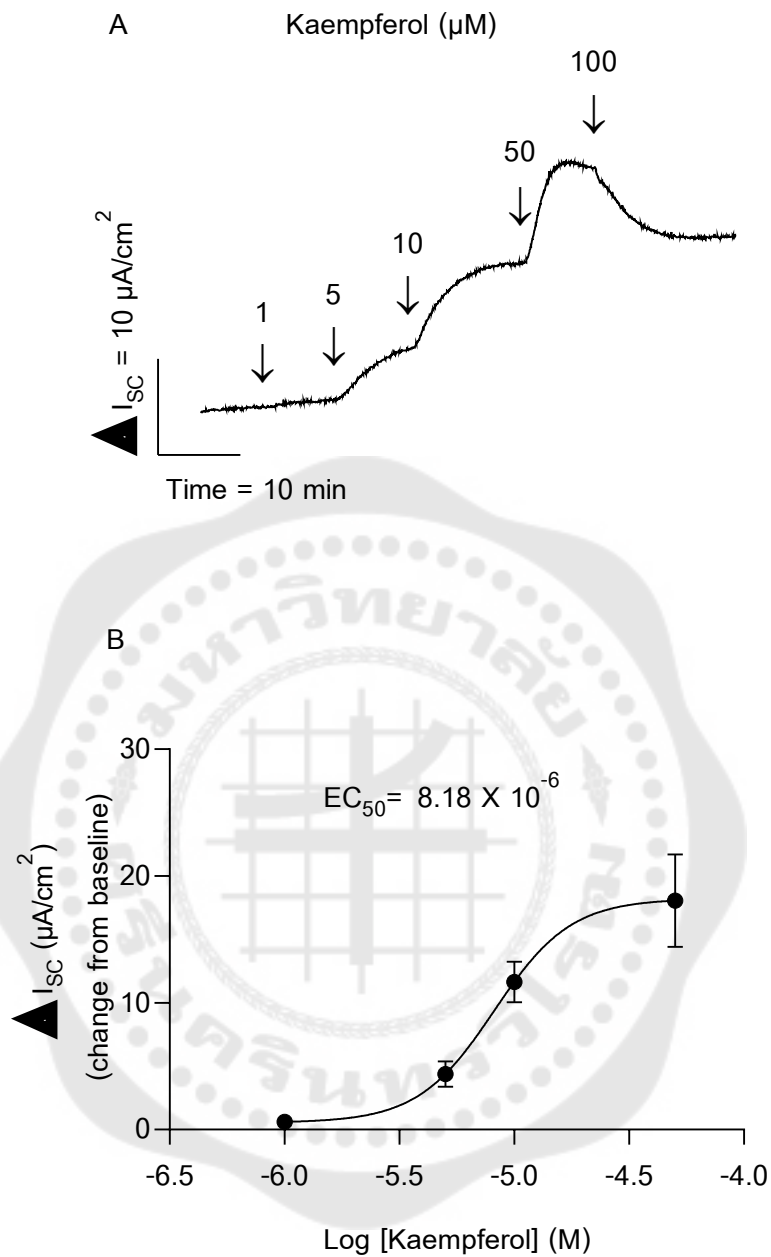


Figure 40 Concentration dependent kaempferol-activated short circuit current. (A) A representative  $I_{\text{SC}}$  tracing showed the accumulative  $I_{\text{SC}}$  response induced by kaempferol at concentrations of 1-100  $\mu\text{M}$  (apical and basolateral) ( $n=3$ ). (B) Concentration-response relationship of kaempferol-activated increase in  $I_{\text{SC}}$  showed an  $\text{EC}_{50}$  value of 8.18  $\mu\text{M}$ . Each value represented mean  $\pm$  SEM ( $n=3$ ).

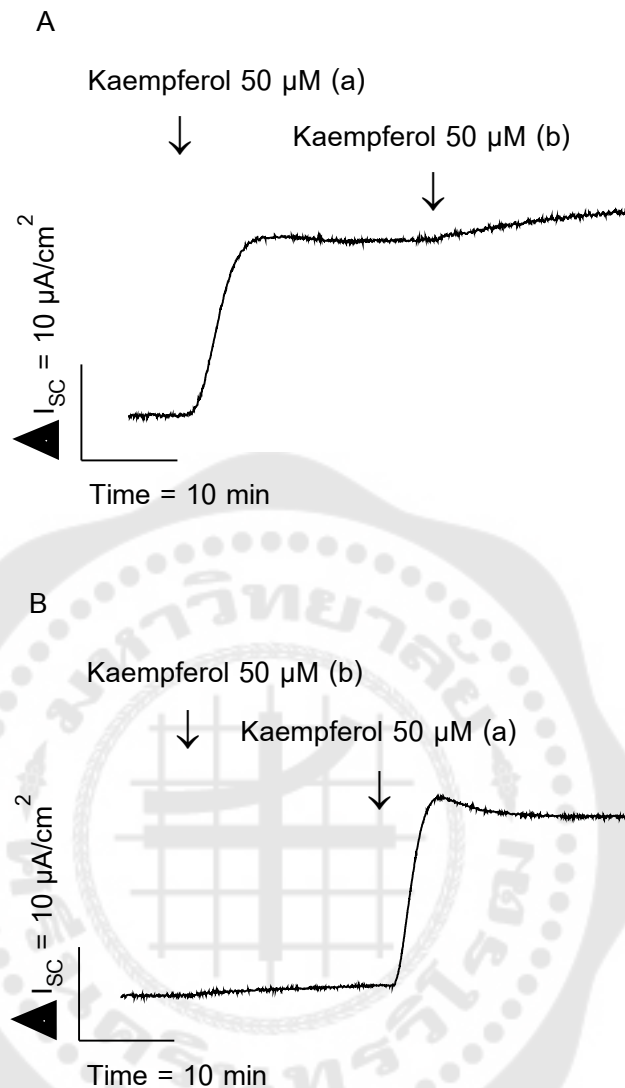


Figure 41 The effect of kaempferol on basal short circuit current when added to each side of the membrane. (A) A representative  $I_{\text{sc}}$  tracing showed an increase in  $I_{\text{sc}}$  response when kaempferol (50  $\mu\text{M}$ ) was first applied in the apical solution and followed by the basolateral addition (n=3). (B) A representative  $I_{\text{sc}}$  tracing showed a small increase in  $I_{\text{sc}}$  response when kaempferol was first added to the basolateral solution and a marked increased  $I_{\text{sc}}$  following the apical addition (n=3).

## 2.2 Ionic basis of kaempferol-stimulated short circuit current

### 2.2.1 Effect of kaempferol on transepithelial sodium ion transport

Since the effect of kaempferol on the basal  $I_{SC}$  was a positive value, this would be due to the movement of cation (e.g.,  $Na^+$ ) from the apical to basolateral compartments (absorption) or the movement of anion (e.g.,  $Cl^-$ ,  $HCO_3^-$ ) from the basolateral to apical compartments (secretion) or a combination of both. We first identified the effect of kaempferol on transepithelial sodium transport by using amiloride, a  $Na^+$  channel blocker. Amiloride is commonly used to block  $Na^+$  transport via the epithelial  $Na^+$  channels (ENaC), the principal cation transport in colonic epithelial cells. As shown in figure 42, an apical addition of amiloride (10  $\mu M$ ) did not change the  $I_{SC}$  from baseline (figure 42A), and a subsequent addition of kaempferol (50  $\mu M$ ) to both solutions produced the increase in  $I_{SC}$  by  $19.18 \pm 0.76 \mu A/cm^2$  within 7-8 min. The average increase in  $I_{SC}$  by kaempferol in the presence of amiloride was not different from that induced by kaempferol alone (figure 42B).

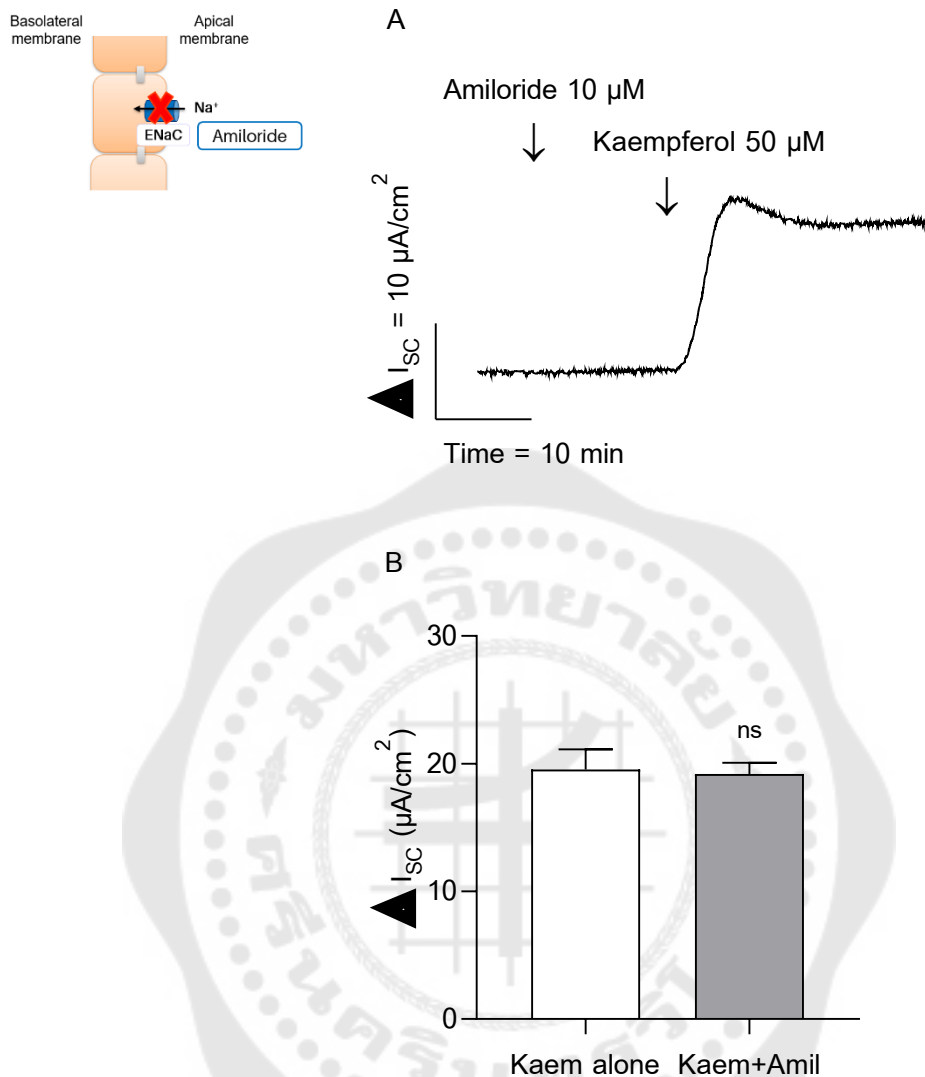


Figure 42 Effect of the Na<sup>+</sup> channel blocker amiloride on the kaempferol-activated short circuit current in T84 cells. (A) A representative  $I_{SC}$  tracing showed the effect of amiloride (10  $\mu$ M, apical) on no change in the  $I_{SC}$  response and a marked increased  $I_{SC}$  following the addition of kaempferol (50  $\mu$ M, apical and basolateral). (B) Bar graph showed average changes in the  $I_{SC}$  responding to kaempferol alone or in the presence of amiloride. Each value represented mean  $\pm$  SEM (n=4). ns = non-statistical difference from kaempferol alone.

### 2.2.2 Effect of kaempferol on transepithelial chloride ion transport

Two major types of  $\text{Cl}^-$  channels involved in  $\text{Cl}^-$  secretion in colonic epithelium are CFTR and  $\text{Ca}^{2+}$ -activated  $\text{Cl}^-$  channel (CaCC). To identify whether the kaempferol-increased  $I_{\text{SC}}$  via CFTR-mediated transepithelial  $\text{Cl}^-$  secretion, we tested the kaempferol response in the presence of a variety of CFTR inhibitors. As shown in figure 43A-C, addition of CFTRinh-172 (50  $\mu\text{M}$ , apical) slightly decreased baseline  $I_{\text{SC}}$  but could not inhibit the kaempferol-increased  $I_{\text{SC}}$  (figure 43A). On the other hand, pretreatment of the monolayer for 10 min with a sulphonylurea drug, glibenclamide (200  $\mu\text{M}$ , apical), did not affect basal  $I_{\text{SC}}$  but it statistically decreased the kaempferol-induced increase in  $I_{\text{SC}}$  by 64% ( $7.06 \pm 0.57 \mu\text{A}/\text{cm}^2$ ,  $n=4$ ) (figure 43B-D) as compared to kaempferol alone. Moreover, pretreatment with 5-Nitro-2-(3-phenylpropylamino)benzoic acid (NPPB) (100  $\mu\text{M}$ , apical) slightly increased basal  $I_{\text{SC}}$  and abolished the kaempferol-increased  $I_{\text{SC}}$  by 84% ( $3.09 \pm 0.12 \mu\text{A}/\text{cm}^2$ ,  $n=4$ ) (figure 43C-D). Although pretreatment with the specific CFTR inhibitor (CFTRinh-172) did not inhibit the kaempferol-increased  $I_{\text{SC}}$ , the addition of CFTRinh-172 after kaempferol treatment decreased the kaempferol response by 48% ( $-9.53 \pm 1.19 \mu\text{A}/\text{cm}^2$ ,  $n=3$ ) (figure 43E).

To examine the effect of kaempferol on CaCC, the cell monolayers were exposed to CaCC inhibitors in the apical solution prior to kaempferol addition. As shown in figure 44A-B, pretreatment with CaCCinh-A01 (30  $\mu\text{M}$ ) or DIDS (200  $\mu\text{M}$ ) for 20 min did not change the basal  $I_{\text{SC}}$  and failed to inhibit the kaempferol induced increase in  $I_{\text{SC}}$  response. The average changes in the kaempferol response in the absence or presence of CaCCinh-A01 or DIDS were shown in figure 44C. Moreover, the addition of the specific CaCC inhibitor (CaCCinh-A01) after kaempferol treatment slightly decreased the kaempferol response by 7% ( $-1.24 \pm 0.02 \mu\text{A}/\text{cm}^2$ ,  $n=3$ ) (figure 44D). To assess the influence of kaempferol on the  $\text{Cl}^-$  uptake step of the cell monolayers through NKCC cotransporter, we applied NKCC blocker bumetanide (200  $\mu\text{M}$ ) into the basolateral solution followed by kaempferol treatment. Bumetanide had no effect on the basal  $I_{\text{SC}}$  and reduced kaempferol-induced  $I_{\text{SC}}$  by 61% ( $7.53 \pm 0.51 \mu\text{A}/\text{cm}^2$ ,  $n=3$ ) (figure 45A-B).

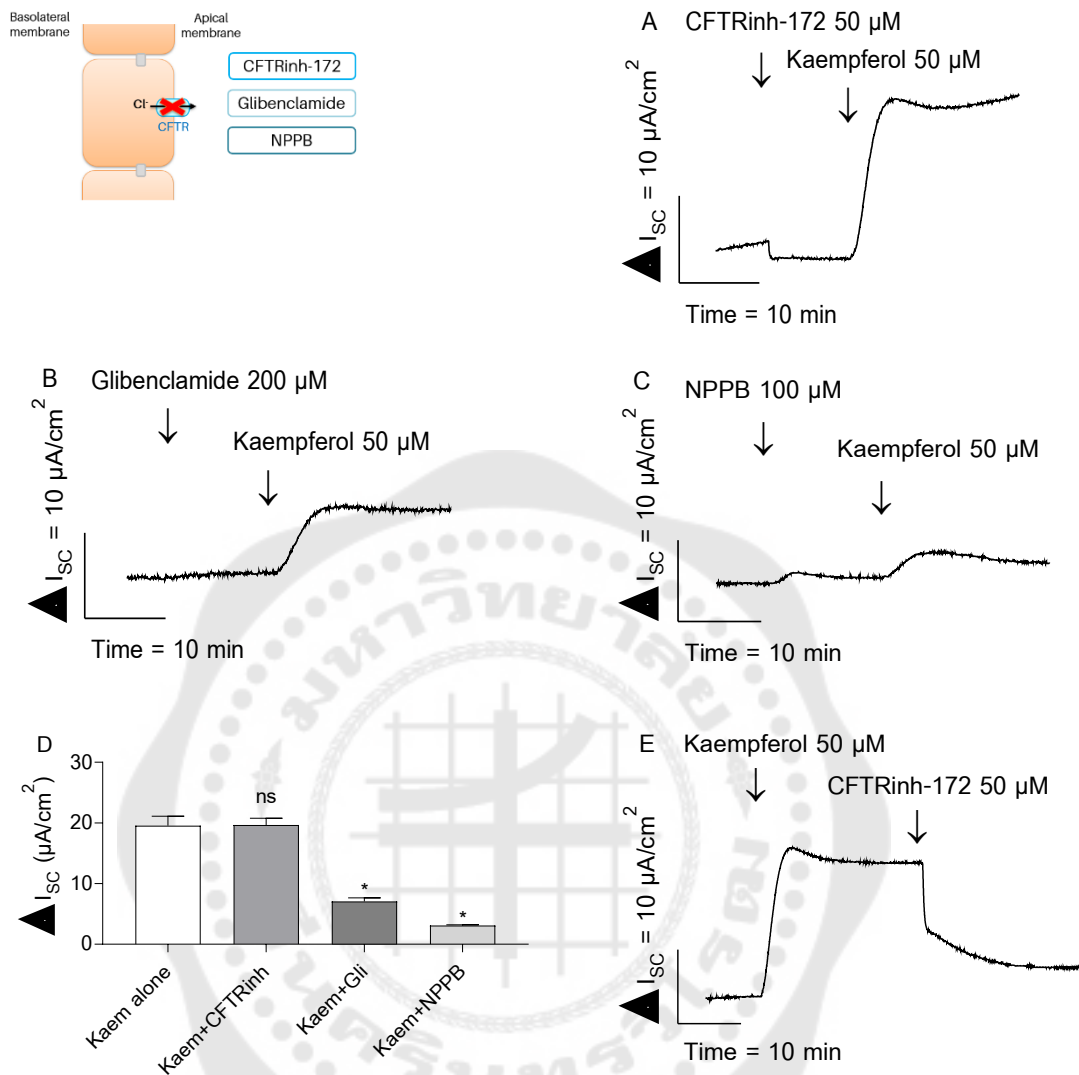


Figure 43 Effect of CFTR  $\text{Cl}^-$  channel inhibitors on the kaempferol-activated short circuit current in T84 cells. Representative  $I_{\text{SC}}$  tracings showed the effect of (A) CFTRinh-172 (50  $\mu\text{M}$ , apical), (B) glibenclamide (200  $\mu\text{M}$ , apical), and (C) NPPB (100  $\mu\text{M}$ , apical) on change in the  $I_{\text{SC}}$  response and a slight increased  $I_{\text{SC}}$  following the addition of kaempferol (50  $\mu\text{M}$ , apical and basolateral). (D) Bar graph showed average changes in the  $I_{\text{SC}}$  responding to kaempferol alone or in the presence of CFTR  $\text{Cl}^-$  channel inhibitors. Each value represented mean  $\pm$  SEM ( $n=3-4$ ). \* $P<0.05$  compared to kaempferol alone by one-way ANOVA and Dunnett's post-hoc test. (E) Representative  $I_{\text{SC}}$  tracings showed the effect of kaempferol following the addition of CFTRinh-172.

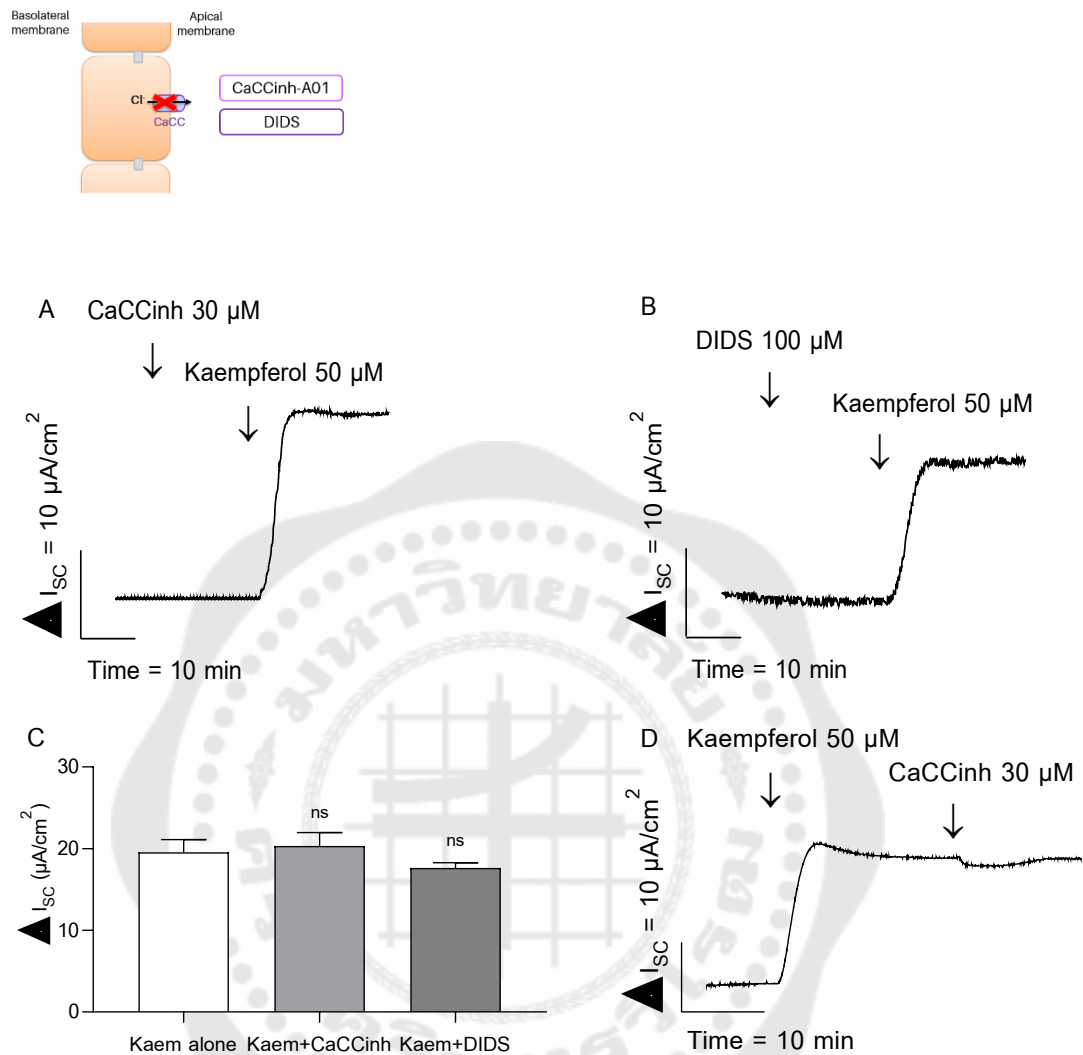


Figure 44 Effect of CaCC Cl<sup>-</sup> channel inhibitors on the kaempferol-activated short circuit current in T84 cells. Representative I<sub>SC</sub> tracings showed the effect of (A) CaCCinh-A01 (30 μM, apical) and (B) DIDS (100 μM, apical) on no change in the I<sub>SC</sub> response and a marked increased I<sub>SC</sub> following the addition of kaempferol (50 μM, apical and basolateral). (C) Bar graph showed average changes in the I<sub>SC</sub> responding to kaempferol alone or in the presence of CaCC Cl<sup>-</sup> channel inhibitors. Each value represented mean ± SEM (n=3). (D) Representative I<sub>SC</sub> tracings showed the effect of kaempferol following the addition of CaCCinh-A01.

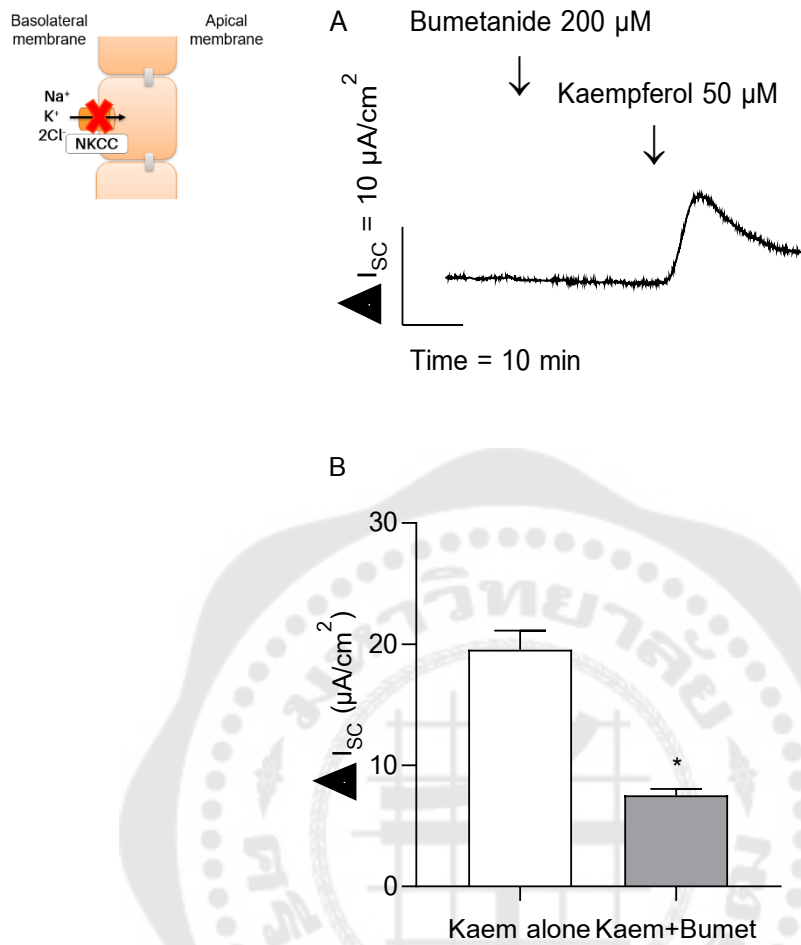
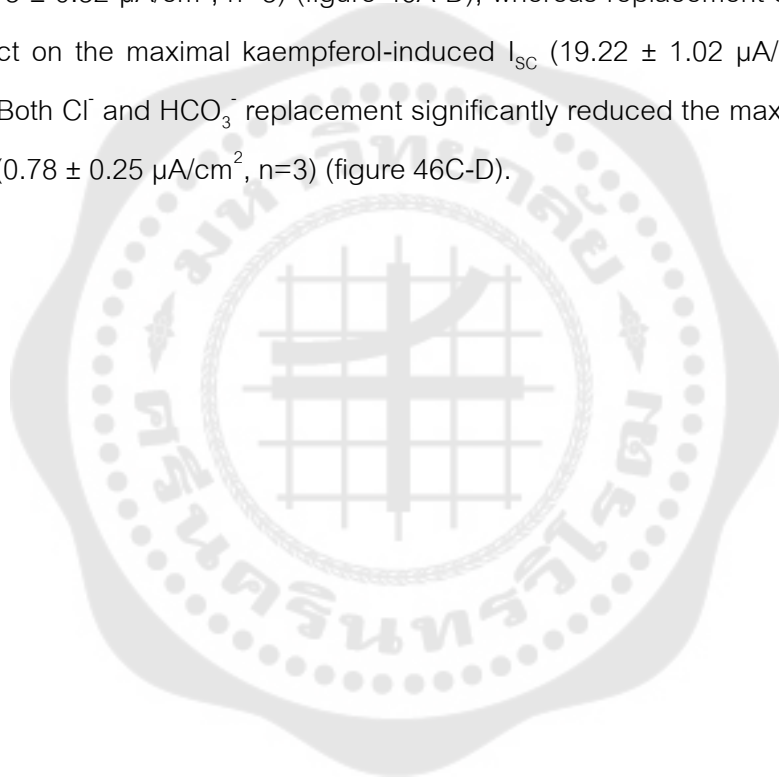


Figure 45 Effect of the NKCC cotransporter blocker bumetanide on the kaempferol-activated short circuit current in T84 cells. (A) A Representative  $I_{\text{SC}}$  tracing showed the effect of NKCC blocker bumetanide (200  $\mu\text{M}$ , basolateral) on a slight decrease in the  $I_{\text{SC}}$  response and a small increased  $I_{\text{SC}}$  following the addition of kaempferol (50  $\mu\text{M}$ , apical and basolateral). (B) Bar graph showed average changes in the  $I_{\text{SC}}$  responding to kaempferol alone or in the presence of bumetanide. Each value represented mean  $\pm$  SEM (n=3). \* $P < 0.05$  compared to kaempferol alone by Student t-test.



### 2.2.3 Effect of ion substitution on kaempferol-increased short circuit current

As the kaempferol-induced increase in  $I_{SC}$  was not inhibited by specific CFTR channel inhibitor CFTR172-inh, anion substitution experiments were also performed to validate the ionic basis of the kaempferol effect on anion secretion. Under normal Ringer's solution, kaempferol 50  $\mu\text{M}$  produced a mean increase in  $I_{SC}$  of  $19.54 \pm 1.57 \mu\text{A}/\text{cm}^2$  ( $n=8$ ). Replacement of  $\text{Cl}^-$  with gluconate salts in both apical and basolateral solutions significantly decreased the maximal kaempferol-induced  $I_{SC}$  by 96% ( $0.73 \pm 0.32 \mu\text{A}/\text{cm}^2$ ,  $n=3$ ) (figure 46A-D), whereas replacement of  $\text{HCO}_3^-$  free had no impact on the maximal kaempferol-induced  $I_{SC}$  ( $19.22 \pm 1.02 \mu\text{A}/\text{cm}^2$ ,  $n=3$ ) (figure 46B-D). Both  $\text{Cl}^-$  and  $\text{HCO}_3^-$  replacement significantly reduced the maximal  $I_{SC}$  response by 96% ( $0.78 \pm 0.25 \mu\text{A}/\text{cm}^2$ ,  $n=3$ ) (figure 46C-D).



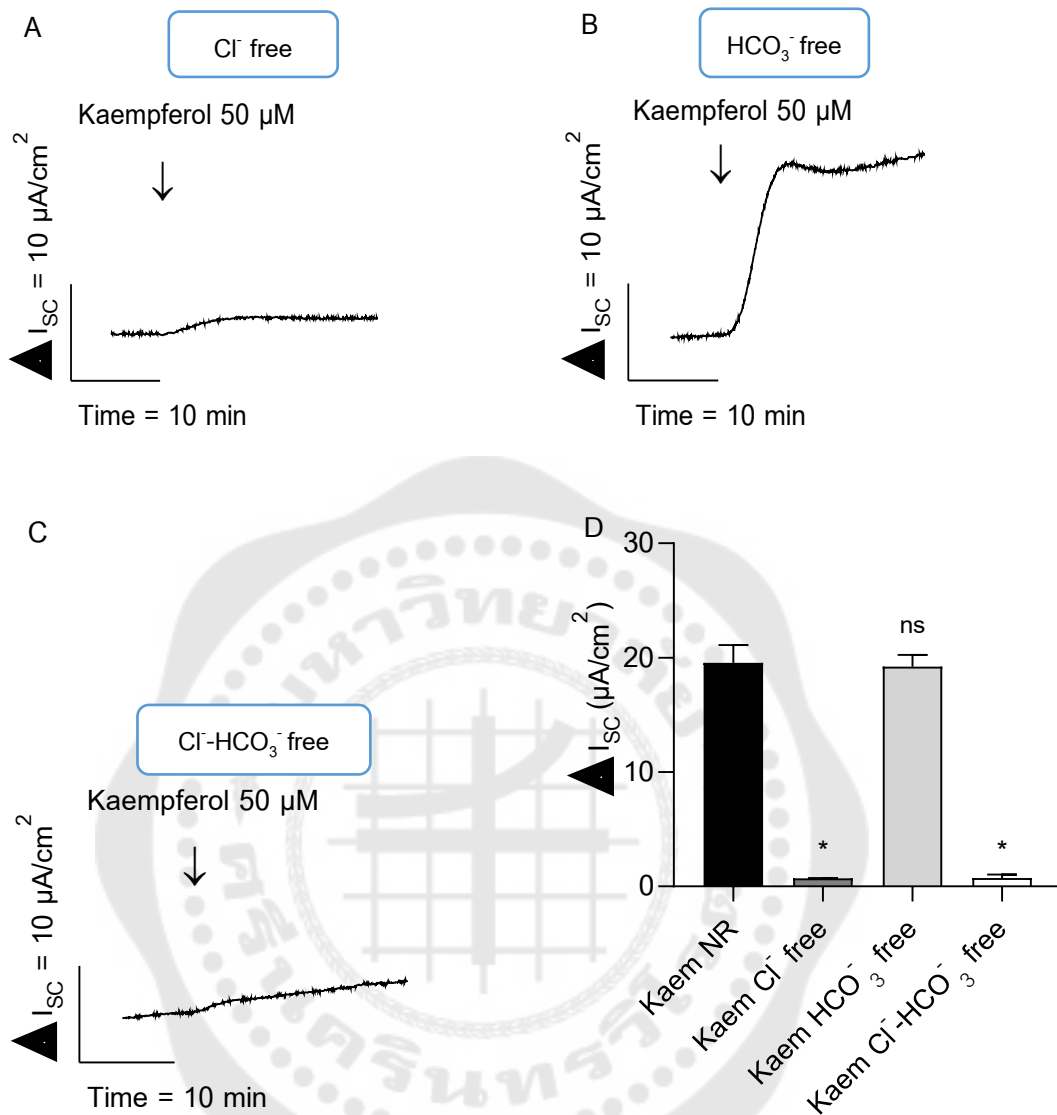


Figure 46 Effect of  $\text{Cl}^-$  and  $\text{HCO}_3^-$  substitution on the kaempferol-activated short circuit current in T84 cells. Representative  $I_{\text{SC}}$  tracings showed the effect of kaempferol (50  $\mu\text{M}$ , apical and basolateral) on the increase in the  $I_{\text{SC}}$  response in (A)  $\text{Cl}^-$  free, (B)  $\text{HCO}_3^-$  free, and (C)  $\text{Cl}^-$ - $\text{HCO}_3^-$  free solution. (D) Bar graph showed average changes in the kaempferol  $I_{\text{SC}}$  response in normal Ringer's (NR),  $\text{Cl}^-$  free,  $\text{HCO}_3^-$  free, or  $\text{Cl}^-$ - $\text{HCO}_3^-$  free solutions. Each value represented mean  $\pm$  SEM ( $n=3$ ). \* $P<0.05$  compared to NR by one-way ANOVA and Dunnett's post-hoc test.

#### 2.2.4 Effect of kaempferol on forskolin-activated chloride secretion

To further investigate the involvement of cAMP in kaempferol-sensitive  $I_{sc}$ , the kaempferol response was determined under  $Cl^-$  secretion activated by forskolin. Forskolin is an adenylate cyclase activator that increases intracellular cAMP synthesis, resulting in CFTR opening and chloride secretion. The kaempferol-sensitive  $I_{sc}$  was determined before and after addition of forskolin as shown in figure 47. Addition of forskolin (10  $\mu$ M, apical and basolateral) induced the maximal  $I_{sc}$  response to  $166.59 \pm 1.76 \mu A/cm^2$  (n=3). A subsequent addition of kaempferol (50  $\mu$ M, apical and basolateral) decreased the forskolin-stimulated  $I_{sc}$  by 59% ( $-98.43 \pm 9.43 \mu A/cm^2$ , n=3) (figure 47A-C). Moreover, pretreatment with kaempferol increased the  $I_{sc}$  and reduced the forskolin-activated  $I_{sc}$  to  $25.81 \pm 2.26 \mu A/cm^2$  (n=4), which was less than the treatment of forskolin alone by 85% (figure 47B-D).

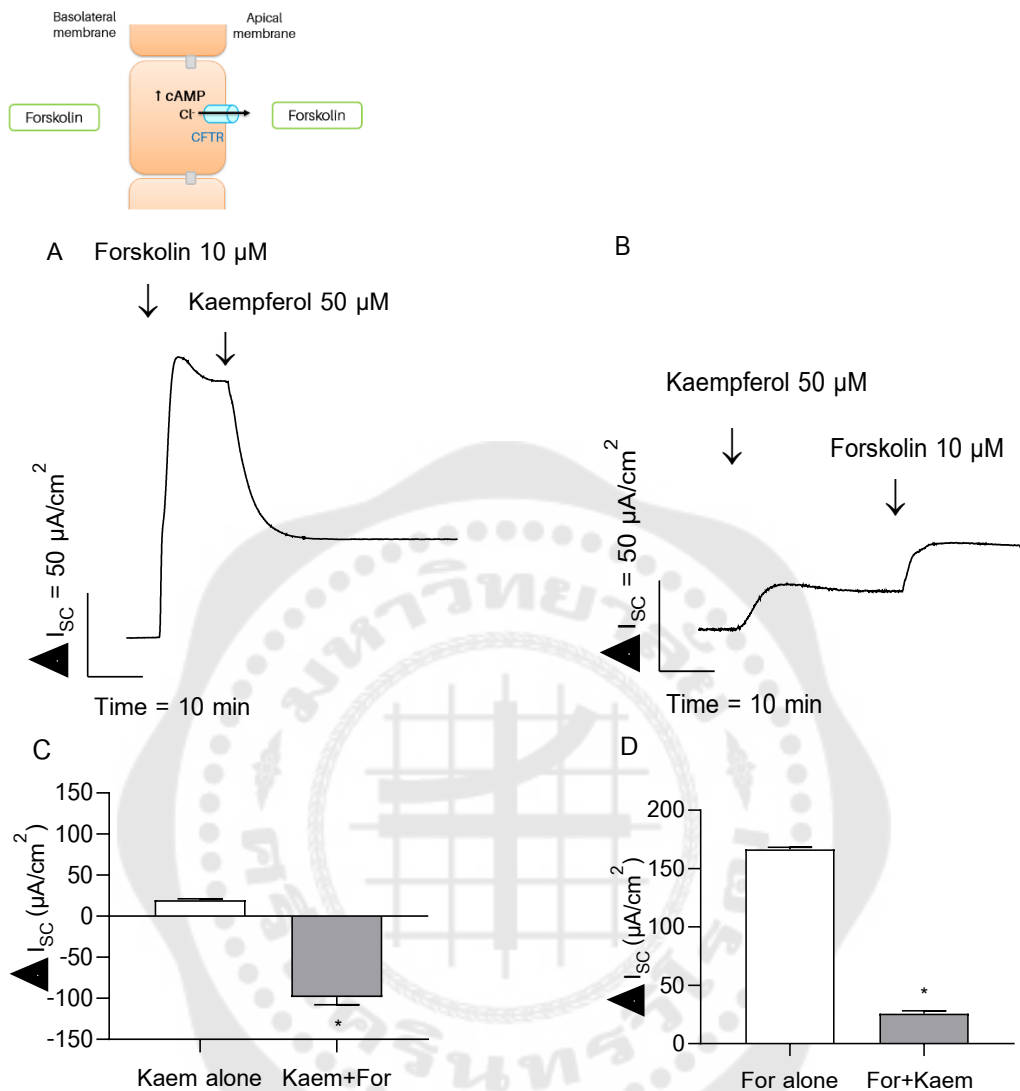


Figure 47 Effect of kaempferol on forskolin-activated transepithelial chloride secretion. (A) A representative  $I_{\text{SC}}$  tracing showed the effect of forskolin (10  $\mu\text{M}$ , apical and basolateral) on a significant increase in the  $I_{\text{SC}}$  response and a marked decreased  $I_{\text{SC}}$  following the addition of kaempferol (50  $\mu\text{M}$ , apical and basolateral). (B) A representative  $I_{\text{SC}}$  tracing showed the effect of kaempferol on the increase in the  $I_{\text{SC}}$  response and an additive increased  $I_{\text{SC}}$  following the addition of forskolin. (C) Bar graph showed average changes in the  $I_{\text{SC}}$  responding to kaempferol alone and in the presence of forskolin, or (D) in the  $I_{\text{SC}}$  responding to forskolin alone and in the presence of kaempferol. Each value represented mean  $\pm$  SEM (n=3-4). \*P<0.05 compared to kaempferol alone or forskolin alone by Student t-test.

### Part 3. The effect of kaempferol on the apical membrane permeability in the permeabilized monolayer

#### 3.1 The effect of kaempferol on the apical chloride current

##### 3.1.1 The direct effect of kaempferol on the apical chloride current

Our experiments found that kaempferol increased  $I_{SC}$  response in the T84 intact monolayer. We further studied the effect of kaempferol on apical membrane permeability in permeabilized T84 cell monolayers. An apical chloride current ( $I_{Cl}$ ) was measured by permeabilizing the basolateral monolayer with amphotericin B and filled with a high-concentrate KCl Ringer solution in the apical side of monolayer and a  $KMeSO_4$  Ringer solution in the basolateral side. The effect of kaempferol with or without various types of channel blockers on the permeabilized monolayer was tested in a similar manner as the intact monolayer. Application of kaempferol (50  $\mu$ M, apical and basolateral) was found to maximally increase  $I_{Cl}$  by  $-59.83 \pm 3.75 \mu A/cm^2$  (n=6) (figure 48A), as shown by the negative deflection of the current. Pretreatment with  $Na^+$  channel blocker amiloride (10  $\mu$ M, apical) slightly decreased the  $I_{Cl}$  baseline ( $0.97 \pm 0.42 \mu A/cm^2$ , n=4), as shown by the slight positive deflection of the current and did not inhibit the stimulatory effect of kaempferol on the  $I_{Cl}$  ( $51.56 \pm 2.30 \mu A/cm^2$ , n=4) (figure 48B). Conversely, pretreatment of CFTR channel inhibitors CFTRinh-172 (50  $\mu$ M, apical) markedly decreased the basal  $I_{Cl}$  and almost completely abolished the kaempferol-induced increase in  $I_{Cl}$  by 99% ( $-0.62 \pm 1.02 \mu A/cm^2$ , n=3) (figure 48C). Likewise, CaCCinh-A01 (30  $\mu$ M, apical), CaCC inhibitor decreased the basal  $I_{Cl}$  and partially inhibited the kaempferol-activated  $I_{Cl}$  by 68% ( $-19.09 \pm 6.34 \mu A/cm^2$ , n=4) (figure 48D). The kaempferol-activated  $I_{Cl}$  was significantly decreased by  $Cl^-$  inhibitors CFTRinh-172 and CaCCinh-A01 compared to kaempferol alone, but not  $Na^+$  channel blocker amiloride (figure 49). Moreover, CaCCinh-A01 completely inhibited the residual  $I_{Cl}$  induced by kaempferol in the presence of CFTRinh-172 (n=3) (figure 50).

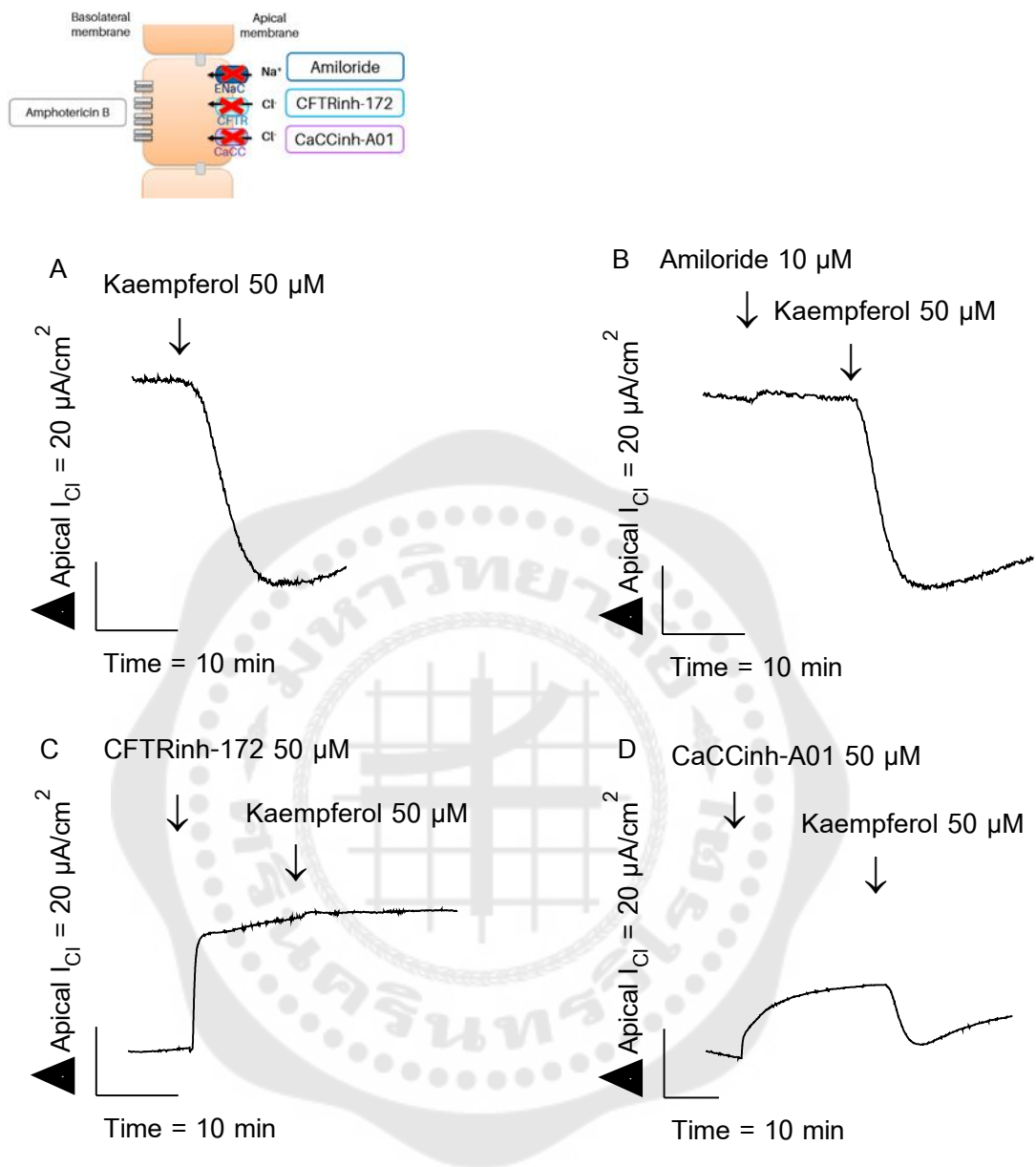


Figure 48 The effect of kaempferol on apical chloride current in the basolaterally permeabilized T84 monolayer. Representative  $I_{Cl}$  tracings showed the effect of (A) kaempferol (50  $\mu$ M, apical and basolateral) on a marked increase in the  $I_{Cl}$  response and the effect of (B) amiloride (10  $\mu$ M, apical), (C) CFTRinh-172 (50  $\mu$ M, apical), or (D) CaCCinh-A01 (30  $\mu$ M, apical) on the decrease in the  $I_{Cl}$  response and the significant increased  $I_{Cl}$ , the completely inhibited the increased  $I_{Cl}$ , or the partially inhibited the increased  $I_{Cl}$ , respectively, following the addition of kaempferol.

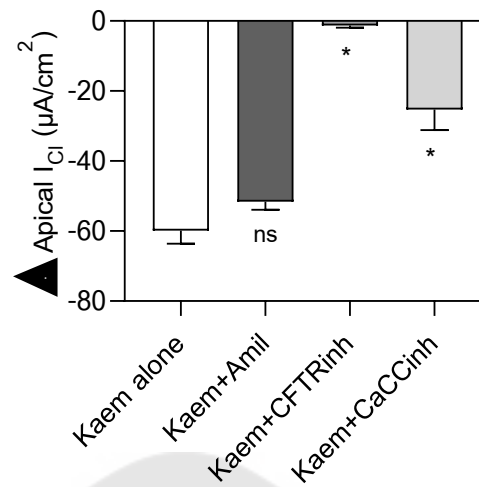


Figure 49 The effect of the  $Na^+$  channel blocker and  $Cl^-$  channel inhibitors on the kaempferol-activated apical chloride current in the basolaterally permeabilized T84 monolayer. Bar graph showed average changes in the  $I_{Cl}$  responding to kaempferol alone or in the presence of amiloride, CFTRinh-172, or CaCCinh-A01. Each value represented mean  $\pm$  SEM (n=3-4). \*P<0.05 compared to kaempferol alone by one-way ANOVA and Dunnett's post-hoc test.

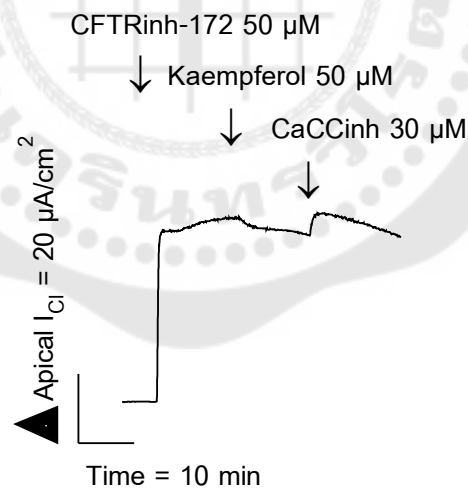


Figure 50 The effect of the CFTR  $Cl^-$  channel inhibitor on the kaempferol-activated apical chloride current in the basolaterally permeabilized T84 monolayer. A Representative  $I_{Cl}$  tracing showed the effect of CFTRinh-172 on a marked decrease in the  $I_{Cl}$  response, a slight increased  $I_{Cl}$  following the addition of kaempferol, and then inhibiting residual kaempferol-increased  $I_{Cl}$  by CaCCinh-A01.

### 3.1.2 The effect of kaempferol on cAMP-activated chloride current

To further investigate the involvement of cAMP in kaempferol-activated  $I_{Cl}$ , the kaempferol response was determined under  $Cl^-$  secretion activated by forskolin or 8cpt-cAMP, respectively. The kaempferol-activated  $I_{Cl}$ , determined before and after adding forskolin or 8cpt-cAMP, was shown in figure 51 or 52. Addition of forskolin (10  $\mu$ M, apical and basolateral) or 8cpt-cAMP (100  $\mu$ M, basolateral) stimulated the maximal  $I_{Cl}$  response to  $-223.85 \pm 0.94 \mu A/cm^2$  (figure 51A-C, n=4) or  $-222.3 \pm 25.39 \mu A/cm^2$  (figure 52A-C, n=3), respectively. After that, addition of kaempferol (50  $\mu$ M, apical and basolateral) were not changed the forskolin or 8cpt-cAMP-stimulated  $I_{Cl}$  from original response pattern (figure 51A-52A). In addition, pretreatment with kaempferol increased the  $I_{Cl}$  and decreased the forskolin or 8cpt-cAMP-activated  $I_{Cl}$  to  $-21.19 \pm 4.99 \mu A/cm^2$  (figure 51B, n=4) or  $-3.01 \pm 0.52 \mu A/cm^2$  (figure 52B, n=3), respectively, which less than the treatment of forskolin alone by 91% (figure 51C) or 8cpt-cAMP alone by 99% (figure 52C).



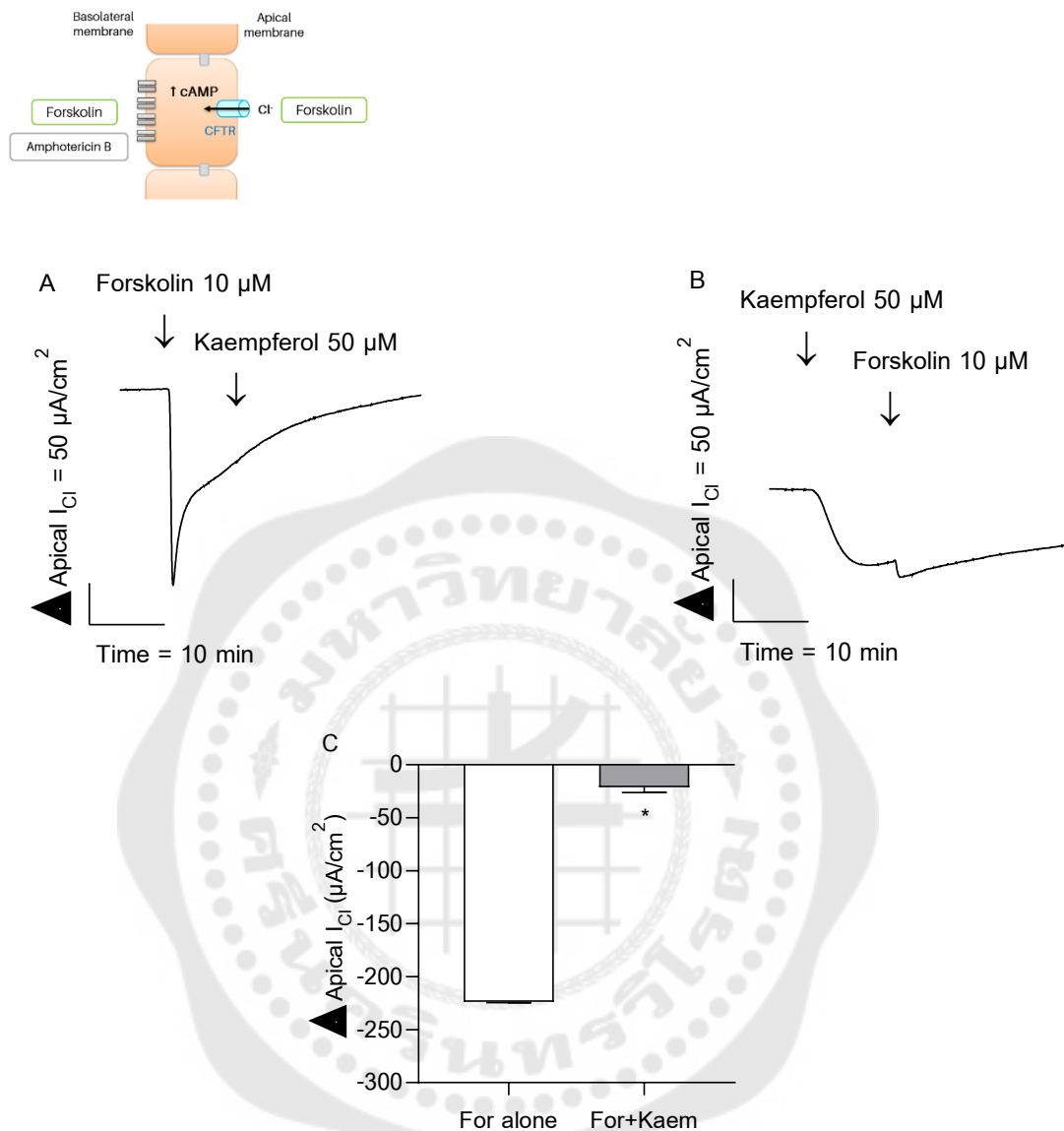


Figure 51 The effect of kaempferol on forskolin-activated chloride current in the basolaterally permeabilized T84 monolayer. (A) A representative  $I_{\text{Cl}^-}$  tracing showed the effect of forskolin (10  $\mu\text{M}$ , apical and basolateral) on a significant increase in the  $I_{\text{Cl}^-}$  response and no increase in the  $I_{\text{Cl}^-}$  response following the addition of kaempferol (50  $\mu\text{M}$ , apical and basolateral). (B) A representative  $I_{\text{Cl}^-}$  tracing showed the effect of kaempferol on the increase in the  $I_{\text{Cl}^-}$  response and a slightly increased  $I_{\text{Cl}^-}$  following the addition of forskolin. (C) Bar graph showed average changes in the  $I_{\text{Cl}^-}$  responding to forskolin alone and in the presence of kaempferol. Each value represented mean  $\pm$  SEM (n=4). \*P<0.05 compared to forskolin alone by Student t-test.

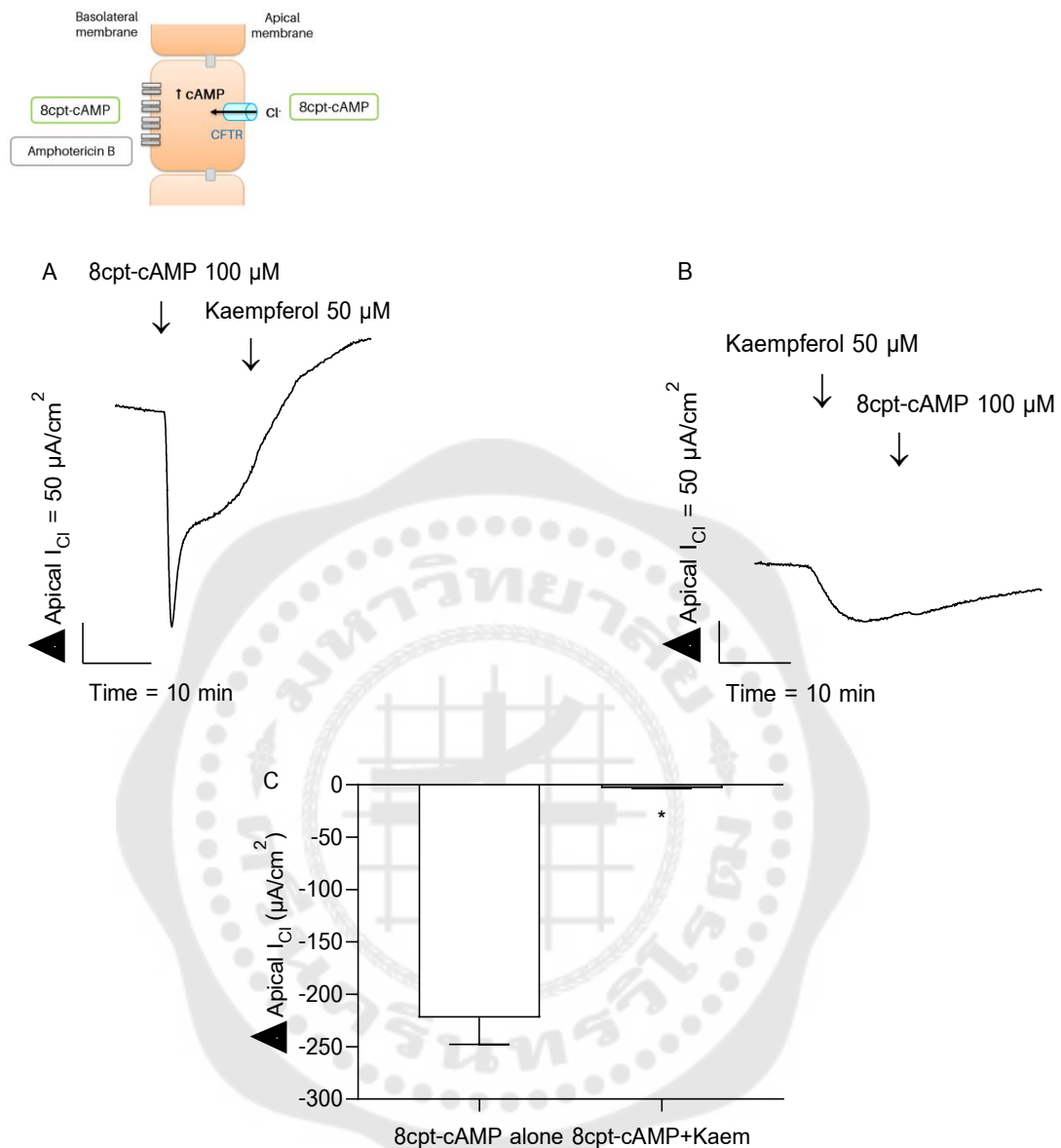


Figure 52 The effect of kaempferol on 8-cpt-cAMP-activated chloride current in the basolaterally permeabilized T84 monolayer. (A) A representative  $I_{Cl}$  tracing showed the effect of 8cpt-cAMP (100  $\mu$ M, basolateral) on a significant increase in the  $I_{Cl}$  response and no increase in the  $I_{Cl}$  response following the addition of kaempferol (50  $\mu$ M, apical and basolateral). (B) A representative  $I_{Cl}$  tracing showed the effect of kaempferol on the increase in the  $I_{Cl}$  response and a small increased  $I_{Cl}$  following the addition of 8cpt-cAMP. (C) Bar graph showed average changes in the  $I_{Cl}$  responding to 8cpt-cAMP alone and in the presence of kaempferol. Each value represented mean  $\pm$  SEM (n=4). \*P<0.05 compared to forskolin alone by Student t-test.

### 3.1.3 The effect of kaempferol on $\text{Ca}^{2+}$ -activated chloride current

To evaluate the involvement of intracellular  $\text{Ca}^{2+}$  in kaempferol-activated  $I_{\text{Cl}}$ , the kaempferol response was examined under increasing intracellular  $\text{Ca}^{2+}$  levels by  $\text{Ca}^{2+}$  ionophore A23187. Pretreatment of the monolayer with  $\text{Ca}^{2+}$  ionophore (1  $\mu\text{M}$ , apical) produced the increased  $I_{\text{Cl}}$  by  $-9.48 \pm 2.17 \mu\text{A}/\text{cm}^2$  (n=4). A subsequent addition of kaempferol (50  $\mu\text{M}$ , apical and basolateral) increased the  $I_{\text{Cl}}$  response to  $-53.07 \pm 1.83 \mu\text{A}/\text{cm}^2$  (n=4) (figure 53A). The kaempferol-activated  $I_{\text{Cl}}$  in the presence of  $\text{Ca}^{2+}$  ionophore was not significantly different compared to kaempferol alone (figure 53B).



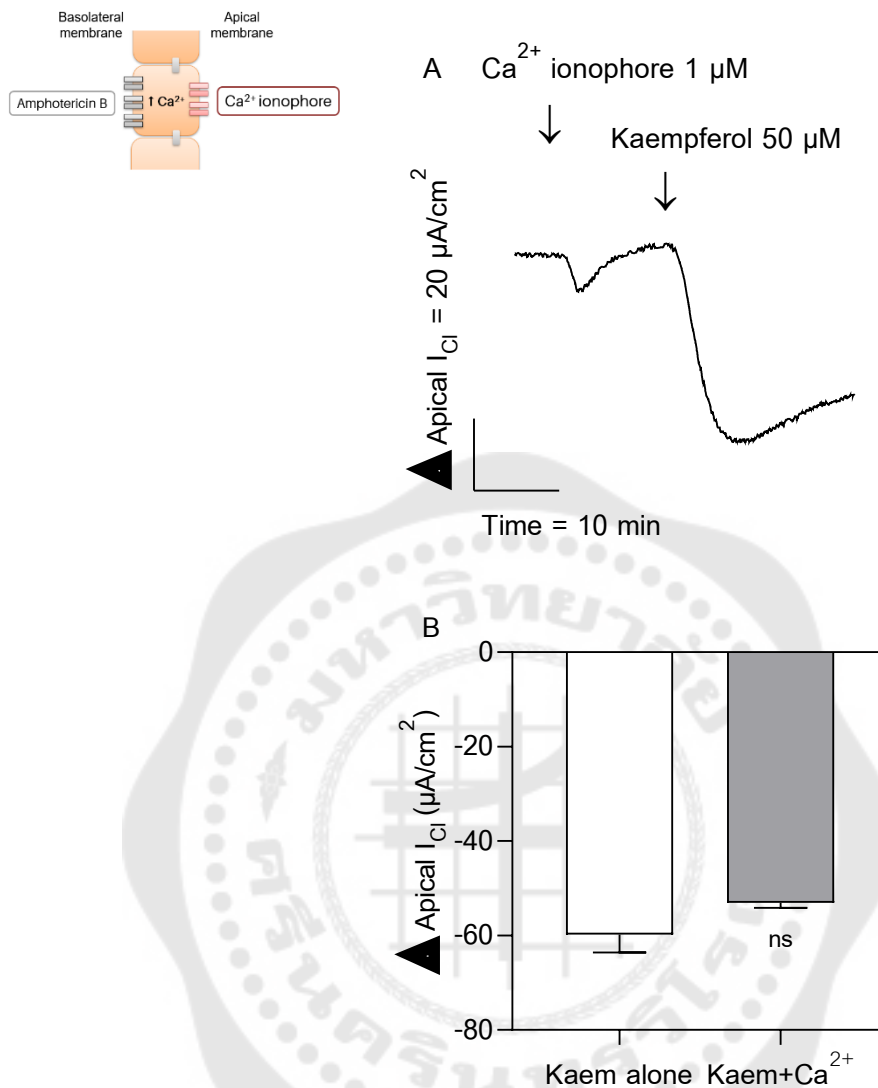


Figure 53 The effect of kaempferol on  $Ca^{2+}$ -activated chloride current in the basolaterally permeabilized T84 monolayer. (A) A representative  $I_{Cl}$  tracing showed the effect of  $Ca^{2+}$  ionophore (1  $\mu M$ , apical) on a slight increase in the  $I_{Cl}$  response and a marked increased  $I_{Cl}$  following the addition of kaempferol (50  $\mu M$ , apical and basolateral). (B) Bar graph showed average changes in the  $I_{Cl}$  responding to kaempferol alone or in the presence of  $Ca^{2+}$  ionophore. Each value represented mean  $\pm$  SEM (n=4).

### 3.2 The effect of kaempferol on the basolateral membrane permeability

To investigate the effect of kaempferol on basolateral membrane permeability, a basolateral potassium current ( $I_{KB}$ ) was assessed by permeabilizing the apical side of monolayers with amphotericin B, bathed with a  $KMeSO_4$  Ringer solution in the apical side and a  $NaMeSO_4$  Ringer solution in the basolateral side. Kaempferol (50  $\mu M$ , apical and basolateral) increased the maximum  $I_{KB}$  by  $9.80 \pm 2.65 \mu A/cm^2$  within 7-8 min, as shown by the positive deflection of the current, and then declined slightly to a constant level above the baseline at  $6.47 \pm 0.83 \mu A/cm^2$  ( $n=5$ , figure 54).

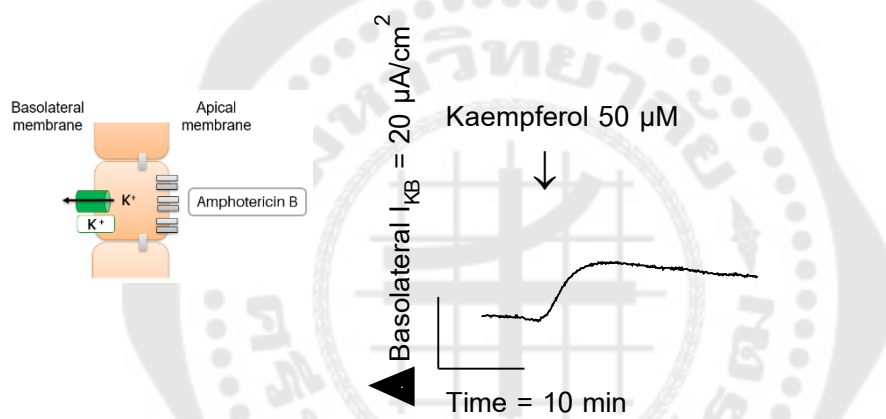
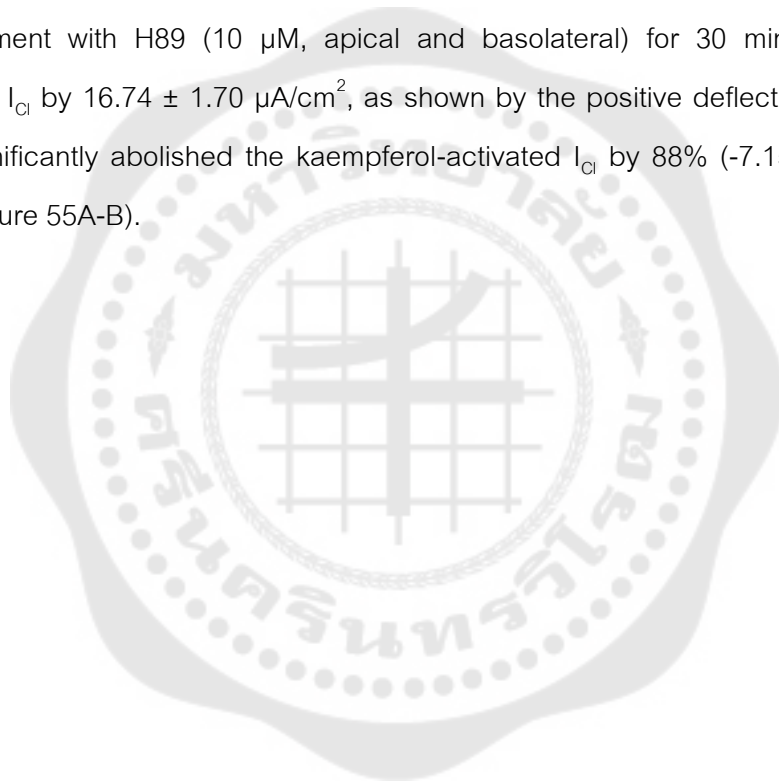


Figure 54 The effect of kaempferol on the basolateral potassium current in the apically permeabilized T84 monolayer. A representative  $I_{KB}$  tracing showed the effect of kaempferol (50  $\mu M$ , apical and basolateral) on the increase in the  $I_{KB}$  response. Each value represented mean  $\pm$  SEM ( $n=5$ ).

#### Part 4. Evaluation of the underlying mechanism of kaempferol through cAMP-dependent protein kinase, tyrosine kinase and tyrosine phosphatase signaling pathway

##### 4.1 The effect of kaempferol on cAMP-dependent protein kinase signaling pathway

To investigate the mechanism of kaempferol-activated  $\text{Cl}^-$  secretion, the protein kinase A inhibitor H89 was used to test the effect of kaempferol mediated by a cAMP-dependent protein kinase. This experiment was carried out in basolateral-to-apical  $\text{Cl}^-$  gradient condition in amphotericin B-permeabilized basolateral membrane. Pretreatment with H89 (10  $\mu\text{M}$ , apical and basolateral) for 30 min decreased the baseline  $I_{\text{Cl}}$  by  $16.74 \pm 1.70 \mu\text{A}/\text{cm}^2$ , as shown by the positive deflection of the current and significantly abolished the kaempferol-activated  $I_{\text{Cl}}$  by 88% ( $-7.15 \pm 2.13 \mu\text{A}/\text{cm}^2$ ,  $n=4$ ) (figure 55A-B).



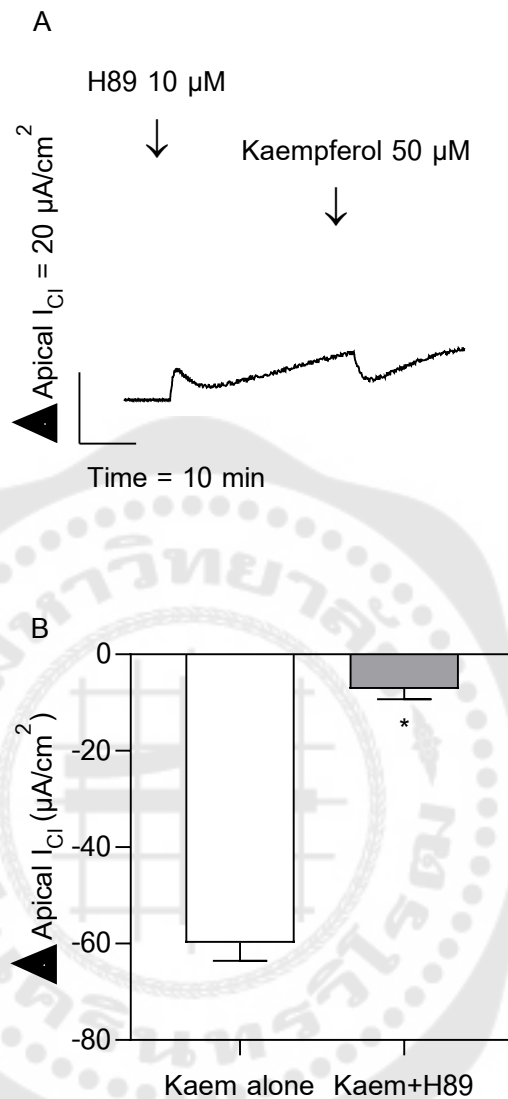


Figure 55 The effect of protein kinase A inhibitor H89 on the kaempferol-activated apical chloride current in the basolaterally permeabilized T84 monolayer. (A) A representative  $I_{\text{Cl}}$  tracing showed the effect of protein kinase A inhibitor H89 (10  $\mu\text{M}$ , apical and basolateral) on a slight decrease in the  $I_{\text{Cl}}$  response and a small increased  $I_{\text{Cl}}$  following the addition of kaempferol to kaempferol (50  $\mu\text{M}$ , apical and basolateral). (B) Bar graph showed average changes in the  $I_{\text{Cl}}$  responding to kaempferol alone and in the presence of H89. Each value represented mean  $\pm$  SEM ( $n=4$ ). \* $P<0.05$  when compared to kaempferol alone by Student t-test.

#### 4.2 The effect of kaempferol on tyrosine kinase and tyrosine phosphatase signaling pathway

Since  $\text{Cl}^-$  secretion through CFTR is also regulated by tyrosine kinase or tyrosine phosphatase. To evaluate the effect of kaempferol-activated  $\text{Cl}^-$  secretion controlled by tyrosine kinase or tyrosine phosphatase, tyrosine kinase inhibitors (AG490 and tyrphostin A23) or tyrosine phosphatase inhibitor (vanadate) were added to the apical and basolateral solutions for 30 minutes before testing by kaempferol. AG490 (10  $\mu\text{M}$ ) or tyrphostin A23 (100  $\mu\text{M}$ ) reduced the baseline  $I_{\text{Cl}}$  by  $-19.73 \pm 5.95 \mu\text{A}/\text{cm}^2$  ( $n=4$ , figure 56A) or  $-15.21 \pm 0.52 \mu\text{A}/\text{cm}^2$  ( $n=3$ , figure 56B) and little inhibited the kaempferol-activated  $I_{\text{Cl}}$  by 16% ( $-50.04 \pm 4.26 \mu\text{A}/\text{cm}^2$ ,  $n=3$ ) (figure 56A-D) or by 16% ( $-50.00 \pm 1.87 \mu\text{A}/\text{cm}^2$ ,  $n=3$ ) (figure 56B-D), respectively. Furthermore, vanadate (100  $\mu\text{M}$ ) reduced the baseline  $I_{\text{Cl}}$  by  $-20.88 \pm 0.96 \mu\text{A}/\text{cm}^2$  ( $n=4$ , figure 56C) and slightly increased the kaempferol-activated  $I_{\text{Cl}}$  by 3% ( $-61.66 \pm 5.06 \mu\text{A}/\text{cm}^2$ ,  $n=3$ ) (figure 56C-D). However, the kaempferol-activated  $I_{\text{Cl}}$  was not significantly different when compared pretreatment with tyrosine kinase inhibitors AG490 or tyrphostin A23 and a tyrosine phosphatase inhibitor vanadate to kaempferol alone (figure 56D).



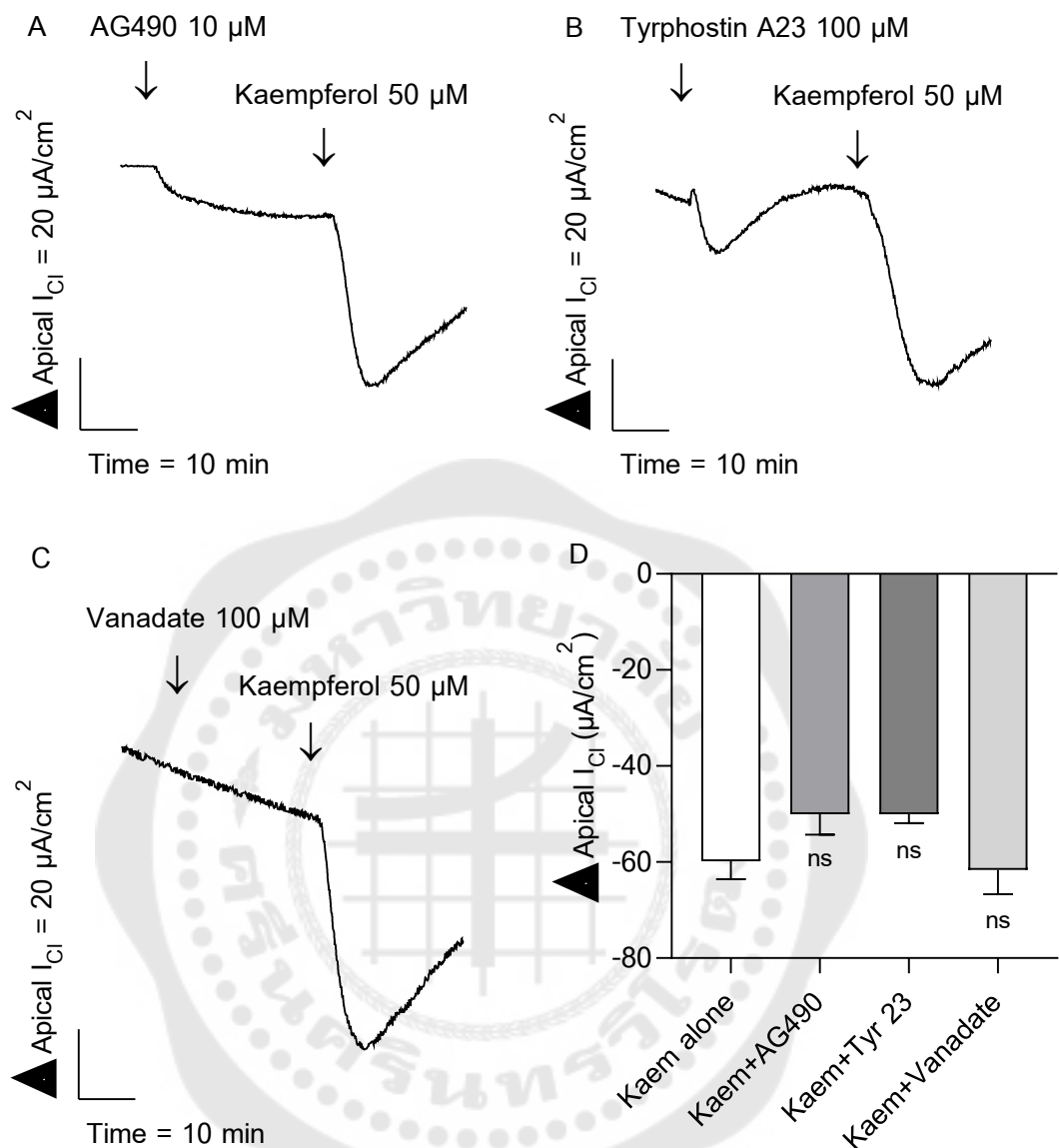


Figure 56 The effect of tyrosine kinase and tyrosine phosphatase inhibitors on the kaempferol-activated apical chloride current in the basolaterally permeabilized T84 monolayer. Representative  $I_{Cl}$  tracings showed the effect of tyrosine kinase inhibitors (A) AG490 (10  $\mu$ M) or (B) tyrphostin A23 (100  $\mu$ M) and the tyrosine phosphatase (C) vanadate (100  $\mu$ M) on the increase in the  $I_{Cl}$  response and a marked increased  $I_{Cl}$  following the addition of kaempferol to kaempferol (50  $\mu$ M, apical and basolateral). (D) Bar graph showed average changes in the  $I_{Cl}$  responding to kaempferol alone and in the presence of AG490, tyrphostin A23, or vanadate. Each value represented mean  $\pm$  SEM (n=3).

### Part 5. The effect of kaempferol on the ion transport protein expression

Our study showed that kaempferol had an acute effect on stimulating chloride secretion mainly through CFTR protein. To study the effect of kaempferol on regulating ion transport at a genomic level, we further investigated the genetic effect of kaempferol on the expression of CFTR protein. The cells were cultured in the complete media until they reached 70-80% confluence before treatment with kaempferol. The cell lysates were collected to determine CFTR protein expressions by western blot analysis. As shown in figure 56, the antibodies of CFTR and  $\beta$ -actin recognized the protein bands with a molecular mass of 165 and 43 kDa, respectively (figure 57A).

The protein band density calculated as the expression ratio of CFTR to  $\beta$ -actin showed that the DMSO group slightly increased the CFTR expression ratio compared to no treatment in the control group but no significant difference. Treatment of the cells with kaempferol (50  $\mu$ M) for 24 h, but not 48 h, significantly increased the CFTR expression (figure 57B) compared to the DMSO. In contrast, treatment with 100  $\mu$ M of kaempferol for 24 h and 48 h did not affect the expression of CFTR (figure 57B). However, CFTR protein expressions were decreased by DMSO and both concentrations of kaempferol when treatment for 48 h compared to treatment for 24 h.

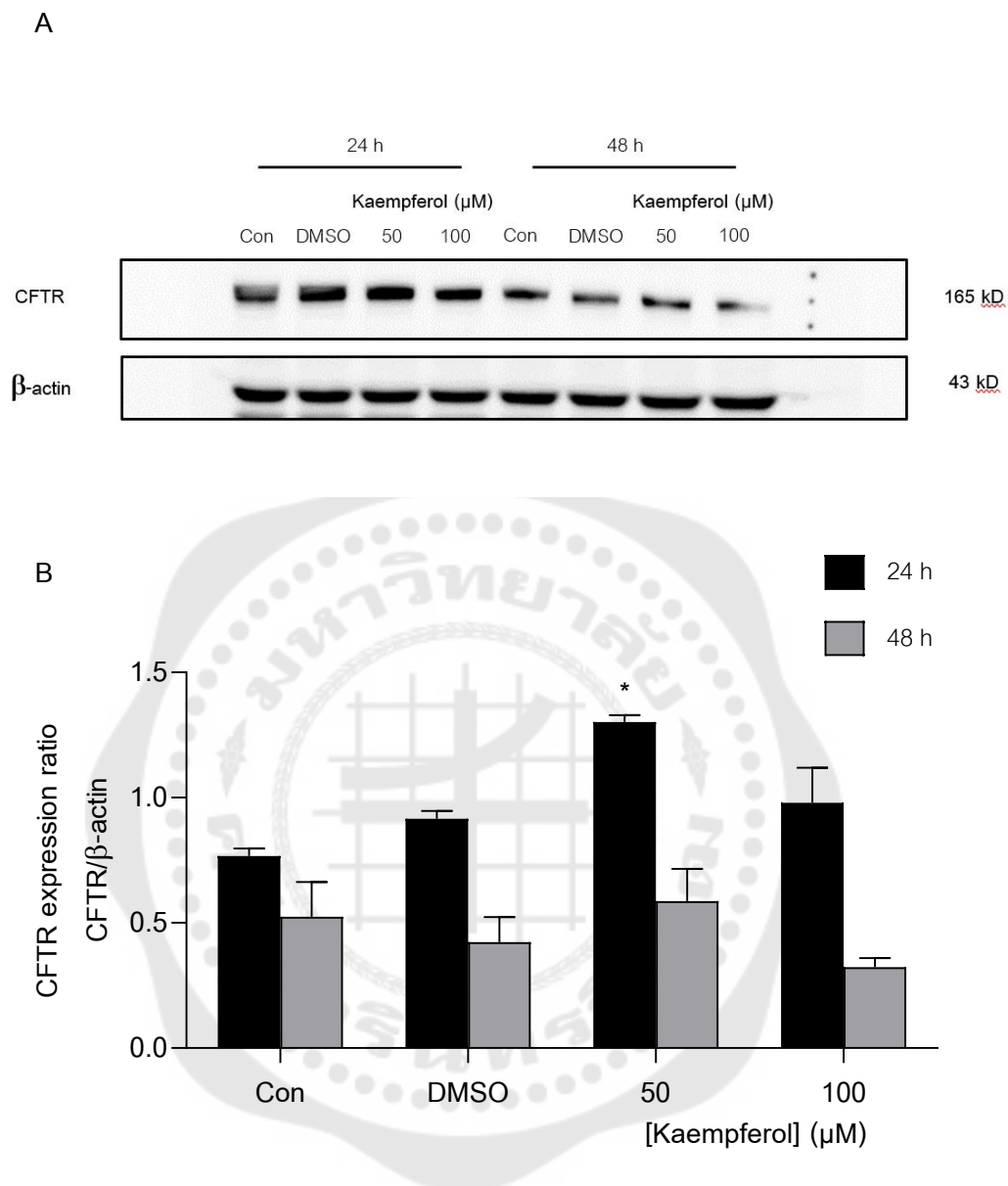


Figure 57 Effect of kaempferol on CFTR protein expression in T84 cells. The cells cultured in complete media (Con) were incubated with DMSO or kaempferol at 50 and 100  $\mu$ M for 24 h or 48 h. Total proteins were extracted to determine the CFTR protein expression by western blot. **(A)** Representative band density of CFTR and  $\beta$ -actin protein expression. **(B)** Densitometric analysis of CFTR expression was normalized to housekeeping protein  $\beta$ -actin. Each value represented mean  $\pm$  SEM (n=3). \*P< 0.05 compared to corresponding DMSO by two-way ANOVA followed by Sidak's multiple comparison post-test.

## CHAPTER 5

### SUMMARY DISCUSSION AND SUGGESTION

The colonic epithelium is essential in maintaining physiological homeostasis by controlling proper  $\text{Na}^+$  absorption and  $\text{Cl}^-$  secretion. The loss of balance or problems in absorption and secretion via the colonic epithelium can result in diarrhea or constipation.<sup>(19)</sup> Flavonoids are a group of natural substances that have been shown to regulate ion transport in rat and human colonic epithelium.<sup>(27, 30, 31, 196)</sup> Kaempferol which is flavanol, a subclass of flavonoids, has been identified as the most potent activator of  $\text{Cl}^-$  secretion in human airway epithelial cells.<sup>(33)</sup> This report by Illek et al. provides information to support that kaempferol can be used as a compound for drug development targeting CFTR activation. Although kaempferol effect on colonic epithelium seems to induce a secretory response,<sup>(197)</sup> the effect and cellular mechanisms of kaempferol on the absorptive and secretory function in colonic epithelial cells remain unknown. This draws our interest in studying the effect and cellular mechanism of kaempferol on the regulation of ion transport in colonic epithelium using the human colonic adenocarcinoma cell line (T84).

First, we evaluated the cytotoxic effect of kaempferol. Our results showed that all concentrations of kaempferol when treated for 24 and 48 h had a percentage of cell viability over 90%, indicating no toxicity to T84 cells. Moreover, kaempferol increased cell viability in a concentration-dependent manner except at the concentration of 100  $\mu\text{M}$ . Our study corresponded with a previous study showing kaempferol is not toxic to other human colon cancer cell lines.<sup>(198)</sup> This study has shown that treatment with a high dose of kaempferol (150  $\mu\text{M}$ ) for 3 h had no cytotoxicity effect on HT-29 and Caco-2 cells, at the same time, also increased the percentage of cell viability. In addition, the high safety of kaempferol on normal epithelial cells has been evidenced.<sup>(199)</sup> Our findings indicated the appropriate and non-toxic concentrations of kaempferol used in the present study.

Our study employed Ussing chamber technique to measure  $I_{\text{sc}}$  which represented the transepithelial ion transport across the T84 cell monolayer. Apical and

basolateral additions of kaempferol at concentrations ranging from 1 - 50  $\mu\text{M}$  stimulated the  $I_{\text{SC}}$  in a concentration-dependent manner, but high concentration (100  $\mu\text{M}$ ) inhibited the  $I_{\text{SC}}$ . The biphasic  $I_{\text{SC}}$  response of kaempferol was not unpredictable. Some flavonols have been shown to exert stimulatory effects at low concentrations and inhibitory effects at high concentrations. For example, flavonol quercetin and kaempferol have been found to have the biphasic  $I_{\text{SC}}$  response in T84, CFTR-transduced fisher rat thyroid (FRT), or human sinonasal epithelial (HSNE) cells.<sup>(197, 200-202)</sup> Likewise, a flavone apigenin has been demonstrated as an activator of CFTR-mediated  $\text{Cl}^-$  currents at low concentrations and a blocker at high concentrations in cells with high CFTR expression.<sup>(203)</sup> The inhibitory effects of flavone and flavonol may be because of the molecular structure as suggested by Illek and Schuier. They have identified the central aromatic-pyrone of the flavone molecule that determines the affinity to the binding site, and the 4'-hydroxyl structure that defines the efficiency as a flavone-based blocker.<sup>(203)</sup> Moreover, quercetin and luteolin are potent inhibitors of  $\text{Cl}^-$  current due to their molecular characteristics of a 4'-hydroxyl and a central-pyrone ring.<sup>(200)</sup> As kaempferol has similar molecular structure to quercetin, it could be anticipated that the inhibitory effect on  $I_{\text{SC}}$  at the high concentration in the present study is possibly due to a 4'-hydroxyl and a central-pyrone ring in the chemical structure of kaempferol. Alternatively, the high kaempferol concentration could affect other unidentified channels or transporters that results in inhibition of  $\text{Cl}^-$  secretion.

In intact monolayer, the increased  $I_{\text{SC}}$  by kaempferol was not changed in the presence of a  $\text{Na}^+$  channel blocker amiloride, suggesting that the effect of kaempferol is not involving  $\text{Na}^+$  absorption. To test the involvement of  $\text{Cl}^-$  secretion in the kaempferol effect by applications of various  $\text{Cl}^-$  channel blockers, we found that the kaempferol-activated  $I_{\text{SC}}$  was markedly inhibited after pretreatment with NPPB and glibenclamide, which are widely used as CFTR and nonselective anion inhibitors.<sup>(82)</sup> In contrast, pretreatment with CFTRinh-172, a selective inhibitor of CFTR, as well as CaCC inhibitors, CaCCinh-A01 and DIDS, failed to inhibit the kaempferol  $I_{\text{SC}}$  response. However, the selective CFTR and CaCC inhibitors did not inhibit the kaempferol-increased  $I_{\text{SC}}$ ; the

addition of CFTRinh-172 after kaempferol treatment showed a marked decrease in the kaempferol response. Nevertheless, CaCCinh-A01 slightly decreased the kaempferol response. These results suggest kaempferol may increase  $I_{sc}$  by activating anion secretion mainly through CFTR. In addition, results from anion substitution experiments revealed that the kaempferol-activated  $I_{sc}$  was abolished in  $Cl^-$  free solution and in  $Cl^-$  and  $HCO_3^-$  free solutions but not  $HCO_3^-$  free solution, indicating that the kaempferol effect depends on  $Cl^-$  secretion. Additionally, the increased  $I_{sc}$  by kaempferol was inhibited in the presence of bumetanide, a specific blocker of basolateral NKCC. All these results support that kaempferol stimulates  $Cl^-$  secretion possibly through CFTR. The finding that specific inhibitor CFTRinh-172 failed to inhibit the kaempferol response could be due to the movement of intracellular  $Cl^-$  out of cells across the apical membrane through other non-CFTR channels.

Since the permeabilized monolayer permits direct passage of ions to channels bypassing the cell membrane, it enables better control of ion concentration gradients and provides specific data on the kinetics and properties of the ion channels. Experiments with permeabilized T84 monolayer help to verify the effect of kaempferol on the specific type of  $Cl^-$  channels and other channels or cotransporters that mediate  $Cl^-$  secretion. Our findings demonstrated that kaempferol increases  $Cl^-$  secretion in T84 cells, which was supported by the following results. Firstly, the kaempferol induced a marked increase in apical  $Cl^-$  current ( $I_{Cl}$ ) which is not sensitive to amiloride. Secondly, the increased  $I_{Cl}$  induced by Kaempferol was completely inhibited after pretreatment with CFTRinh-172. This was correlated with the significant inhibition of the kaempferol-stimulated  $I_{sc}$  by glibenclamide and NPPB in intact monolayers. These results indicate that kaempferol activates  $Cl^-$  secretion mainly via the CFTR channels. Thirdly, the kaempferol-stimulated  $I_{Cl}$  was about 60% inhibited by CaCCinh-A01, suggesting that kaempferol-stimulated  $Cl^-$  secretion is in part mediated through CaCC. Lastly, the residual kaempferol-stimulated  $I_{Cl}$  in the presence of CFTRinh-172 was inhibited by CaCCinh-A01. All together indicate that kaempferol stimulates  $Cl^-$  secretion via activating apical  $Cl^-$  current mainly through CFTR and partially through CaCC.

The kaempferol results obtained from permeabilized monolayers contrast with those obtained from intact monolayers in that the kaempferol-induced increase in  $I_{Cl}$ , but not  $I_{SC}$ , was not inhibited by both CFTRinh-172 and CaCCinh-A01. These different responses could be possibly due to different experimental conditions. In our experiments, intact monolayers were bathed with the same Normal Ringer's solution in apical and basolateral membranes to eliminate chemical driving force. In contrast, permeabilized monolayers were bathed with a high-concentrated KCl Ringer solution in the apical membrane and a  $KMeSO_4$  Ringer solution as an intracellular solution in the basolateral membrane, which creates a  $Cl^-$  concentration gradient. The high  $Cl^-$  gradient solutions will create electrochemical driving force for apical  $Cl^-$  current through existing open  $Cl^-$  channel as evidenced by high basal  $I_{Cl}$ , as compared to a little change in basal  $I_{SC}$ , which was markedly abolished by CFTR blockers. This CFTR blocker also inhibited a successive kaempferol  $I_{Cl}$  response. Although a previous patch-clamp study has demonstrated that binding of CFTRinh-172 occurs on both open and closed states of CFTR channels, the apparent binding affinity appears to be increased in conditions of the NBD dimerized open state.<sup>(204)</sup> Thus, CFTRinh-172 could be more likely to bind to CFTR channels in the open state, which can result in more effective inhibition of CFTR activity. In addition, CFTRinh-172 has a single negative charge at physiological pH, and thus its ability into the cytoplasm is dependent on cell plasma membrane potential.<sup>(82)</sup> Nevertheless, the result of kaempferol-stimulated  $I_{SC}$  not being inhibited by CaCCinh-A01 was still unexplained. Our results contradicted the previous study showing that the increased  $I_{SC}$  by quercetin, a flavonol structurally similar to kaempferol, was completely abolished by CaCCinh-A01 in human colon adenocarcinoma cells (HT-29).<sup>(196)</sup>

Basically,  $Na^+K^+$ -ATPase cooperatively working with NKCC cotransporters and  $K^+$  channels at the basolateral membrane is required to generate the electrochemical driving force for  $Cl^-$  secretion. The  $Cl^-$  secretory process starts with the active entry of  $Cl^-$  across the basolateral membrane via the NKCC cotransporters, which uses the  $Na^+K^+$ -ATPase established inwardly directed  $Na^+$  gradient to accumulate  $Cl^-$  above its electrochemical equilibrium.<sup>(205)</sup> This process causes  $Cl^-$  move out of the cell through

opening apical  $\text{Cl}^-$  channels. In the meantime, recycle of  $\text{K}^+$  through basolateral  $\text{K}^+$  channels for properly function of the  $\text{Na}^+-\text{K}^+$ -ATPase will sustain a hyperpolarized driving force for  $\text{Cl}^-$  secretion.<sup>(114)</sup> Our experiment with apically permeabilized T84 monolayer bathed with high gradient  $\text{K}^+$  solution revealed the direct effect of kaempferol on stimulation of basolateral  $\text{K}^+$  current ( $I_{\text{KB}}$ ). Kaempferol produced an initial increase followed by a slight decrease in  $I_{\text{KB}}$ . The subsequent slight decrease in the  $I_{\text{KB}}$  was likely a result of a slight decrease in the  $I_{\text{SC}}$ . Unfortunately, the specific types of  $\text{K}^+$  channels that respond to kaempferol are currently unclear and under investigation. This finding together with the result of kaempferol-stimulated  $I_{\text{SC}}$  being inhibited by the NKCC inhibitor bumetanide supports the kaempferol effect on stimulating  $\text{Cl}^-$  secretion across the T84 monolayer. This increased  $I_{\text{KB}}$  also hyperpolarizes the basolateral membrane leading to  $\text{Cl}^-$  exit through apical  $\text{Cl}^-$  channels. Meanwhile, NKCC increases  $\text{Cl}^-$  accumulation within cells. Taken together, all results from both intact and permeabilized monolayers support that kaempferol enhances  $\text{Cl}^-$  secretion by promoting the driving force created by NKCC cotransporters and basolateral  $\text{K}^+$  channels. Our findings correspond to previous data showing flavonol-induced  $\text{Cl}^-$  secretion by activating CFTR and basolateral NKCC.<sup>(206)</sup> Furthermore, many flavonoids have been shown activation of basolateral  $\text{K}^+$  channels.<sup>(28, 162, 196, 207, 208)</sup>

To further explore the kaempferol effect on modulation of cAMP-activated  $\text{Cl}^-$  secretion, kaempferol was applied before and after forskolin, an activator of adenylate cyclase or 8cpt-cAMP, an activator of cAMP-dependent protein kinase. Our results showed that kaempferol-stimulated  $I_{\text{Cl}}$  was completely inhibited in the presence of forskolin or 8cpt-cAMP. On the other hand, the forskolin/8cpt-cAMP-stimulated  $I_{\text{Cl}}$  was almost completely abolished in the presence of kaempferol. This non-additive effect of kaempferol and cAMP dependent agonists resembles those of genistein in previous studies.<sup>(207, 208)</sup> This finding indicates that kaempferol and cAMP dependent agonists may share a common  $\text{Cl}^-$  secretory pathway that involves cAMP-dependent  $\text{Cl}^-$  secretion via CFTR. The involvement of CFTR in the kaempferol response is consistent with the results showing that the specific CFTR blocker abolished the kaempferol-stimulated  $I_{\text{Cl}}$ . In the



present study, we did not measure the effect of kaempferol on the cAMP level in T84 cells. However, previous studies in T84 cells and human airway cells found that isoflavone genistein and quercetin stimulated  $\text{Cl}^-$  secretion without an increase in intracellular cAMP.<sup>(201, 209, 210)</sup> Due to its chemical structure similar to those flavonoid compounds, it could be possible that kaempferol stimulates  $\text{Cl}^-$  secretion through cAMP-independent signaling pathway. Overall, it could be likely that kaempferol may stimulate  $\text{Cl}^-$  secretion via cAMP-dependent or cAMP-independent signaling pathways or the direct activation of CFTR without an increase in intracellular cAMP.<sup>(201, 209, 210)</sup>

Our findings in intact and permeabilized monolayers that pretreatment with kaempferol inhibited forskolin/8cpt-cAMP-activated  $\text{Cl}^-$  secretion also suggests an inhibitory effect of kaempferol under condition of activated  $\text{Cl}^-$  secretion. Due to limited study of kaempferol effect on cAMP-activated  $\text{Cl}^-$  secretion in colonic epithelium, the inhibitory action of other flavonoids on the activated  $\text{Cl}^-$  secretion has been evidenced. Flavonols quercetin and morin have been shown to decrease forskolin-stimulated  $I_{\text{SC}}$  in T84 cells<sup>(200)</sup> while the flavone naringenin has been demonstrated to diminish the forskolin-activated  $I_{\text{SC}}$  in human and rat colons.<sup>(211)</sup> Additionally recent reports have shown that pretreatment with flavonol quercetin abolishes forskolin-stimulated  $I_{\text{SC}}$  in renal epithelial A6 cells.<sup>(206, 212)</sup> However, the effect of kaempferol on inhibiting the forskolin-stimulated  $I_{\text{SC}}$  is still unexplained. Only one report has mentioned that four weeks of treatment with quercetin reduces the  $\text{Na}^+/\text{K}^+$ -ATPase function by impairment of the  $\text{Na}^+$  binding site affinity.<sup>(213)</sup>

Moreover, the inhibitory effect of kaempferol may be related to activating other signaling pathways. For example, adenosine monophosphate-stimulated kinase (AMPK), a cellular metabolic sensor, has been reported to inhibit CFTR and reduce cAMP-activated  $\text{Cl}^-$  secretion.<sup>(214)</sup> Although previous studies have not investigated the effect of kaempferol on regulating ion transport through the AMPK signaling pathway, studies of anti-cancer effects have mostly found that kaempferol can induce AMPK activation.<sup>(215, 216)</sup> Furthermore, kaempferol may activate  $\text{Ca}^{2+}$ -dependent  $\text{Cl}^-$  secretion across intestinal epithelial cells, which can also activate other signaling pathways.

Activation of epidermal growth factor receptor (EGFR) and mitogen-activated protein kinase (MAPK) has been shown to downregulate epithelial  $K^+$  and  $Cl^-$  channel activity and inhibit secretion in T84 cells.<sup>(217-219)</sup> In a study of airway mucin secretion, kaempferol has been demonstrated to regulate gene expression and production of mucin by regulating the phosphorylation of EGFR, MAPK, and extracellular signal-regulated kinase (ERK) in human airway epithelial cells.<sup>(220)</sup> However, the effect of kaempferol controlling ion transport through the EGFR/MAPK signaling pathway remains unknown. Therefore, in the present study, the inhibited  $I_{SC}$  at a high concentration of kaempferol could be because of the activation of different signaling pathways. The net  $Cl^-$  secretion could be due to the counteraction between the inhibitory effect and the stimulatory effect of kaempferol on  $Cl^-$  channels. For this reason, the inhibiting effect of kaempferol may have consequences for its therapeutic use and should be studied further.

As previously mentioned, kaempferol may activate  $Cl^-$  secretion partially through CaCC. Our result demonstrated the kaempferol induced increase in  $I_{Cl}$  was not affected by  $Ca^{2+}$  ionophore, a mobile ion carrier used to increase intracellular  $Ca^{2+}$  levels. This finding indicates that the effect of kaempferol may not involve intracellular  $Ca^{2+}$  signaling pathway. However, the cellular mechanism by which kaempferol partially modulates  $Cl^-$  secretion via CaCC remains unexplained.

Flavonoids have been reported to regulate  $Cl^-$  secretion through the modulation of the protein kinase A (PKA) system and the phosphorylation status of CFTR by protein kinases and protein phosphatases.<sup>(33, 209, 210)</sup> In the present result, a protein kinase A (PKA) inhibitor (H89) reduced the basal  $I_{Cl}$  and abolished the kaempferol-increased  $I_{Cl}$ , suggesting that the inhibition of PKA involves a kaempferol response in the T84 cells. Meanwhile, the inhibitory effect of H89 on the basal  $I_{Cl}$  is indicative of reducing  $Cl^-$  secretion via inhibition of PKA activity, as has been observed in decreasing basal  $I_{SC}$  by H89 in Calu-3 airway epithelial cells.<sup>(221)</sup> However, the kaempferol-increased  $I_{Cl}$  was not significantly affected in the presence of tyrosine kinase inhibitors tyrphostin A23 and AG490. Accordingly, we suggest that tyrosine kinase inhibition is irrelevant to the kaempferol-stimulated  $Cl^-$  secretion. Likewise, the kaempferol response was not

inhibited in the presence of a tyrosine phosphatase inhibitor vanadate, suggesting that tyrosine dephosphorylation does not mediate the kaempferol effect on  $\text{Cl}^-$  secretion. All the current findings in the T84 cells demonstrate that the kaempferol activating  $\text{Cl}^-$  secretion via CFTR appears to be mediated by a protein kinase A-dependent phosphorylation pathway.

Kaempferol is a well-known phytoestrogen because of a structure similar to estrogen.<sup>(222)</sup> Kaempferol acts as a potential natural estrogen competitor with its binding affinity to estrogen receptor lower than that of natural estrogen. However, the low-affinity binding value shows a stable interaction.<sup>(223)</sup> Since previous studies have demonstrated that phytoestrogen genistein increases CFTR expression,<sup>(224)</sup> thus there is a possibility that phytoestrogen kaempferol also increases CFTR expression. In our experiments, we tested the effect of kaempferol (50  $\mu\text{M}$ ) for 24 h and found that it increased the CFTR protein expression in T84 cells. This observation corresponds with studies of other flavonoid compounds. For example, treatment with phytoestrogen genistein for 24 h has increased CFTR expression in kidney BHK cells.<sup>(224)</sup> Investigators have indicated that genistein regulates the expression of ion transport proteins and estrogen receptors via the estrogen receptors (ER)-mediated pathway by binding both ER- $\alpha$  and ER- $\beta$  subtypes.<sup>(225)</sup> Therefore, we hypothesized that kaempferol might also up-regulate the CFTR protein expression through modulating receptors of estrogen and the ER-mediated pathway, probably because kaempferol is structurally related to the estrogen. Nevertheless, CFTR protein expressions of control and all treatment groups were decreased when treatment for 48 h compared to 24 h. Several studies have provided important information for this point by investigating the effects of endoplasmic reticulum (ER) stress on the synthesis, intracellular processing, and half-life of newly synthesized proteins,<sup>(226, 227)</sup> especially in endogenous CFTR synthesis and processing. They have suggested that T84 cells must be grown under optimal conditions for experiments. For example, it is essential to change the culture media every day in order to avoid nutrient starvation that induces ER stress and reduces CFTR transcription.<sup>(226)</sup> Thus, our results

demonstrating decreased CFTR protein expressions in continuous treatment for 48 h may be due to nutrient starvation, which lead to decreased CFTR transcription.

Kaempferol is frequently taken orally in glycosidic forms with different polarities. High-polarity glycosides are poorly absorbed, whereas low-polarity glycosides are readily absorbed. In the colon, the normal floras metabolize kaempferol glycoside to aglycones, which are subsequently converted to 4-methyl phenol, 4-hydroxyphenyl acetic acid, and phloroglucinol. Following that, the absorbed part of kaempferol is metabolized in the liver into glucuronides and sulfate-conjugates,<sup>(167-169)</sup> after which it is absorbed into the systemic circulation and distributed to various tissues.<sup>(170, 171)</sup> Previous research has found that the 3-glucuronide compound of kaempferol is the most abundant component in plasma.<sup>(173)</sup> Several human studies have revealed that kaempferol concentrations in plasma are restricted to nanomolar levels after oral ingestion. For example, a study by Radtke investigated a daily intake of 4.7 mg of kaempferol and found that they have a plasma kaempferol concentration of 10.7 nM.<sup>(228)</sup> Another study has discovered that ingesting 27 mg of kaempferol daily as tea results in a plasma concentration of 52 nM.<sup>(174)</sup> In addition, researchers also have suggested that flavonols are poorly absorbed in the human gut and high concentrations are found in the intestinal lumen.<sup>(229)</sup> For this reason, kaempferol may be appropriate for treatment in the intestinal lumen. In the present study, kaempferol administration into both the apical and basolateral solution bathing the T84 cell monolayers produced a significant increase in the  $I_{SC}$ . Kaempferol reached a maximal response within 7-8 minutes after administration, suggesting that this compound has immediate action. However, kaempferol added apically produced a higher  $I_{SC}$  than kaempferol added basolaterally, owing to greater accessibility of the compound on the apical side. Therefore, the action of kaempferol on  $Cl^-$  secretion in the intestinal lumen may be applied for therapeutic use.

The entire findings from our research can be summarized and presented as graphical model in figure 58. Kaempferol preferentially acts on the apical membrane of T84 cell monolayer to stimulate  $Cl^-$  secretion. The kaempferol induced  $Cl^-$  secretion was accomplished by activating apical  $Cl^-$  current mainly through CFTR and partially through

CaCC channels as well as activating basolateral  $K^+$  current through unidentified  $K^+$  channels. The activated  $K^+$  channels will hyperpolarize the basolateral membrane and then sustain an electrochemical driving force for  $Cl^-$  exit through apical  $Cl^-$  channels. Additional kaempferol effect on stimulation of NKCC helps to promote  $Cl^-$  loading and secretion. The cellular mechanism of kaempferol on stimulating  $Cl^-$  secretion via CFTR appears to involve cAMP-protein kinase A signaling pathway. Additionally, kaempferol may exert genetic action on  $Cl^-$  secretory process by upregulating CFTR gene expression, resulting in increased expression of CFTR proteins. Overall, the new findings of this study indicate that kaempferol may promote  $Cl^-$  secretion into the intestinal lumen.

Alterations in ion transport activity and function lead to ion transport-related disorders which require medication for treatment.<sup>(23, 24)</sup> In the elderly, chronic constipation results from decreased cAMP-dependent  $Cl^-$  secretion and reduced non-goblet cells in colonic crypts which is the site of fluid and anion secretions.<sup>(20, 21)</sup> Furthermore, the decrease in  $Cl^-$  secretion reported in cystic fibrosis patients is due to impairing functional CFTR.<sup>(22)</sup> It results in a reduction of fluid secretion from the intestinal crypts into the intestinal lumen. In contrast, secretory diarrhea has been related to enterotoxins from various bacteria that produce the increases in cAMP to activate CFTR channels, leading to overstimulation of  $Cl^-$  secretion.<sup>(68)</sup> For this reason, kaempferol may be used as a pharmacological treatment for constipation by promoting  $Cl^-$  secretion and enhancing CFTR protein expression. In addition, kaempferol may be used as an alternative substance to treat cystic fibrosis by stimulating  $Cl^-$  secretion via CaCC. On the other hand, the inhibitory effect of kaempferol on forskolin-stimulated  $I_{sc}$  may be applied as a pharmacological therapy for secretory diarrhea associated with cAMP-activated  $Cl^-$  secretion.

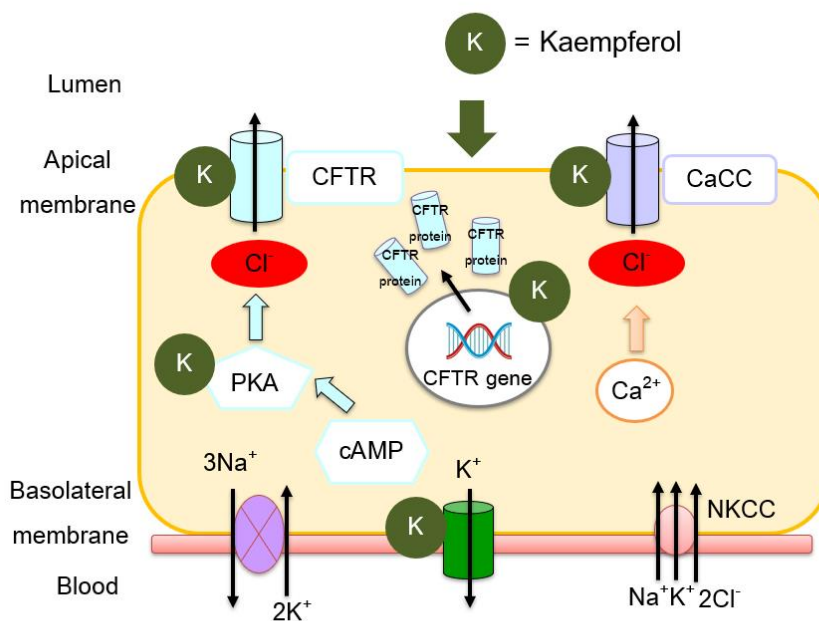


Figure 58 The model illustrates the effect and cellular mechanism of kaempferol on T84 cells.

### Conclusion

The present study employed the Ussing chamber technique to investigate the effect of kaempferol on the ion transport in intact and permeabilized colonic epithelial T84 cell by using several pharmacological blockers and anion substitution experiments. The cellular mechanism of kaempferol in regulating apical Cl<sup>-</sup> current was also identified using substances or inhibitors involving cAMP, intracellular Ca<sup>2+</sup>, tyrosine kinase, and tyrosine phosphatase signaling pathways. Lastly, the genetic effect of kaempferol on the expression of CFTR proteins was examined using a western blot.

Through the study, the following conclusions can be drawn:

1. Kaempferol treatment at concentrations of 1, 5, 10, 50, and 100  $\mu$ M for 24 and 48 h had no cytotoxic effect on T84 cells.

2. Apical and basolateral addition of kaempferol exerted a biphasic short circuit current ( $I_{SC}$ ) response. Concentrations of less than 50  $\mu$ M produced a concentration dependent increased  $I_{SC}$  whereas high concentration inhibited  $I_{SC}$ .

3. In intact T84 cell monolayers, the increased  $I_{SC}$  induced by kaempferol under normal condition and anion replacement experiment indicates that kaempferol stimulates  $Cl^-$  secretion without affecting  $Na^+$  absorption.

4. Experiments with amphotericin B-permeabilized monolayer confirmed the stimulating effect of kaempferol on  $Cl^-$  secretion through activating apical  $Cl^-$  current, mainly through CFTR and partially through CaCC, and activating basolateral  $K^+$  current.

5. Kaempferol failed to increase  $I_{Cl}$  in the presence of cAMP-dependent agonist or cAMP analog (8cpt-cAMP). Conversely, pretreatment of kaempferol almost abolished the cAMP-activated  $Cl^-$  secretion. This indicates that kaempferol response may involve cAMP-dependent  $Cl^-$  secretion via CFTR.

6. Additional data showed that kaempferol modulates  $Cl^-$  secretion via the cAMP-protein kinase A signaling pathway but not intracellular  $Ca^{2+}$ , tyrosine kinase, and tyrosine phosphatase signaling pathways.

7. Kaempferol 50  $\mu$ M when treated for 24 h had a genetic effect on upregulating the CFTR protein expression.

Our findings provide functional information of the effect and cellular mechanisms of kaempferol on regulating  $Cl^-$  secretion in the colonic epithelium. The  $Cl^-$  secretory function helps to promote fluid secretion into the intestinal lumen. Overall, kaempferol could be used as a pharmacotherapeutic treatment in the gastrointestinal tract by boosting mucosal hydration, which is beneficial for treating constipation.

## REFERENCES

1. Kunzelmann K, Mall M. Electrolyte transport in the mammalian colon: mechanisms and implications for disease. *Physiol Rev.* 2002;82(1):245-89.
2. Kashlan OB, Kleyman TR. Epithelial Na<sup>+</sup> channel regulation by cytoplasmic and extracellular factors. *Exp Cell Res.* 2012;318(9):1011-9.
3. Greger R, Bleich M, Leipziger J, Ecke D, Mall M, Kunzelmann K. Regulation of ion transport in colonic crypts. *Physiology.* 1997;12(2):62-6.
4. Han J, Lee SH, Giebisch G, Wang T. Potassium channelopathies and gastrointestinal ulceration. *Gut Liver.* 2016;10(6):881-9.
5. World Health O. Readings on diarrhoea : student manual. Public Health Pap; 1992.
6. Saint-Criq V, Gray MA. Role of CFTR in epithelial physiology. *Cell Mol Life Sci.* 2017;74(1):93-115.
7. Frizzell RA, Hanrahan JW. Physiology of epithelial chloride and fluid secretion. *Cold Spring Harb Perspect Med.* 2012;2(6):a009563.
8. Murek M, Kopic S, Geibel J. Evidence for intestinal chloride secretion. *Exp Physiol.* 2010;95(4):471-8.
9. Kleuss C. Adenylate Cyclase\*. In: Enna SJ, Bylund DB, editors. *xPharm: The comprehensive pharmacology reference.* New York: Elsevier; 2007. p. 1-12.
10. Gadsby DC, Nairn AC. Control of CFTR channel gating by phosphorylation and nucleotide hydrolysis. *Physiol Rev.* 1999;79(1 Suppl):S77-s107.
11. Kunzelmann K. The cystic fibrosis transmembrane conductance regulator and its function in epithelial transport. *Rev Physiol Biochem Pharmacol.* 1999;137:1-70.
12. Billet A, Hanrahan JW. The secret life of CFTR as a calcium-activated chloride channel. *J Physiol.* 2013;591(21):5273-8.
13. Billet A, Luo Y, Balghi H, Hanrahan JW. Role of tyrosine phosphorylation in the muscarinic activation of the cystic fibrosis transmembrane conductance regulator (CFTR). *J Biol Chem.* 2013;288(30):21815-23.
14. Billet A, Jia Y, Jensen T, Riordan JR, Hanrahan JW. Regulation of the cystic fibrosis



transmembrane conductance regulator anion channel by tyrosine phosphorylation. *FASEB J.* 2015;29(9):3945-53.

15. O'Malley KE, Farrell CB, O'Boyle KM, Baird AW. Cholinergic activation of Cl<sup>-</sup> secretion in rat colonic epithelia. *Eur J Pharmacol.* 1995;275(1):83-9.

16. Schultheiss G, Frings M, Diener M. Carbachol-induced Ca<sup>2+</sup> entry into rat colonic epithelium. *Ann N Y Acad Sci.* 2000;915:260-3.

17. Ando H, Kawaai K, Mikoshiba K. IRBIT: a regulator of ion channels and ion transporters. *Biochim Biophys Acta.* 2014;1843(10):2195-204.

18. Park S, Shcheynikov N, Hong JH, Zheng C, Suh SH, Kawaai K, et al. Irbit mediates synergy between Ca<sup>2+</sup> and cAMP signaling pathways during epithelial transport in mice. *Gastroenterology.* 2013;145(1):232-41.

19. Argoff CE. Opioid-induced Constipation: A review of health-related quality of life, patient Burden, practical clinical considerations, and the impact of peripherally acting  $\mu$ -opioid receptor antagonists. *Clin J Pain.* 2020;36(9):716-22.

20. Braaten B, Madara JL, Donowitz M. Age-related loss of nongoblet crypt cells parallels decreased secretion in rabbit descending colon. *Am J Physiol.* 1988;255(1 Pt 1):G72-84.

21. Veeze HJ, Halley DJ, Bijman J, de Jongste JC, de Jonge HR, Sinaasappel M. Determinants of mild clinical symptoms in cystic fibrosis patients. Residual chloride secretion measured in rectal biopsies in relation to the genotype. *J Clin Invest.* 1994;93(2):461-6.

22. Boucher RC, Cotton CU, Gatzky JT, Knowles MR, Yankaskas JR. Evidence for reduced Cl<sup>-</sup> and increased Na<sup>+</sup> permeability in cystic fibrosis human primary cell cultures. *J Physiol.* 1988;405:77-103.

23. Roomans GM. Pharmacological treatment of the ion transport defect in cystic fibrosis. *Expert Opin Investig Drugs.* 2001;10(1):1-19.

24. Newton TJ. Respiratory care of the hospitalized patient with cystic fibrosis. *Respir Care.* 2009;54(6):769-75; discussion 75-6.

25. Marunaka Y. Actions of quercetin, a flavonoid, on ion transporters: its physiological

roles. *Ann N Y Acad Sci.* 2017;1398(1):142-51.

26. Panche AN, Diwan AD, Chandra SR. Flavonoids: an overview. *J Nutr Sci.* 2016;5:e47.

27. Cermak R, Vujcic Z, Scharrer E, Wolfram S. The impact of different flavonoid classes on colonic Cl<sup>-</sup> secretion in rats. *Biochem Pharmacol.* 2001;62(8):1145-51.

28. Cermak R, Kuhn G, Wolfram S. The flavonol quercetin activates basolateral K<sup>+</sup> channels in rat distal colon epithelium. *Br J Pharmacol.* 2002;135(5):1183-90.

29. Yu B, Jiang Y, Jin L, Ma T, Yang H. Role of Quercetin in modulating chloride transport in the intestine. *Front Physiol.* 2016;7(549).

30. Yue GG, Yip TW, Huang Y, Ko WH. Cellular mechanism for potentiation of Ca<sup>2+</sup>-mediated Cl<sup>-</sup> secretion by the flavonoid baicalein in intestinal epithelia. *J Biol Chem.* 2004;279(38):39310-6.

31. Ko WH, Law VW, Yip WC, Yue GG, Lau CW, Chen ZY, et al. Stimulation of chloride secretion by baicalein in isolated rat distal colon. *Am J Physiol Gastrointest Liver Physiol.* 2002;282(3):G508-18.

32. Nguyen TD, Canada AT, Heintz GG, Gettys TW, Cohn JA. Stimulation of secretion by the T84 colonic epithelial cell line with dietary flavonols. *Biochem Pharmacol.* 1991;41(12):1879-86.

33. Illek B, Fischer H. Flavonoids stimulate Cl conductance of human airway epithelium in vitro and in vivo. *Am J Physiol.* 1998;275(5):L902-10.

34. Devriese S, Van den Bossche L, Van Welden S, Holvoet T, Pinheiro I, Hindryckx P, et al. T84 monolayers are superior to Caco-2 as a model system of colonocytes. *Histochem Cell Biol.* 2017;148(1):85-93.

35. Ao M, Sarathy J, Domingue J, Alrefai WA, Rao MC. Chenodeoxycholic acid stimulates Cl<sup>-</sup> secretion via cAMP signaling and increases cystic fibrosis transmembrane conductance regulator phosphorylation in T84 cells. *Am J Physiol Cell Physiol.* 2013;305(4):C447-56.

36. Cheng LK, O'Grady G, Du P, Egbuji JU, Windsor JA, Pullan AJ. Gastrointestinal system. *Wiley Interdiscip Rev Syst Biol Med.* 2010;2(1):65-79.

37. Greenwood-Van Meerveld B, Johnson AC, Grundy D. Gastrointestinal physiology and function. *Handb Exp Pharmacol*. 2017;239:1-16.
38. Liao DH, Zhao JB, Gregersen H. Gastrointestinal tract modelling in health and disease. *World J Gastroenterol*. 2009;15(2):169-76.
39. Stromberg PE, Coopersmith CM. Epithelium, Proliferation of. In: Johnson LR, editor. *Encyclopedia of gastroenterology*. New York: Elsevier; 2004. p. 725-30.
40. Kong S, Zhang YH, Zhang W. Regulation of intestinal epithelial cells properties and functions by amino acids. *Biomed Res Int*. 2018;2018:2819154.
41. Kim YS, Ho SB. Intestinal goblet cells and mucins in health and disease: recent insights and progress. *Curr Gastroenterol Rep*. 2010;12(5):319-30.
42. Cox HM. Neuroendocrine peptide mechanisms controlling intestinal epithelial function. *Curr Opin Pharmacol*. 2016;31:50-6.
43. Gribble FM, Reimann F. Enteroendocrine cells: chemosensors in the intestinal epithelium. *Annu Rev Physiol*. 2016;78:277-99.
44. Latorre R, Sternini C, De Giorgio R, Greenwood-Van Meerveld B. Enteroendocrine cells: a review of their role in brain-gut communication. *Neurogastroenterol Motil*. 2016;28(5):620-30.
45. Bevins CL, Salzman NH. Paneth cells, antimicrobial peptides and maintenance of intestinal homeostasis. *Nat Rev Microbiol*. 2011;9(5):356-68.
46. Corr SC, Gahan CC, Hill C. M-cells: origin, morphology and role in mucosal immunity and microbial pathogenesis. *FEMS Immunol Med Microbiol*. 2008;52(1):2-12.
47. Howitt MR, Lavoie S, Michaud M, Blum AM, Tran SV, Weinstock JV, et al. Tuft cells, taste-chemosensory cells, orchestrate parasite type 2 immunity in the gut. *Science*. 2016;351(6279):1329-33.
48. Zhou B, Yuan Y, Zhang S, Guo C, Li X, Li G, et al. Intestinal flora and disease mutually shape the regional immune system in the intestinal tract. *Front Immunol*. 2020;11:575.
49. Jasper H. Intestinal Stem Cell Aging: Origins and Interventions. *Annu Rev Physiol*. 2020;82:203-26.

50. Moog F. The lining of the small intestine. *Sci Am.* 1981;245(5):154-8, 60, 62 et passiom.
51. Andrews CN, Storr M. The pathophysiology of chronic constipation. *Can J Gastroenterol.* 2011;25 Suppl B(Suppl B):16b-21b.
52. Azzouz LL, Sharma S. Physiology, large intestine. *StatPearls.* Treasure Island (FL): StatPearls Publishing Copyright © 2021, StatPearls Publishing LLC.; 2021.
53. Lee B, Moon KM, Kim CY. Tight junction in the intestinal epithelium: its association with diseases and regulation by phytochemicals. *J Immunol Res.* 2018;2018:2645465-.
54. Assémat E, Bazellières E, Pallesi-Pocachard E, Le Bivic A, Massey-Harroche D. Polarity complex proteins. *Biochim Biophys Acta.* 2008;1778(3):614-30.
55. Parikh K, Antanaviciute A, Fawkner-Corbett D, Jagielowicz M, Aulicino A, Lagerholm C, et al. Colonic epithelial cell diversity in health and inflammatory bowel disease. *Nature.* 2019;567(7746):49-55.
56. Barrett KE, Keely SJ. Chloride secretion by the intestinal epithelium: molecular basis and regulatory aspects. *Annu Rev Physiol.* 2000;62:535-72.
57. Zihni C, Mills C, Matter K, Balda MS. Tight junctions: from simple barriers to multifunctional molecular gates. *Nat Rev Mol Cell Biol.* 2016;17(9):564-80.
58. Tang VW, Goodenough DA. Paracellular ion channel at the tight junction. *Biophys J.* 2003;84(3):1660-73.
59. González-Mariscal L, Tapia R, Chamorro D. Crosstalk of tight junction components with signaling pathways. *Biochim Biophys Acta.* 2008;1778(3):729-56.
60. Harhaj NS, Antonetti DA. Regulation of tight junctions and loss of barrier function in pathophysiology. *Int J Biochem Cell Biol.* 2004;36(7):1206-37.
61. Reddy MM, Stutts MJ. Status of fluid and electrolyte absorption in cystic fibrosis. *Cold Spring Harb Perspect Med.* 2013;3(1):a009555-a.
62. Rao MC. Physiology of electrolyte transport in the gut: implications for disease. *compr physiol.* 2019;9(3):947-1023.
63. Halm DR. Physiologic Influences of Transepithelial K<sup>+</sup> Secretion. In: Hamilton KL, Devor DC, editors. *Basic epithelial ion transport principles and function: ion channels and*

transporters of epithelia in health and disease - Vol 1. Cham: Springer International Publishing; 2020. p. 337-93.

64. Lucas M. Lack of applicability of the enterocyte chloride ion secretion paradigm to the pathology of cystic fibrosis. *Arch Asthma Allergy Immunol.* 2017;1:061-85.
65. Rajendran VM, Sandle GI. Colonic potassium absorption and secretion in health and disease. *Compr Physiol.* 2018;8(4):1513-36.
66. Sorensen MV, Matos JE, Sausbier M, Sausbier U, Ruth P, Praetorius HA, et al. Aldosterone increases KCa1.1 (BK) channel-mediated colonic K<sup>+</sup> secretion. *J Physiol.* 2008;586(17):4251-64.
67. Galizia L, Ojea A, Kotsias BA. [Amiloride sensitive sodium channels (ENaC) and their regulation by proteases]. *Medicina.* 2011;71(2):179-82.
68. Kunzelmann K, Mall M. Electrolyte transport in the mammalian colon: mechanisms and implications for disease. *Physiol Rev.* 2002;82(1):245-89.
69. Warnock DG. The amiloride-sensitive endothelial sodium channel and vascular tone. *Hypertension.* 2013;61(5):952-4.
70. Horisberger JD, Chraïbi A. Epithelial sodium channel: a ligand-gated channel?. *Nephron Physiol.* 2004;96(2):p37-41.
71. Garty H, Benos DJ. Characteristics and regulatory mechanisms of the amiloride-blockable Na<sup>+</sup> channel. *Physiol Rev.* 1988;68(2):309-73.
72. Loffing J, Schild L. Functional domains of the epithelial sodium channel. *J Am Soc Nephrol.* 2005;16(11):3175-81.
73. Riordan JR, Rommens JM, Kerem B, Alon N, Rozmahel R, Grzelczak Z, et al. Identification of the cystic fibrosis gene: cloning and characterization of complementary DNA. *Science.* 1989;245(4922):1066-73.
74. Kunzelmann K, Nitschke R. Defects in processing and trafficking of cystic fibrosis transmembrane conductance regulator. *Exp Nephrol.* 2000;8(6):332-42.
75. Riordan JR. CFTR function and prospects for therapy. *Annu Rev Biochem.* 2008;77:701-26.
76. Welsh MJ, Smith AE. Molecular mechanisms of CFTR chloride channel dysfunction

in cystic fibrosis. *Cell*. 1993;73(7):1251-4.

77. Sheppard DN, Welsh MJ. Structure and function of the CFTR chloride channel. *Physiol Rev*. 1999;79(1 Suppl):S23-45.

78. Bozoky Z, Krzeminski M, Muhandiram R, Birtley JR, Al-Zahrani A, Thomas PJ, et al. Regulatory R region of the CFTR chloride channel is a dynamic integrator of phospho-dependent intra- and intermolecular interactions. *Proc Natl Acad Sci U S A*. 2013;110(47):E4427-36.

79. Ahsan MK, Tchernychev B, Kessler MM, Solinga RM, Arthur D, Linde CI, et al. Linaclotide activates guanylate cyclase-C/cGMP/protein kinase-II-dependent trafficking of CFTR in the intestine. *Physiol Rep*. 2017;5(11).

80. Li C, Naren AP. CFTR chloride channel in the apical compartments: spatiotemporal coupling to its interacting partners. *Integr Biol (Camb)*. 2010;2(4):161-77.

81. Mall M, Bleich M, Schürlein M, Kuhr J, Seydewitz HH, Brandis M, et al. Cholinergic ion secretion in human colon requires coactivation by cAMP. *Am J Physiol*. 1998;275(6):G1274-81.

82. Verkman AS, Synder D, Tradtrantip L, Thiagarajah JR, Anderson MO. CFTR inhibitors. *Curr Pharm Des*. 2013;19(19):3529-41.

83. Thiagarajah JR, Song Y, Haggie PM, Verkman AS. A small molecule CFTR inhibitor produces cystic fibrosis-like submucosal gland fluid secretions in normal airways. *FASEB J*. 2004;18(7):875-7.

84. Barish ME. A transient calcium-dependent chloride current in the immature *Xenopus* oocyte. *J Physiol*. 1983;342:309-25.

85. Eggermont J. Calcium-activated chloride channels: (un)known, (un)loved?. *Proc Am Thorac Soc*. 2004;1(1):22-7.

86. Ferrera L, Zegarra-Moran O, Galletta LJ. Ca<sup>2+</sup>-activated Cl<sup>-</sup> channels. *Compr Physiol*. 2011;1(4):2155-74.

87. Caputo A, Caci E, Ferrera L, Pedemonte N, Barsanti C, Sondo E, et al. TMEM16A, a membrane protein associated with calcium-dependent chloride channel activity. *Science*. 2008;322(5901):590-4.

88. He Q, Halm ST, Zhang J, Halm DR. Activation of the basolateral membrane Cl<sup>-</sup> conductance essential for electrogenic K<sup>+</sup> secretion suppresses electrogenic Cl<sup>-</sup> secretion. *Exp Physiol*. 2011;96(3):305-16.
89. Ko EA, Jin BJ, Namkung W, Ma T, Thiagarajah JR, Verkman AS. Chloride channel inhibition by a red wine extract and a synthetic small molecule prevents rotaviral secretory diarrhoea in neonatal mice. *Gut*. 2014;63(7):1120-9.
90. Ousingsawat J, Mirza M, Tian Y, Roussa E, Schreiber R, Cook DI, et al. Rotavirus toxin NSP4 induces diarrhea by activation of TMEM16A and inhibition of Na<sup>+</sup> absorption. *Pflugers Arch*. 2011;461(5):579-89.
91. Schroeder BC, Cheng T, Jan YN, Jan LY. Expression cloning of TMEM16A as a calcium-activated chloride channel subunit. *Cell*. 2008;134(6):1019-29.
92. Yang YD, Cho H, Koo JY, Tak MH, Cho Y, Shim WS, et al. TMEM16A confers receptor-activated calcium-dependent chloride conductance. *Nature*. 2008;455(7217):1210-5.
93. Ferrera L, Caputo A, Galiotta LJ. TMEM16A protein: a new identity for Ca<sup>2+</sup>-dependent Cl<sup>-</sup> channels. *Physiology (Bethesda, Md)*. 2010;25(6):357-63.
94. Dang S, Feng S, Tien J, Peters CJ, Bulkley D, Lolicato M, et al. Cryo-EM structures of the TMEM16A calcium-activated chloride channel. *Nature*. 2017;552(7685):426-9.
95. Paulino C, Kalienkova V, Lam AKM, Neldner Y, Dutzler R. Activation mechanism of the calcium-activated chloride channel TMEM16A revealed by cryo-EM. *Nature*. 2017;552(7685):421-5.
96. Hwang SJ, Basma N, Sanders KM, Ward SM. Effects of new-generation inhibitors of the calcium-activated chloride channel anoctamin 1 on slow waves in the gastrointestinal tract. *Br J Pharmacol*. 2016;173(8):1339-49.
97. De La Fuente R, Namkung W, Mills A, Verkman AS. Small-molecule screen identifies inhibitors of a human intestinal calcium-activated chloride channel. *Mol Pharmacol*. 2008;73(3):758-68.
98. Clarke LL, Boucher RC. Chloride secretory response to extracellular ATP in human normal and cystic fibrosis nasal epithelia. *Am J Physiol*. 1992;263(2 Pt 1):C348-56.

99. Gabriel SE, Makhlina M, Martsen E, Thomas EJ, Lethem MI, Boucher RC. Permeabilization via the P2X7 purinoreceptor reveals the presence of a  $\text{Ca}^{2+}$ -activated  $\text{Cl}^-$  conductance in the apical membrane of murine tracheal epithelial cells. *J Biol Chem*. 2000;275(45):35028-33.
100. Grubb BR, Paradiso AM, Boucher RC. Anomalies in ion transport in CF mouse tracheal epithelium. *Am J Physiol*. 1994;267(1 Pt 1):C293-300.
101. Willumsen NJ, Boucher RC. Activation of an apical  $\text{Cl}^-$  conductance by  $\text{Ca}^{2+}$  ionophores in cystic fibrosis airway epithelia. *Am J Physiol*. 1989;256(2 Pt 1):C226-33.
102. Flores CA, Cid LP, Sepúlveda FV, Niemeyer MI. TMEM16 proteins: the long awaited calcium-activated chloride channels?. *Braz J Med Biol Res*. 2009;42(11):993-1001.
103. Benedetto R, Ousingsawat J, Wanitchakool P, Zhang Y, Holtzman MJ, Amaral M, et al. Epithelial chloride transport by CFTR requires TMEM16A. *Sci Rep*. 2017;7(1):12397.
104. Schreiber R, Faria D, Skryabin BV, Wanitchakool P, Rock JR, Kunzelmann K. Anoctamins support calcium-dependent chloride secretion by facilitating calcium signaling in adult mouse intestine. *Pflugers Arch*. 2015;467(6):1203-13.
105. Sandle GI, Hunter M. Apical potassium (BK) channels and enhanced potassium secretion in human colon. *QJM*. 2010;103(2):85-9.
106. Matos JE, Sausbier M, Beranek G, Sausbier U, Ruth P, Leipziger J. Role of cholinergic-activated  $\text{KCa}1.1$  (BK),  $\text{KCa}3.1$  (SK4) and  $\text{KV}7.1$  (KCNQ1) channels in mouse colonic  $\text{Cl}^-$  secretion. *Acta Physiol (Oxf)*. 2007;189(3):251-8.
107. Rechkemmer G, Halm DR. Aldosterone stimulates K secretion across mammalian colon independent of Na absorption. *Proc Natl Acad Sci U S A*. 1989;86(1):397-401.
108. Cheepala S, Hulot JS, Morgan JA, Sassi Y, Zhang W, Naren AP, et al. Cyclic nucleotide compartmentalization: contributions of phosphodiesterases and ATP-binding cassette transporters. *Annu Rev Pharmacol Toxicol*. 2013;53:231-53.
109. Zhang J, Halm ST, Halm DR. Adrenergic activation of electrogenic  $\text{K}^+$  secretion in guinea pig distal colonic epithelium: desensitization via the Y2-neuropeptide receptor. *Am J Physiol Gastrointest Liver Physiol*. 2009;297(2):G278-91.



110. Zhang J, Halm ST, Halm DR. Adrenergic activation of electrogenic  $K^+$  secretion in guinea pig distal colonic epithelium: involvement of beta1- and beta2-adrenergic receptors. *Am J Physiol Gastrointest Liver Physiol.* 2009;297(2):G269-77.
111. Heinke B, Hörger S, Diener M. Mechanisms of carbachol-induced alterations in  $K^+$  transport across the rat colon. *Eur J Pharmacol.* 1998;362(2-3):199-206.
112. Burckhardt BC, Gögelein H. Small and maxi  $K^+$  channels in the basolateral membrane of isolated crypts from rat distal colon: single-channel and slow whole-cell recordings. *Pflugers Arch.* 1992;420(1):54-60.
113. Loo DD, Kaunitz JD.  $Ca^{2+}$  and cAMP activate  $K^+$  channels in the basolateral membrane of crypt cells isolated from rabbit distal colon. *J Membr Biol.* 1989;110(1):19-28.
114. McNamara B, Winter DC, Cuffe JE, O'Sullivan GC, Harvey BJ. Basolateral  $K^+$  channel involvement in forskolin-activated chloride secretion in human colon. *J Physiol.* 1999;519 Pt 1(Pt 1):251-60.
115. Lohrmann E, Burhoff I, Nitschke RB, Lang HJ, Mania D, Englert HC, et al. A new class of inhibitors of cAMP-mediated  $Cl^-$  secretion in rabbit colon, acting by the reduction of cAMP-activated  $K^+$  conductance. *Pflugers Arch.* 1995;429(4):517-30.
116. Warth R, Riedemann N, Bleich M, Van Driessche W, Busch AE, Greger R. The cAMP-regulated and 293B-inhibited  $K^+$  conductance of rat colonic crypt base cells. *Pflugers Arch.* 1996;432(1):81-8.
117. Heitzmann D, Warth R. Physiology and pathophysiology of potassium channels in gastrointestinal epithelia. *Physiol Rev.* 2008;88(3):1119-82.
118. Cuthbert AW, Hickman ME, Thorn P, MacVinish LJ. Activation of  $Ca^{2+}$ - and cAMP-sensitive  $K^+$  channels in murine colonic epithelia by 1-ethyl-2-benzimidazolone. *Am J Physiol.* 1999;277(1):C111-20.
119. Devor DC, Singh AK, Frizzell RA, Bridges RJ. Modulation of  $Cl^-$  secretion by benzimidazolones. I. Direct activation of a  $Ca^{2+}$ -dependent  $K^+$  channel. *Am J Physiol.* 1996;271(5 Pt 1):L775-84.
120. Devor DC, Singh AK, Gerlach AC, Frizzell RA, Bridges RJ. Inhibition of intestinal  $Cl^-$

secretion by clotrimazole: direct effect on basolateral membrane  $K^+$  channels. *Am J Physiol.* 1997;273(2 Pt 1):C531-40.

121. Rufo PA, Merlin D, Riegler M, Ferguson-Maltzman MH, Dickinson BL, Brugnara C, et al. The antifungal antibiotic, clotrimazole, inhibits chloride secretion by human intestinal T84 cells via blockade of distinct basolateral  $K^+$  conductances. Demonstration of efficacy in intact rabbit colon and in an in vivo mouse model of cholera. *J Clin Invest.* 1997;100(12):3111-20.

122. Ikuma M, Kashgarian M, Binder HJ, Rajendran VM. Differential regulation of NHE isoforms by sodium depletion in proximal and distal segments of rat colon. *Am J Physiol.* 1999;276(2):G539-49.

123. Padan E. Functional and structural dynamics of NhaA, a prototype for  $Na^+$  and  $H^+$  antiporters, which are responsible for  $Na^+$  and  $H^+$  homeostasis in cells. *Biochim Biophys Acta.* 2014;1837(7):1047-62.

124. Rajendran VM, Binder HJ. Characterization of Na-H exchange in apical membrane vesicles of rat colon. *J Biol Chem.* 1990;265(15):8408-14.

125. Rajendran VM, Geibel J, Binder HJ. Chloride-dependent Na-H exchange. A novel mechanism of sodium transport in colonic crypts. *J Biol Chem.* 1995;270(19):11051-4.

126. Rajendran VM, Geibel J, Binder HJ. Characterization of apical membrane  $Cl^-$  dependent Na/H exchange in crypt cells of rat distal colon. *Am J Physiol Gastrointest Liver Physiol.* 2001;280(3):G400-5.

127. Höglund P, Haila S, Scherer SW, Tsui LC, Green ED, Weissenbach J, et al. Positional candidate genes for congenital chloride diarrhea suggested by high-resolution physical mapping in chromosome region 7q31. *Genome Res.* 1996;6(3):202-10.

128. Jacob P, Rossmann H, Lamprecht G, Kretz A, Neff C, Lin-Wu E, et al. Down-regulated in adenoma mediates apical  $Cl^-/HCO_3^-$  exchange in rabbit, rat, and human duodenum. *Gastroenterology.* 2002;122(3):709-24.

129. Melvin JE, Park K, Richardson L, Schultheis PJ, Shull GE. Mouse down-regulated in adenoma (DRA) is an intestinal  $Cl^-/HCO_3^-$  exchanger and is up-regulated in colon of mice lacking the NHE3  $Na^+/H^+$  exchanger. *J Biol Chem.* 1999;274(32):22855-61.

130. Walker NM, Simpson JE, Yen PF, Gill RK, Rigsby EV, Brazill JM, et al. Down-regulated in adenoma Cl/HCO<sub>3</sub> exchanger couples with Na/H exchanger 3 for NaCl absorption in murine small intestine. *Gastroenterology*. 2008;135(5):1645-53.e3.
131. Wang Z, Petrovic S, Mann E, Soleimani M. Identification of an apical Cl<sup>-</sup>/HCO<sub>3</sub><sup>-</sup> exchanger in the small intestine. *Am J Physiol Gastrointest Liver Physiol*. 2002;282(3):G573-9.
132. Bastl CP, Schulman G, Cragoe EJ, Jr. Low-dose glucocorticoids stimulate electroneutral NaCl absorption in rat colon. *Am J Physiol*. 1989;257(6 Pt 2):F1027-38.
133. Saksena S, Singla A, Goyal S, Katyal S, Bansal N, Gill RK, et al. Mechanisms of transcriptional modulation of the human anion exchanger SLC26A3 gene expression by IFN- $\gamma$ . *Am J Physiol Gastrointest Liver Physiol*. 2010;298(2):G159-66.
134. Saksena S, Tyagi S, Goyal S, Gill RK, Alrefai WA, Ramaswamy K, et al. Stimulation of apical Cl<sup>-</sup>/HCO<sub>3</sub><sup>-</sup>(OH<sup>-</sup>) exchanger, SLC26A3 by neuropeptide Y is lipid raft dependent. *Am J Physiol Gastrointest Liver Physiol*. 2010;299(6):G1334-43.
135. Singla A, Dwivedi A, Saksena S, Gill RK, Alrefai WA, Ramaswamy K, et al. Mechanisms of lysophosphatidic acid (LPA) mediated stimulation of intestinal apical Cl<sup>-</sup>/OH<sup>-</sup> exchange. *Am J Physiol Gastrointest Liver Physiol*. 2010;298(2):G182-9.
136. Delpire E, Gagnon KB. Na<sup>+</sup>-K<sup>+</sup>-2Cl<sup>-</sup> Cotransporter (NKCC) Physiological Function in Nonpolarized Cells and Transporting Epithelia. *Compr Physiol*. 2018;8(2):871-901.
137. Greger R. Role of CFTR in the colon. *Ann Rev Physiol*. 2000;62:467-91.
138. Matthews JB. Molecular regulation of Na<sup>+</sup>-K<sup>+</sup>-2Cl<sup>-</sup> cotransporter (NKCC1) and epithelial chloride secretion. *World J Surg*. 2002;26(7):826-30.
139. Palfrey HC, Rao MC. Na/K/Cl co-transport and its regulation. *J Exp Biol*. 1983;106:43-54.
140. Zimmerman AL. Chapter 35 - Cyclic nucleotide-gated ion channels. In: Sperelakis N, editor. *Cell physiology source book* (fourth edition). San Diego: Academic Press; 2012. p. 621-32.
141. Tresguerres M, Levin LR, Buck J. Intracellular cAMP signaling by soluble adenylyl cyclase. *Kidney Int*. 2011;79(12):1277-88.

142. Halm ST, Zhang J, Halm DR. beta-Adrenergic activation of electrogenic  $K^+$  and  $Cl^-$  secretion in guinea pig distal colonic epithelium proceeds via separate cAMP signaling pathways. *Am J Physiol Gastrointest Liver Physiol*. 2010;299(1):G81-95.
143. Liu F, Zhang Z, Csanady L, Gadsby DC, Chen J. Molecular structure of the human CFTR ion channel. *Cell*. 2017;169(1):85-95.e8.
144. Mihályi C, Iordanov I, Torocsik B, Csanady L. Simple binding of protein kinase A prior to phosphorylation allows CFTR anion channels to be opened by nucleotides. *Proc Natl Acad Sci U S A*. 2020;117(35):21740-6.
145. Alasbahi RH, Melzig MF. Forskolin and derivatives as tools for studying the role of cAMP. *Pharmazie*. 2012;67(1):5-13.
146. Krakstad C, Christensen AE, Doskeland SO. cAMP protects neutrophils against TNF-alpha-induced apoptosis by activation of cAMP-dependent protein kinase, independently of exchange protein directly activated by cAMP (Epac). *J Leukoc Biol*. 2004;76(3):641-7.
147. Kunzelmann K, Mehta A. CFTR: a hub for kinases and crosstalk of cAMP and  $Ca^{2+}$ . *FEBS J*. 2013;280(18):4417-29.
148. Xu Z, Yao G, Niu W, Fan H, Ma X, Shi S, et al. Calcium ionophore (A23187) rescues the activation of unfertilized oocytes after intracytoplasmic sperm injection and chromosome analysis of blastocyst after activation. *Front Endocrinol (Lausanne)*. 2021;12:692082.
149. Rottgen TS, Nickerson AJ, Rajendran VM. Calcium-activated  $Cl^-$  channel: insights on the molecular identity in epithelial tissues. *Int J Mol Sci*. 2018;19(5):1432.
150. Barro-Soria R, Aldehni F, Almaça J, Witzgall R, Schreiber R, Kunzelmann K. ER-localized bestrophin 1 activates  $Ca^{2+}$ -dependent ion channels TMEM16A and SK4 possibly by acting as a counterion channel. *Pflugers Arch*. 2010;459(3):485-97.
151. Neussert R, Müller C, Milenkovic VM, Strauss O. The presence of bestrophin-1 modulates the  $Ca^{2+}$  recruitment from  $Ca^{2+}$  stores in the ER. *Pflugers Arch*. 2010;460(1):163-75.
152. Wolf W, Kilic A, Schrul B, Lorenz H, Schwappach B, Seedorf M. Yeast Ist2 recruits

the endoplasmic reticulum to the plasma membrane and creates a ribosome-free membrane microcompartment. *PLoS One*. 2012;7(7):e39703.

153. Currie MG, Fok KF, Kato J, Moore RJ, Hamra FK, Duffin KL, et al. Guanylin: an endogenous activator of intestinal guanylate cyclase. *Proc Natl Acad Sci U S A*. 1992;89(3):947-51.

154. Bakre MM, Sopory S, Visweswariah SS. Expression and regulation of the cGMP-binding, cGMP-specific phosphodiesterase (PDE5) in human colonic epithelial cells: role in the induction of cellular refractoriness to the heat-stable enterotoxin peptide. *J Cell Biochem*. 2000;77(1):159-67.

155. Fischer H, Machen TE. The tyrosine kinase p60c-src regulates the fast gate of the cystic fibrosis transmembrane conductance regulator chloride channel. *Biophys J*. 1996;71(6):3073-82.

156. Cesaro L, Marin O, Venerando A, Donella-Deana A, Pinna LA. Phosphorylation of cystic fibrosis transmembrane conductance regulator (CFTR) serine-511 by the combined action of tyrosine kinases and CK2: the implication of tyrosine-512 and phenylalanine-508. *Amino Acids*. 2013;45(6):1423-9.

157. Venerando A, Cesaro L, Marin O, Donella-Deana A, Pinna LA. A "SYDE" effect of hierarchical phosphorylation: possible relevance to the cystic fibrosis basic defect. *Cell Mol Life Sci*. 2014;71(12):2193-6.

158. Ma J, Zhao J, Drumm ML, Xie J, Davis PB. Function of the R Domain in the Cystic Fibrosis Transmembrane Conductance Regulator Chloride Channel\*. *J Biol Chem*. 1997;272(44):28133-41.

159. Szabó K, Szakács G, Hegeds T, Sarkadi B. Nucleotide occlusion in the human cystic fibrosis transmembrane conductance regulator. Different patterns in the two nucleotide binding domains. *J Biol Chem*. 1999;274(18):12209-12.

160. Banbury DN, Oakley JD, Sessions RB, Banting G. Tyrphostin A23 inhibits internalization of the transferrin receptor by perturbing the interaction between tyrosine motifs and the medium chain subunit of the AP-2 adaptor complex. *J Biol Chem*. 2003;278(14):12022-8.

161. Seo IA, Lee HK, Shin YK, Lee SH, Seo SY, Park JW, et al. Janus kinase 2 inhibitor AG490 inhibits the STAT3 signaling pathway by suppressing protein translation of gp130. *Korean J Physiol Pharmacol.* 2009;13(2):131-8.
162. Deachapunya C, Poonyachoti S. Activation of chloride secretion by isoflavone genistein in endometrial epithelial cells. *Cell Physiol Biochem.* 2013;32(5):1473-86.
163. Khalil AA, Jameson MJ. Sodium orthovanadate inhibits proliferation and triggers apoptosis in oral squamous cell carcinoma in vitro. *Biochem (Mosc).* 2017;82(2):149-55.
164. Panche AN, Diwan AD, Chandra SR. Flavonoids: an overview. *J Nutr Sci.* 2016;5:e47-e.
165. Hossen MJ, Uddin MB, Ahmed SSU, Yu ZL, Cho JY. Kaempferol: review on natural sources and bioavailability. 2016. p. 101-50.
166. Alam W, Khan H, Shah MA, Cauli O, Saso L. Kaempferol as a dietary anti-inflammatory agent: current therapeutic standing. *Molecules.* 2020;25(18):4073.
167. Gee JM, Johnson IT. Polyphenolic compounds: interactions with the gut and implications for human health. *Curr Med Chem.* 2001;8(11):1245-55.
168. Crespy V, Morand C, Besson C, Cotellet N, Vezin H, Demigne C, et al. The splanchnic metabolism of flavonoids highly differed according to the nature of the compound. *Am J Physiol Gastrointest Liver Physiol.* 2003;284(6):G980-8.
169. Lehtonen HM, Lehtinen O, Suomela JP, Viitanen M, Kallio H. Flavonol glycosides of sea buckthorn (*Hippophae rhamnoides* ssp. *sinensis*) and lingonberry (*Vaccinium vitis-idaea*) are bioavailable in humans and monoglucuronidated for excretion. *J Agric Food Chem.* 2010;58(1):620-7.
170. Bokkenheuser VD, Shackleton CH, Winter J. Hydrolysis of dietary flavonoid glycosides by strains of intestinal *Bacteroides* from humans. *Biochem J.* 1987;248(3):953-6.
171. Schneider H, Blaut M. Anaerobic degradation of flavonoids by *Eubacterium ramulus*. *Arch Microbiol.* 2000;173(1):71-5.
172. Dabeek WM, Marra MV. Dietary Quercetin and kaempferol: bioavailability and potential cardiovascular-related bioactivity in humans. *Nutrients.* 2019;11(10).

173. DuPont MS, Day AJ, Bennett RN, Mellon FA, Kroon PA. Absorption of kaempferol from endive, a source of kaempferol-3-glucuronide, in humans. *Eur J Clin Nutr.* 2004;58(6):947-54.
174. de Vries JH, Hollman PC, Meyboom S, Buysman MN, Zock PL, van Staveren WA, et al. Plasma concentrations and urinary excretion of the antioxidant flavonols quercetin and kaempferol as biomarkers for dietary intake. *Am J Clin Nutr.* 1998;68(1):60-5.
175. Chen AY, Chen YC. A review of the dietary flavonoid, kaempferol on human health and cancer chemoprevention. *Food Chem.* 2013;138(4):2099-107.
176. Lin W-C, Lin J-Y. Berberine down-regulates the Th1/Th2 cytokine gene expression ratio in mouse primary splenocytes in the absence or presence of lipopolysaccharide in a preventive manner. *Int Immunopharmacol.* 2011;11(12):1984-90.
177. Ren J, Lu Y, Qian Y, Chen B, Wu T, Ji G. Recent progress regarding kaempferol for the treatment of various diseases (Review). *Exp Ther Med.* 2019;18(4):2759-76.
178. Niering P, Michels G, Watjen W, Ohler S, Steffan B, Chovolou Y, et al. Protective and detrimental effects of kaempferol in rat H4IIE cells: Implication of oxidative stress and apoptosis. *Toxicol Appl Pharmacol.* 2005;209(2):114-22.
179. Mira L, Fernandez MT, Santos M, Rocha R, Florêncio MH, Jennings KR. Interactions of flavonoids with iron and copper ions: a mechanism for their antioxidant activity. *Free radic res.* 2002;36(11):1199-208.
180. Pietta PG. Flavonoids as antioxidants. *J Nat Prod.* 2000;63(7):1035-42.
181. Hu Y, Cheng Z, Heller LI, Krasnoff SB, Glahn RP, Welch RM. Kaempferol in red and pinto bean seed (*Phaseolus vulgaris* L.) coats inhibits iron bioavailability using an in vitro digestion/human Caco-2 cell model. *J Agric Food Chem.* 2006;54(24):9254-61.
182. Lemos C, Peters GJ, Jansen G, Martel F, Calhau C. Modulation of folate uptake in cultured human colon adenocarcinoma Caco-2 cells by dietary compounds. *Eur J Nutr.* 2007;46(6):329-36.
183. Li C, Li X, Choi J-S. Enhanced bioavailability of etoposide after oral or intravenous administration of etoposide with kaempferol in rats. *Arch Pharmacol Res.* 2009;32(1):133-8.

184. Barrett KE. Positive and negative regulation of chloride secretion in T84 cells. *Am J Physiol.* 1993;265(4 Pt 1):C859-68.
185. Dharmasathaphorn K, McRoberts JA, Mandel KG, Tisdale LD, Masui H. A human colonic tumor cell line that maintains vectorial electrolyte transport. *Am J Physiol.* 1984;246(2 Pt 1):G204-8.
186. Chantret I, Barbat A, Dussaux E, Brattain MG, Zweibaum A. Epithelial polarity, villin expression, and enterocytic differentiation of cultured human colon carcinoma cells: a survey of twenty cell lines. *Cancer Res.* 1988;48(7):1936-42.
187. Bolte G, Wolburg H, Beuermann K, Stocker S, Stern M. Specific interaction of food proteins with apical membranes of the human intestinal cell lines Caco-2 and T84. *Clin Chim Acta.* 1998;270(2):151-67.
188. Sambuy Y, De Angelis I, Ranaldi G, Scarino ML, Stamatii A, Zucco F. The Caco-2 cell line as a model of the intestinal barrier: influence of cell and culture-related factors on Caco-2 cell functional characteristics. *Cell Biol Toxicol.* 2005;21(1):1-26.
189. Natoli M, Leoni BD, D'Agnano I, D'Onofrio M, Brandi R, Arisi I, et al. Cell growing density affects the structural and functional properties of Caco-2 differentiated monolayer. *J Cell Physiol.* 2011;226(6):1531-43.
190. Banks M, Golder M, Farthing M, Burleigh D. Intracellular potentiation between two second messenger systems may contribute to cholera toxin induced intestinal secretion in humans. *Gut.* 2004;53:50-7.
191. Nichols JM, Maiellaro I, Abi-Jaoude J, Curci S, Hofer AM. "Store-operated" cAMP signaling contributes to  $Ca^{2+}$ -activated  $Cl^{-}$  secretion in T84 colonic cells. *Am J Physiol Gastrointest Liver Physiol.* 2015;309(8):G670-G9.
192. Weiglmeier PR, Rosch P, Berkner H. Cure and curse: E. coli heat-stable enterotoxin and its receptor guanylyl cyclase C. *Toxins (Basel).* 2010;2(9):2213-29.
193. Ao M, Sarathy J, Domingue J, Alrefai WA, Rao MC. Chenodeoxycholic acid stimulates  $Cl^{-}$  secretion via cAMP signaling and increases cystic fibrosis transmembrane conductance regulator phosphorylation in T84 cells. *Am J Physiol Cell Physiol.* 2013;305(4):C447-C56.



194. Kuete V, Fokou FW, Karaosmanoglu O, Beng VP, Sivas H. Cytotoxicity of the methanol extracts of *Elephantopus mollis*, *Kalanchoe crenata* and 4 other Cameroonian medicinal plants towards human carcinoma cells. *BMC Complement Altern Med*. 2017;17(1):280-.
195. Bhattacharya S, Sae-Tia S, Fries BC. Candidiasis and mechanisms of antifungal resistance. *Antibiotics (Basel)*. 2020;9(6):312.
196. Yu B, Jiang Y, Jin L, Ma T, Yang H. Role of quercetin in modulating chloride transport in the intestine. *Front Physiol*. 2016;7:549.
197. Nguyen TD, Canada AT, Heintz GG, Gettys TW, Cohn JA. Stimulation of secretion by the T84 colonic epithelial cell line with dietary flavonols. *Biochem Pharmacol*. 1991;41(12):1879-86.
198. Kim JD, Liu L, Guo W, Meydani M. Chemical structure of flavonols in relation to modulation of angiogenesis and immune-endothelial cell adhesion. *J Nutr Biochem*. 2006;17(3):165-76.
199. Boonmasawai S, Leesombun A, Chaichoun K, Taowan J, Sariya L, Thongjuy O. Effects of the three flavonoids; kaempferol, quercetin, and myricetin on Baby hamster kidney (BHK-21) cells and Human hepatocellular carcinoma cell (HepG2) cells proliferations and total Erk1/2 protein expression. 2017.
200. Schuier M, Sies H, Illek B, Fischer H. Cocoa-related flavonoids inhibit CFTR-mediated chloride transport across T84 human colon epithelia. *J Nutr*. 2005;135(10):2320-5.
201. Pyle LC, Fulton JC, Sloane PA, Backer K, Mazur M, Prasain J, et al. Activation of the cystic fibrosis transmembrane conductance regulator by the flavonoid quercetin: potential use as a biomarker of  $\Delta$ F508 cystic fibrosis transmembrane conductance regulator rescue. *Am J Respir Cell Mol Biol*. 2010;43(5):607-16.
202. Zhang S, Smith N, Schuster D, Azbell C, Sorscher EJ, Rowe SM, et al. Quercetin increases cystic fibrosis transmembrane conductance regulator-mediated chloride transport and ciliary beat frequency: therapeutic implications for chronic rhinosinusitis. *Am J Rhinol Allergy*. 2011;25(5):307-12.

203. Illek B, Lizarzaburu ME, Lee V, Nantz MH, Kurth MJ, Fischer H. Structural determinants for activation and block of CFTR-mediated chloride currents by apigenin. *Am J Physiol Cell Physiol.* 2000;279(6):C1838-C46.
204. de Jonge HR, Ardelean MC, Bijvelds MJC, Vergani P. Strategies for cystic fibrosis transmembrane conductance regulator inhibition: from molecular mechanisms to treatment for secretory diarrhoeas. *FEBS letters.* 2020;594(23):4085-108.
205. Saint-Criq V, Gray MA. Role of CFTR in epithelial physiology. *Cell Mol Life Sci.* 2017;74(1):93-115.
206. Niisato N, Nishino H, Nishio K, Marunaka Y. Cross talk of cAMP and flavone in regulation of cystic fibrosis transmembrane conductance regulator (CFTR) Cl<sup>-</sup> channel and Na<sup>+</sup>/K<sup>+</sup>/2Cl<sup>-</sup> cotransporter in renal epithelial A6 cells. *Biochem Pharmacol.* 2004;67(4):795-801.
207. Hwang TC, Wang F, Yang IC, Reenstra WW. Genistein potentiates wild-type and delta F508-CFTR channel activity. *Am J Physiol.* 1997;273(3 Pt 1):C988-98.
208. Baker MJ, Hamilton KL. Genistein stimulates electrogenic Cl<sup>-</sup> secretion in mouse jejunum. *Am J Physiol Cell Physiol.* 2004;287(6):C1636-45.
209. Sears CL, Firoozmand F, Mellander A, Chambers FG, Eromar IG, Bot AG, et al. Genistein and tyrphostin 47 stimulate CFTR-mediated Cl<sup>-</sup> secretion in T84 cell monolayers. *Am J Physiol.* 1995;269(6 Pt 1):G874-82.
210. Illek B, Fischer H, Machen TE. Alternate stimulation of apical CFTR by genistein in epithelia. *Am J Physiol.* 1996;270(1 Pt 1):C265-75.
211. Collins D, Kopic S, Geibel JP, Hogan AM, Medani M, Baird AW, et al. The flavonone naringenin inhibits chloride secretion in isolated colonic epithelia. *Eur J Pharmacol.* 2011;668(1-2):271-7.
212. Sun H, Niisato N, Nishio K, Hamilton KL, Marunaka Y. Distinct action of flavonoids, myricetin and quercetin, on epithelial Cl<sup>-</sup> secretion: useful tools as regulators of Cl<sup>-</sup> secretion. *Biomed Res Int.* 2014;2014:902735.
213. Mezesova L, Bartekova M, Javorkova V, Vlkovicova J, Breier A, Vrbjar N. Effect of quercetin on kinetic properties of renal Na,K-ATPase in normotensive and hypertensive

rats. *J Physiol Pharmacol*. 2010;61(5):593-8.

214. Kongsuphol P, Cassidy D, Hieke B, Treharne KJ, Schreiber R, Mehta A, et al. Mechanistic insight into control of CFTR by AMPK. *J Biol Chem*. 2009;284(9):5645-53.

215. Huang WW, Tsai SC, Peng SF, Lin MW, Chiang JH, Chiu YJ, et al. Kaempferol induces autophagy through AMPK and AKT signaling molecules and causes G2/M arrest via downregulation of CDK1/cyclin B in SK-HEP-1 human hepatic cancer cells. *Int J Oncol*. 2013;42(6):2069-77.

216. Han B, Yu YQ, Yang QL, Shen CY, Wang XJ. Kaempferol induces autophagic cell death of hepatocellular carcinoma cells via activating AMPK signaling. *Oncotarget*. 2017;8(49):86227-39.

217. Clark JA, Black AR, Leontieva OV, Frey MR, Pysz MA, Kunneva L, et al. Involvement of the ERK signaling cascade in protein kinase C-mediated cell cycle arrest in intestinal epithelial cells. *J Biol Chem*. 2004;279(10):9233-47.

218. Keely SJ, Barrett KE. p38 mitogen-activated protein kinase inhibits calcium-dependent chloride secretion in T84 colonic epithelial cells. *Am J Physiol Cell Physiol*. 2003;284(2):C339-48.

219. Keely SJ, Uribe JM, Barrett KE. Carbachol stimulates transactivation of epidermal growth factor receptor and mitogen-activated protein kinase in T84 cells. Implications for carbachol-stimulated chloride secretion. *J Biol Chem*. 1998;273(42):27111-7.

220. Li X, Jin F, Lee HJ, Lee CJ. Kaempferol Regulates the Expression of Airway MUC5AC Mucin Gene via I $\kappa$ B $\alpha$ -NF- $\kappa$ B p65 and p38-p44/42-Sp1 Signaling Pathways. *Biomol Ther (Seoul)*. 2021;29(3):303-10.

221. Loffing J, Moyer BD, McCoy D, Stanton BA. Exocytosis is not involved in activation of Cl<sup>-</sup> secretion via CFTR in Calu-3 airway epithelial cells. *Am J Physiol Cell Physiol*. 1998;275(4):C913-C20.

222. Singh D, Kumari K, Ahmed S. CHAPTER 17 - Natural herbal products for cancer therapy. In: Jain B, Pandey S, editors. *Understanding Cancer*: Academic Press; 2022. p. 257-68.

223. Yani S, Taupiqurrohman O, Siti R, Ida K, Epa P. In silico analysis of kaempferol as

- a competitor of estrogen on estrogen receptor alpha of endometrial cancer In silico analysis of kaempferol as a competitor of estrogen on estrogen receptor alpha of endometrial cancer. *J Phys Conf Ser.* 2019;1402.
224. Schmidt A, Hughes LK, Cai Z, Mendes F, Li H, Sheppard DN, et al. Prolonged treatment of cells with genistein modulates the expression and function of the cystic fibrosis transmembrane conductance regulator. *Br J Pharmacol.* 2008;153(6):1311-23.
225. Staar S, Richter DU, Makovitzky J, Briese V, Bergemann C. Stimulation of endometrial glandular cells with genistein and daidzein and their effects on ERalpha- and ERbeta-mRNA and protein expression. *Anticancer Res.* 2005;25(3a):1713-8.
226. Rab A, Bartoszewski R, Jurkuvenaite A, Wakefield J, Collawn JF, Bebok Z. Endoplasmic reticulum stress and the unfolded protein response regulate genomic cystic fibrosis transmembrane conductance regulator expression. *Am J Physiol Cell Physiol.* 2007;292(2):C756-C66.
227. Varga K, Jurkuvenaite A, Wakefield J, Hong JS, Guimbellot JS, Venglarik CJ, et al. Efficient intracellular processing of the endogenous cystic fibrosis transmembrane conductance regulator in epithelial cell lines. *J Biol Chem.* 2004;279(21):22578-84.
228. Radtke J, Linseisen J, Wolfram G. Fasting plasma concentrations of selected flavonoids as markers of their ordinary dietary intake. *Eur J Nutr.* 2002;41(5):203-9.
229. Sun H, Niisato N, Nishio K, Hamilton KL, Marunaka Y. Distinct action of flavonoids, myricetin and quercetin, on epithelial Cl<sup>-</sup> secretion: useful tools as regulators of Cl<sup>-</sup> secretion. *Biomed Res Int.* 2014;2014:902735-.



## VITA

NAME Janjira Thaweewattanodom

DATE OF BIRTH 12 August 1993

PLACE OF BIRTH Chumphon, Thailand

INSTITUTIONS ATTENDED 2012-2015 Bachelor of Nursing Science (B.N.S.) (1st Hons.)  
from Srinakharinwirot University Prasarnmitr, Bangkok

HOME ADDRESS 116/1 Village No.16 Phato, Phato, Chumphon, Thailand

PUBLICATION -

AWARD RECEIVED -

